

WALL JET MODEL  
FOR CEILING FAN APPLICATIONS IN  
BROILER HOUSES

by

Neal Elwood Blackwell

Dissertation submitted to the Faculty of the  
Virginia Polytechnic Institute and State University  
in partial fulfillment of the requirements for the degree of  
DOCTOR OF PHILOSOPHY

in

Environmental Science and Engineering

APPROVED:

\_\_\_\_\_  
D. H. Vaughan, Chairman

\_\_\_\_\_  
J. S. Cundiff

\_\_\_\_\_  
T. E. Diller

\_\_\_\_\_  
H. A. Hughes

\_\_\_\_\_  
W. D. Weaver

December, 1985

Blacksburg, Virginia

WALL JET MODEL  
FOR CEILING FAN APPLICATIONS  
IN BROILER HOUSES

by

Neal Elwood Blackwell

Committee Chairman: David H. Vaughan  
Environmental Science and Engineering

(ABSTRACT)

A model was developed to predict velocity profiles of radial wall jets produced by ceiling fans and flowing over broiler chickens. Broilers were modeled by balloons with paper cylinders simulating the necks. Wall jet data was recorded for 91.5, 83.8 and 71.1 cm radius fans that were rated at 220, 160, and 108 W, respectively. Each fan was suspended 2.44 m above the floor and operated at four speeds.

Applications of the model include 1) calculation of optimum design specifications for ceiling fan applications in broiler houses and 2) prediction of data for managerial decisions concerning existing ceiling fan applications. Model inputs are the fan radius and the characteristic velocity. The characteristic velocity was defined as the maximum air velocity 30 cm below the blades.

The wall jet model was interfaced with a broiler growth model for heat stressed broilers to simulate summer conditions and to predict the additional weight gain due to the wall jet. Also, the wall jet was developed to predict the air velocity near the litter to aid litter management decisions.

Ceiling fan applications in the southeast, used in conjunction with the summer model, have the potential of increasing summer broiler production by 10% and decreasing fan energy consumption by 8 to 12%. The model may be used to optimize the benefit to the producer.

To

Dr. David Harris Vaughan,  
a wise researcher, author, speaker and counselor  
and to his wife and family,

who shared their husband and father with me for ten years,

I dedicate this dissertation  
with much thankfulness to God  
for you.

## ACKNOWLEDGEMENTS

This was a cooperative effort of the Agricultural Engineering Department at Virginia Polytechnic Institute and State University in Blacksburg, VA and the Biological and Agricultural Engineering Department at North Carolina State University in Raleigh, N.C. This work was a part of Hatch project S-149 entitled "Optimize Efficiency of Energy Utilization in Agricultural Housing Systems" (Hatch 622357).

Appreciation is extended to Dr. D. H. Vaughan, Chairman, Dr. J. S. Cundiff, Dr. T. E. Diller, Dr. H. A. Hughes and Dr. W. D. Weaver Jr. for serving as members of my graduate committee.

Appreciation is also expressed to the following people: Dr. G. R. Baughman, Dr. R. W. Bottcher, Dr. C. G. Bowers, Mr. G. B. Blum, Dr. W. F. McClure, and Dr. F. J. Hassler for invaluable assistance in data collection at North Carolina State University.

Many thanks to my former roommates , , and . Your friendship and encouragement over the past three years was a gift from God.

Also, many thanks to the several hundred other friends and relatives who have meant so much during these past three years. I wish I had space to list all of you!

A special thanks to my parents, , who introduced me to my Creator and gave me purpose in life.

"As you do not know the path of the wind, or how the body is formed in the mother's womb, so you cannot understand the work of God, the Maker of all things."

Ecc1. 11:5

"When I consider your heavens, the work of your fingers,  
The moon and the stars, which you have set into place,  
what is man that you are mindful of him. . .?  
O LORD, our Lord, how majestic is your name in all the earth!"

Ps. 8:3, 4, 9

"I will praise you, O LORD, with all my heart;  
I will tell of all your wonders.  
I will be glad and rejoice in you;  
I will sing praise to your name, O Most High."

Ps. 9:1, 2

## TABLE OF CONTENTS

	<u>Page</u>
TITLE PAGE . . . . .	i
ABSTRACT . . . . .	ii
ACKNOWLEDGMENTS . . . . .	v
TABLE OF CONTENTS . . . . .	vi
LIST OF FIGURES . . . . .	ix
LIST OF TABLES . . . . .	xiv
 Chapter	
I. INTRODUCTION . . . . .	1
II. REVIEW OF LITERATURE . . . . .	9
III. PROBLEM DEFINITION AND OBJECTIVES . . . . .	12
Problem Definition . . . . .	12
Objectives . . . . .	12
IV. THEORETICAL BACKGROUND FOR MODEL FORMULATION . . . . .	13
Theoretical Factors Affecting Wall Jet Model . . . . .	13
Factors Affecting Wall Jet Model . . . . .	13
Regions of Flow . . . . .	13
Linear Relationships . . . . .	15
Annular Free Jets . . . . .	15
Similar Velocity Profiles . . . . .	15
Fan Height. . . . .	15
Wall Jet Obstructions . . . . .	18
Wall Jet Interaction . . . . .	18
Characteristic Velocity and Data Correlation. . . . .	19
V. EXPERIMENTAL METHODS AND MATERIALS . . . . .	20
Experimental Procedure . . . . .	20
Surface Pressure in the Impingement Region . . . . .	21
Background: Wall Jet Measurement Procedure . . . . .	21
Fans . . . . .	22
Wall Jet Measurements and Balloon Orientation . . . . .	22
Wall Jets Flowing Over Smooth Floor . . . . .	22
Wall Jets Flowing Over Broilers with Necks Down . . . . .	25
Wall Jets Flowing Over Broilers with Necks Up . . . . .	29

TABLE OF CONTENTS  
(continued)

	<u>Page</u>
Wall Jet Sensitivity to Uniform Broiler Spacing . . . . .	29
Wall Jet Sensitivity to Large Gaps between Groups of Broilers . . . . .	33
Characteristic Velocity . . . . .	33
Instrumentation and Data Collection . . . . .	33
Velocity Measurements . . . . .	33
Psychometric Properties of Air . . . . .	35
Data Processing . . . . .	36
Temperature Correction of Velocity Data . . . . .	36
 VI. EXPERIMENTAL RESULTS AND MODEL DEVELOPMENT . . . . .	 48
Stagnation Ring . . . . .	48
Characteristic Velocity. . . . .	50
Wall Jet Model: Smooth Floor . . . . .	50
Wall Jet Model: Broilers With Necks Down . . . . .	61
Wall Jet Model: Broilers With Necks Up . . . . .	69
Model Sensitivity to Balloon Spacing . . . . .	83
Model Sensitivity to Large Gaps Between Groups of Balloons . . . . .	83
Velocity Decay . . . . .	83
 VII. APPLICATION . . . . .	 92
Summer Routine . . . . .	92
Background: Weight Gain of Heat Stressed Broilers . . . . .	92
Summer Routine Development . . . . .	96
Insights for Summer Ceiling Fan Applications . . . . .	104
Winter Routine . . . . .	105
Background: Litter Conditions . . . . .	105
Winter Routine Development . . . . .	106
Insights for Winter Ceiling Fan Applications . . . . .	106
 VIII CONCLUSIONS, SAFETY AND FUTURE WORK . . . . .	 109
Conclusions . . . . .	109
Future Work . . . . .	109
Safety . . . . .	110
Fan Standards . . . . .	110
Future Ceiling Fan Concept . . . . .	111
Updated Broiler Growth Model . . . . .	113

TABLE OF CONTENTS  
(continued)

	<u>Page</u>
Ceiling Fan Applications for Air Exchange . . .	113
Inclusion of the Reduction of Risk in the Summer Routine . . . . .	115
LITERATURE CITED . . . . .	116
Appendix	
A. SUMMER ROUTINE: BROILER1 USER MANUAL . . . . .	121
B. WINTER ROUTINE: USER MANUAL . . . . .	141
C. UNCERTAINTY ANALYSIS . . . . .	146
VITA . . . . .	149



## LIST OF FIGURES

		<u>Page</u>
Figure 1.	Horizontal view of a blower fan application in a poultry house . . . . .	3
Figure 2.	Top view of a blower fan application in a poultry house . . . . .	4
Figure 3.	Air flow patterns produced by jets exiting sidewall slotted inlets . . . . .	5
Figure 4.	Wall jet characteristics and development (Striegl, 1982) . . . . .	7
Figure 5.	Circles formed by heat stressed broilers huddled beneath ceiling fans . . . . .	10
Figure 6.	Schematic of impinging jet (Striegl, 1982) . . . . .	14
Figure 7.	Velocity scale for a wall jet flowing over a flat plate . . . . .	16
Figure 8.	Characteristic lengths for a wall jet flowing over a flat plate . . . . .	17
Figure 9.	Orientation of wall jet measurements with respect to balloons . . . . .	23
Figure 10.	Probe locations above the smooth floor . . . . .	24
Figure 11.	Water balloons used to physically model broilers sitting with necks down . . . . .	26
Figure 12.	Shape and size of the floor space where the balloons were located . . . . .	27
Figure 13.	Probe locations over the top of the balloons . . . . .	28
Figure 14.	Probe locations 3 cm in front of the balloons . . . . .	30
Figure 15.	Water balloons with paper necks used to physically model broilers sitting with necks up . . . . .	31
Figure 16.	Probe locations 3 cm in front of the balloons with necks . . . . .	32

LIST OF FIGURES (Continued)

		<u>Page</u>
Figure 17.	Orientation of wall jet measurements with respect to a gap produced by missing rows of balloons . . . . .	34
Figure 18.	Calibration curve for metal clad sensor ("Model 1266") of "Model 1053B Hot Wire Anemometer" . .	38
Figure 19.	Calibration curve for metal clad sensor ("Model 1266") of "Model 1053B Hot Wire Anemometer" . .	39
Figure 20.	Velocity versus pressure drop curves for wind chamber calibration of sensor at 68 F and one atmosphere (Thermal-Systems, Inc., n.d.) . . .	42
Figure 21.	Calibration curve for metal clad sensor ("Model 1266") of "Model 1053 Hot Wire Anemometer" . .	43
Figure 22.	Comparison of known and corrected mass flux . .	46
Figure 23.	Corrected and uncorrected velocity profiles of wall jet at a radial distance of 286.5 cm, measured 3 cm in front of a balloon and produced by the 91.5 cm radius fan operating at a characteristic velocity of 4.922 m/s . . .	47
Figure 24.	Surface pressure on a smooth floor at varying radial distances from the fan centerline and with a fan height of 2.44 m . . . . .	49
Figure 25.	Annular free jet, 30 cm below the blades, produced by the 91.5 cm radius fan operating at four characteristic velocities . . . . .	51
Figure 26.	Annular free jet, 30 cm below the blades, produced by the 83.8 cm radius fan operating at four characteristic velocities . . . . .	52
Figure 27.	Annular free jet, 30 cm below the blades, produced by the 71.1 cm radius fan operating at four characteristic velocities . . . . .	53
Figure 28.	Velocity profile of a wall jet at a radius of 337 cm flowing over a smooth floor and produced by a 83.3 cm radius fan operating at a characteristic velocity of 3.348 m/s . . . .	54

LIST OF FIGURES (Continued)

		<u>Page</u>
Figure 29.	Nondimensional velocity profiles for wall jets flowing over a smooth floor . . . . .	55
Figure 30.	Inverse of the maximum velocity of wall jets flowing over a smooth floor . . . . .	56
Figure 31.	Inverse of the maximum velocity of wall jets flowing over a smooth floor . . . . .	57
Figure 32.	Nondimensionalized velocity scale of wall jets flowing over a smooth floor . . . . .	59
Figure 33.	Characteristic length of wall jets flowing over a smooth floor . . . . .	60
Figure 34.	Velocity profile of a wall jet at a radius of 378 cm flowing over a balloon and produced by a 91.5 cm radius fan operating at a characteristic velocity of 4.074 m/s . . . . .	62
Figure 35.	Nondimensional velocity profiles for wall jets flowing over balloons . . . . .	62
Figure 36.	Inverse of the maximum velocity of wall jets flowing over balloons . . . . .	63
Figure 37.	Nondimensionalized velocity scale of wall jets flowing over balloons . . . . .	64
Figure 38.	Characteristic length of wall jets flowing over balloons . . . . .	65
Figure 39.	Velocity profile of wall jet at a radial distance of 286.5 cm, measured 3 cm in front of a balloon and produced by the 91.5 cm radius fan operating at a characteristic velocity of 4.922 m/s . . . . .	67
Figure 40.	Nondimensional velocity profile for wall jets 3 cm in front of balloons . . . . .	68
Figure 41.	Nondimensionalized velocity scale of wall jets 3 cm in front of balloons . . . . .	70

LIST OF FIGURES (Continued)

	<u>Page</u>
Figure 42. Characteristic length of wall jets 3 cm in front of balloons . . . . .	71
Figure 43. Velocity profiles of wall jet at a radial distance of 204.5 cm, 3 cm in front of a balloon with a neck and produced by the 91.5 cm radius fan operating at four characteristic velocities . . . . .	72
Figure 44. Characteristic length of wall jets flowing over balloons with necks . . . . .	73
Figure 45. Nondimensional velocity profile for wall jets, in region one, flowing over balloons with necks . . . . .	75
Figure 46. Nondimensional velocity profile for wall jets, in region two, flowing over balloons with necks . . . . .	76
Figure 47. Inverse of the maximum velocity of wall jets flowing over balloons with necks and produced by a 91.5 cm radius fan operating at four characteristic velocities . . . . .	79
Figure 48. Inverse of the maximum velocity of wall jets flowing over balloons with necks and produced by an 83.8 cm radius fan operating at two characteristic velocities . . . . .	80
Figure 49. Inverse of the maximum velocity of wall jets flowing over balloons with necks and produced by a 71.1 cm radius fan operating at two characteristic velocities . . . . .	81
Figure 50. Nondimensionalized velocity scale of wall jets flowing over balloons with necks . . . . .	82
Figure 51. Characteristic length of wall jets flowing over balloons (with necks) at two balloon spacings . . . . .	84
Figure 52. Nondimensionalized velocity scale of wall jets flowing over balloons (with necks) at two balloon spacings . . . . .	85

LIST OF FIGURES (Continued)

		<u>Page</u>
Figure 53.	Nondimensional velocity profile for wall jets flowing over balloons (with necks) at two balloon spacings . . . . .	86
Figure 54.	Wall jet velocity profiles for two gap spacings (characteristic velocity = 3.348 m/s, R = 83.8 cm, r = 253 cm) . . . . .	87
Figure 55.	Nondimensional velocity profile for wall jets flowing over balloons (with necks) at two gap spacings . . . . .	88
Figure 56.	Nondimensionalized velocity scale of wall jets flowing over balloons (with necks) at two gap spacings . . . . .	89
Figure 57.	Characteristic length of wall jets flowing over balloons (with necks) at two gap spacings . . .	90
Figure 58.	Comparison of nondimensionalized velocities of wall jets . . . . .	91
Figure 59.	Flowchart for Summer Routine BROILER1 . . . . .	129
Figure 60.	Flowchart for Winter Routines NECKDN and NECKUP . . . . .	143
Figure 61.	Air velocity effect on growth of 7 week old male broilers tested for 2 weeks in a diurnally cycling hot, humid environment (Drury, 1967) . .	93
Figure 62.	Broiler growth at varying ages measured in 1964 and 1983 . . . . .	95
Figure 63.	Ceiling fan with blade extensions and resulting air flow patterns . . . . .	112
Figure 64.	Ceiling fan application for air circulation and air exchange . . . . .	114

## LIST OF TABLES

		<u>Page</u>
Table 1.	Data for the Summer Routine Example Problem . .	100
Table 2.	Output for the Summer Routine Example Problem: Ceiling Fans Compared to No Fans (Zero Air Flow) . . . . .	101
Table 3.	Output for Summer Routine Example Problem: Ceiling Fans Compared to Alternative Air Circulators . . . . .	102
Table 4.	Output for Summer Routine Example: Combinations of Fan Characteristics and the Predicted Results . . . . .	103
Table 5.	Output for Winter Routine Example Problem: $r = 400$ cm, $R = 91.5$ cm and $UC = 4.990$ m/s . .	108
Table 6.	Listing of Variable Names for BROILER1 . . . .	123
Table 7.	FORTTRAN Coding for the Summer Routine (BROILER1) . . . . .	130
Table 8.	Coding for NECKDN for the HP-41C Series of Calculators . . . . .	144
Table 9.	Coding for NECKUP for the HP-41C Series of Calculators . . . . .	145

## CHAPTER I

### INTRODUCTION

Interest in energy conservation and improved management practices for air circulation in the proximity of broiler chickens, hereafter called broilers, has prompted research on ceiling fan applications in broiler houses. Ceiling fans, which are paddle-bladed fans that hang from the ceiling, have the potential to decrease the amount of energy used to ventilate live broiler production facilities. The energy required to ventilate a broiler house represents the second largest cost in live broiler production (Hughes, 1985). Energy savings of 8-12% are expected with the proper use of ceiling fans (Hughes, 1985). Energy consumption of individual ceiling fans ranges from 50 to 200 W.

Ceiling fans also have the potential to increase air circulation in the proximity of broilers and reduce problems, which may result from a lack of air circulation. Winter problems include: 1) relatively high ammonia concentrations in the air, 2) damp and caked litter and 3) air temperature stratification. Problems associated with high ammonia concentrations in the air include decreased feed efficiency, decreased weight gain and an increased susceptibility to disease (Anderson et al., 1964; Charles and Payne, 1966; Kling and Quarles, 1974; Quarles and Kling, 1974; Reece, et al., 1981). Damp litter enhances the growth of microorganisms. Also, damp litter and cool air may chill broilers because poor air circulation allows warm air to rise to the ceiling and cold air to fall to the floor.

A lack of air circulation in the summer magnifies heat stress. Heat stress depresses the appetite of broilers thereby decreasing weight gain (Drury, 1966 and Deaton et al., 1978). Furthermore, extreme heat stress can kill broilers (Kempster, 1938; Joiner and Huston, 1957; Siegel and Drury, 1968b; Sammelwitz, 1967).

Ceiling fan applications during the summer have several advantages over the use of blowers and slotted inlets. Blowers are exhaust fans that are removed from the walls in summer and positioned to produce a jet of air that travels horizontally along the length of the building (Figure 1). At least 75% of the jet is above the broilers and does not contribute to increasing the velocity around the broilers. A top view of a blower application (Figure 2) illustrates that portions of the floor area are poorly ventilated, because the jets travel in one direction. Blowers that are positioned high and tilted downward are special cases of ceiling fans.

Slotted inlets produce two-dimensional wall jets that attach to the floor and distribute the jet along the floor (Figure 3) (Timmons, 1984). The disadvantages of slotted inlets are: 1) the slots are difficult and expensive to retrofit to an existing building, 2) slotted inlets cannot be used in the open-wall broiler houses that are common in the Southeast, and 3) additional inlets must be installed near the ceiling because inlets near the floor are not suitable for winter ventilation.

Ceiling fans are advantageous to blowers because they produce wall jets which flow over the floor where broilers are located. Wall jets are defined as jets of air which flow along a boundary, such as a wall



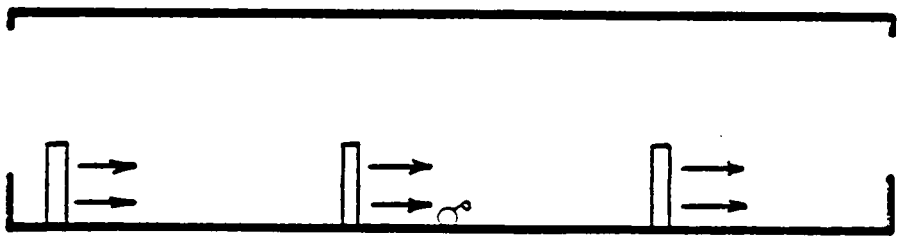


FIGURE 1. HORIZONTAL VIEW OF A BLOWER FAN APPLICATION IN A POULTRY HOUSE.

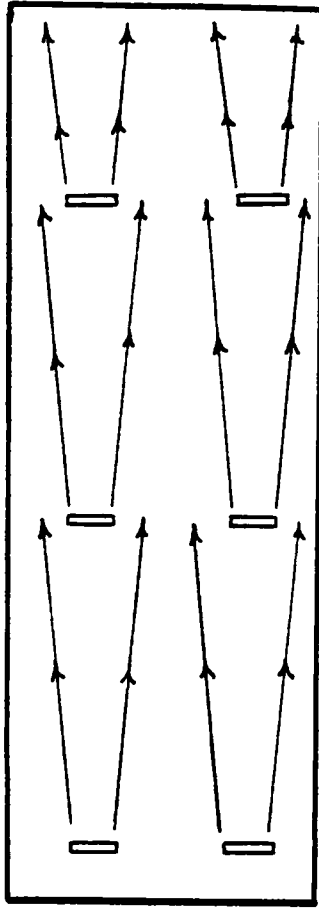


FIGURE 2. TOP VIEW OF A BLOWER FAN APPLICATION IN A  
POULTRY HOUSE.

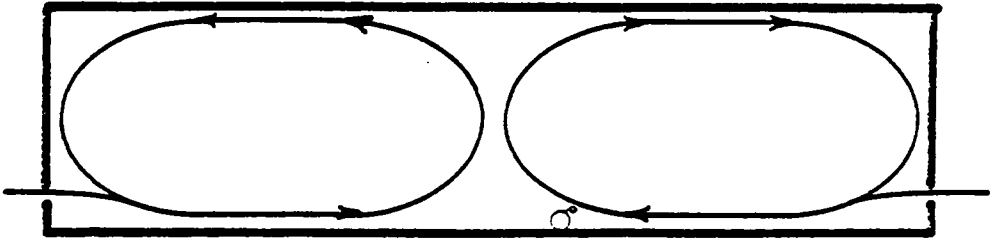


FIGURE 3. AIR FLOW PATTERNS PRODUCED BY JETS EXITING  
SIDEWALL SLOTTED INLETS.

or a floor. Wall jets, traveling along the ceiling, are commonly used for winter ventilation because wall jets decay slower than free jets. Free jets do not flow along a boundary, therefore a large amount of air is entrained and the jets decay rapidly. Two parameters are required to characterize a wall jet: 1) the maximum velocity ( $U_{MAX}$ ) and 2) the characteristic length ( $B$ ) (Figure 4). The characteristic length is the height from the floor to the position where the velocity is equal to one-half of the maximum velocity.

Ceiling fans produce annular, free jets which impinge upon the floor and produce a radial wall jet. Ceiling fans are advantageous over blowers because the corresponding radial wall jets are axisymmetric, thereby ventilating the floor in all radial directions. Also, the wall jets remain close to the floor and impinge upon the broilers. Hence, ceiling fans distribute jets of air in an efficient way. In comparison to slotted inlets, ceiling fans may be characterized as movable inlets which are not restricted to the side walls because they can be hung wherever a ceiling support is available. Hence, ceiling fans can be spaced to produce wall jets at many positions along the floor.

In summary, ceiling fans are beneficial because: 1) the fans can be easily retrofitted to existing buildings, 2) fan height and spacing are adjustable, 3) relatively uniform velocities are produced in the space occupied by the broilers, 4) energy consumption is relatively small, and 5) the wall jet is confined to the space where the broilers are located.

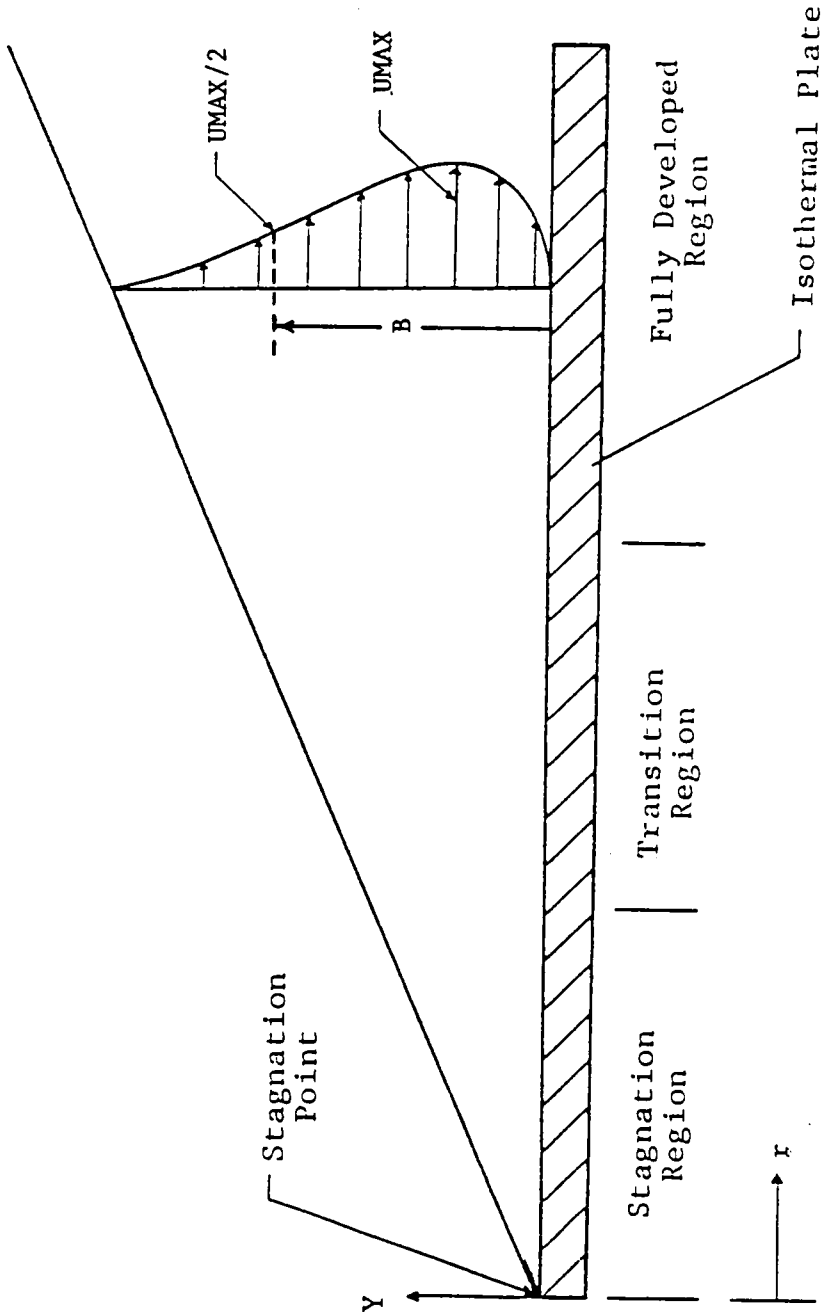


FIGURE 4. WALL JET CHARACTERISTICS AND DEVELOPMENT (STRIEGL, 1982).

Ceiling fan research is needed because 75% of the broilers in the United States are produced in the area from eastern Texas to North Carolina where stress conditions are common in the summer (Reece, 1981). Summer heat stress in the Southeast causes mortalities between 3 to 10% of the initial broiler population (Timmons and Baughman, 1982). One of the main research needs is to develop a technique to calculate proper spacing of ceiling fans in broiler applications. Timmons and Baughman (1982) suggested a fan spacing of 5.77 m, but their report was based on wall jets flowing over a floor with no broilers present. Also, the recommendation did not vary with fan diameter or speed. Research is needed to answer the following questions: 1) which diameter fan should be used, 2) what speeds should the fans operate in winter and summer, 3) how does the presence of the broilers affect the wall jet, 4) how does broiler spacing effect the wall jet, 5) how does the wall jet differ when the broilers are in a restful state with their necks down versus when the broilers are in an alert state with their necks up, 6) what safety hazards do ceiling fans present, and 7) how ceiling fan design can be improved for broiler applications.

## CHAPTER II

### REVIEW OF LITERATURE

No literature was found that included any reports on models which predict wall jets produced by ceiling fans. Data from two ceiling fan studies have been reported in unpublished papers. The author collected the data reported by Timmons and Baughman (1984). The study by Hughes and Wu (1985) was conducted at VPI & SU and the author observed data collection. These experiments have shown that annular free jets impinging on flat plates produce axisymmetrical, radial wall jets. The reports of these studies include criteria for ceiling fan applications, but these recommendations are based on data for flow over flat floors. No reports have included the results of flow over broilers.

Timmons and Baughman (1984) initially became interested in measuring velocities of wall jets from ceiling fans when they observed a broiler operation where the fans were apparently spaced too far apart (Baughman, 1984). The heat stressed birds huddled beneath the fans and formed circles with empty floor area between the circles (Figure 5). To recommend proper fan spacing, Timmons and Baughman (1984) determined the velocity of wall jets at varying radii. The radial wall jets were produced by a 1.56 m diameter, 55 W, ceiling fan (Agri fan 190 a7). Velocity measurements were made with a hot-wire anemometer and a time integrating digital voltmeter. They concluded: 1) air velocities of 1.0 m/s and higher were maintained within a radius of 3.4 m from the fan centerline; 2) fan heights (above the floor) ranging from 1.8 to 3.7 m

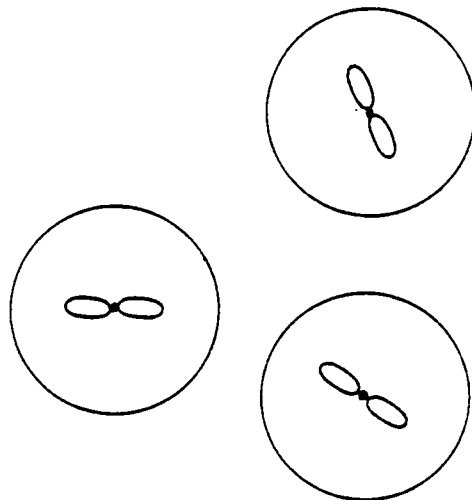


FIGURE 5. CIRCLES FORMED BY HEAT STRESSED BROILERS  
HUDDLED BENEATH CEILING FANS.



had little effect on the wall jet velocity; 3) the fan reduced temperature stratification in an insulated roof broiler house. These researchers also reported wall jet velocities produced by a 1.32 m diameter, 115 W, ceiling fan (Fasco PF52CR) and a 1.42 m diameter, 82 W, ceiling fan (Dayton AC569). They concluded that under their operating conditions, the differences in fan diameter, fan height, blade design, and fan speed had little effect on the characteristics of the wall jet.

Hughes and Wu (1985) reported radial wall jets created by nine different ceiling fans. The jets flowed over a flat floor. Velocity measurements were made with four-inch propeller-type, vane anemometers interfaced with a frequency counter. They concluded: 1) fan heights ranging from 2.1 to 2.4 m did not significantly affect the velocity of the wall jet and 2) the radial wall jet was axisymmetrical. When the fan blades rotated in the reverse direction, the wall jet at floor level was dependent on room geometry because the wall jet stuck nearby walls and were drawn back into the fan.

## CHAPTER III

### PROBLEM DEFINITION AND OBJECTIVES

#### Problem Definition

Design and improved management recommendations are needed for ceiling fan applications in broiler houses. Ceiling fans produce air circulation in the space occupied by broilers and reduce the energy costs required for ventilation.

#### Objectives

The goal of this research was to develop software to predict ceiling fan performance. Specific objectives were: 1) to develop a wall jet model to predict the velocity of the wall jet impinging upon broilers located at varying radii from the center line, 2) interface the wall jet model to a broiler growth model that predicts the weight gain of heat stressed broilers as a function of air velocity, 3) develop a computer routine to calculate the optimum combination of fan diameter, fan speed and fan spacing for a given broiler house, and 4) develop a computer routine to predict the velocity of the wall jet one centimeter above litter to aid litter management decisions.

CHAPTER IV  
THEORETICAL BACKGROUND FOR MODEL FORMULATION

Theoretical Factors Affecting Wall Jet Model

Determination of the mathematical form of the wall jet model required an investigation of: 1) wall jets produced by round and annular free jets issuing from orifices and impinging flat plates, 2) wall jets produced by annular free jets issuing from ceiling fans and impinging flat plates, 3) wall jets flowing over obstructions, 4) interacting wall jets, and 5) radial variation of turbulence in round free jets.

Regions of Flow. Round jets issuing from orifices and impinging on flat plates produce three regions of flow (Figure 6) (Striegl, 1982). The three regions are the free jet region, the impingement region and the wall jet region. Air in the free jet region flows downward due to the momentum imparted by the pressure difference across the orifice. An impingement region is produced by the free jet impinging on the flat plate. The impingement of the jet on the plate produces a pressure. The pressure in the impingement region causes the jet to change direction. The direction of the jet approaches horizontal as the jet exits the impingement region. The jet accelerates as it exits the impingement region because the pressure decreases. A wall jet region is produced as the jet decelerates and flows radially over the plate. The impingement of annular free jets produced by ceiling fans cause wall

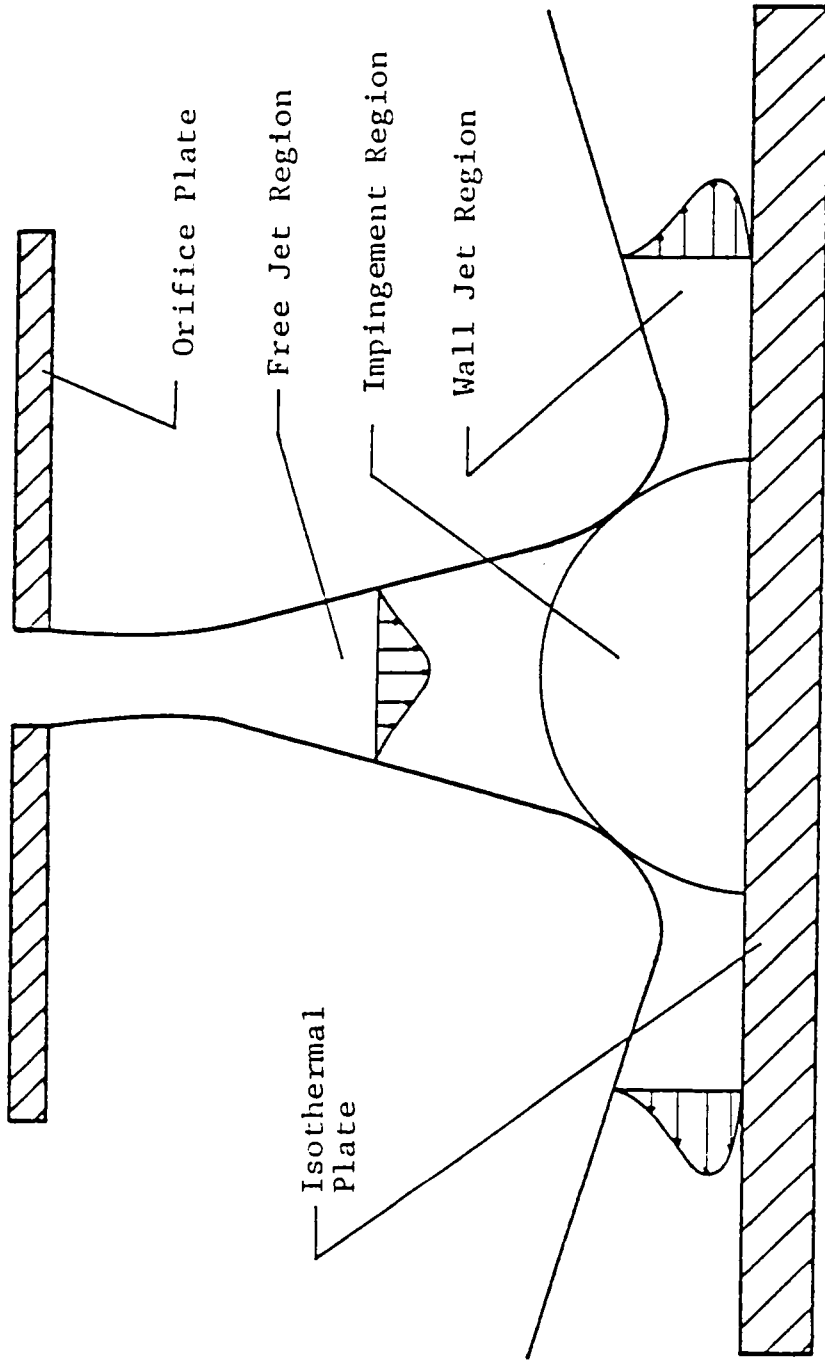


FIGURE 6. SCHEMATIC OF IMPINGING JET (STRIEGL, 1982).

jets in the same way as round free jets produced by round orifices. Hence, ceiling fans are analogous to orifices and floors are analogous to flat plates.

Linear Relationships. Linear relationships are advantageous because the equations are simple. There is a linear relationship between the inverse of the maximum velocity and the radial distance a radial wall jet has traveled (Figure 7)(Tsuei, 1962 and Poreh et al., 1967; Bakke, 1957). Also, the characteristic length is linearly related to the radial distance of the jet (Figure 8).

Annular Free Jets. Annual free jets impinging on flat plates produce radial wall jets with similar velocity profiles (Maki et al., 1980; Timmons and Baughman, 1984). Velocity profiles are termed similar if the nondimensional profiles are equal. The advantage of similar velocity profiles is that the profiles at varying radius can be predicted with one regression equation. Ceiling fans, like annular orifices, produce annular free jets that impinge the floor and produce radial wall jets with similar velocity profiles.

Fan Height. Fan heights between 1.8 and 3.7 m are not critical to the velocity of the wall jet because the deceleration of a jet prior to the impingement region is small compared to the deceleration in the pressure dominated, impingement region (Timmons and Baughman, 1984; Hughes and Wu, 1985, and Tani and Komatsu, 1964). A free jet exits a

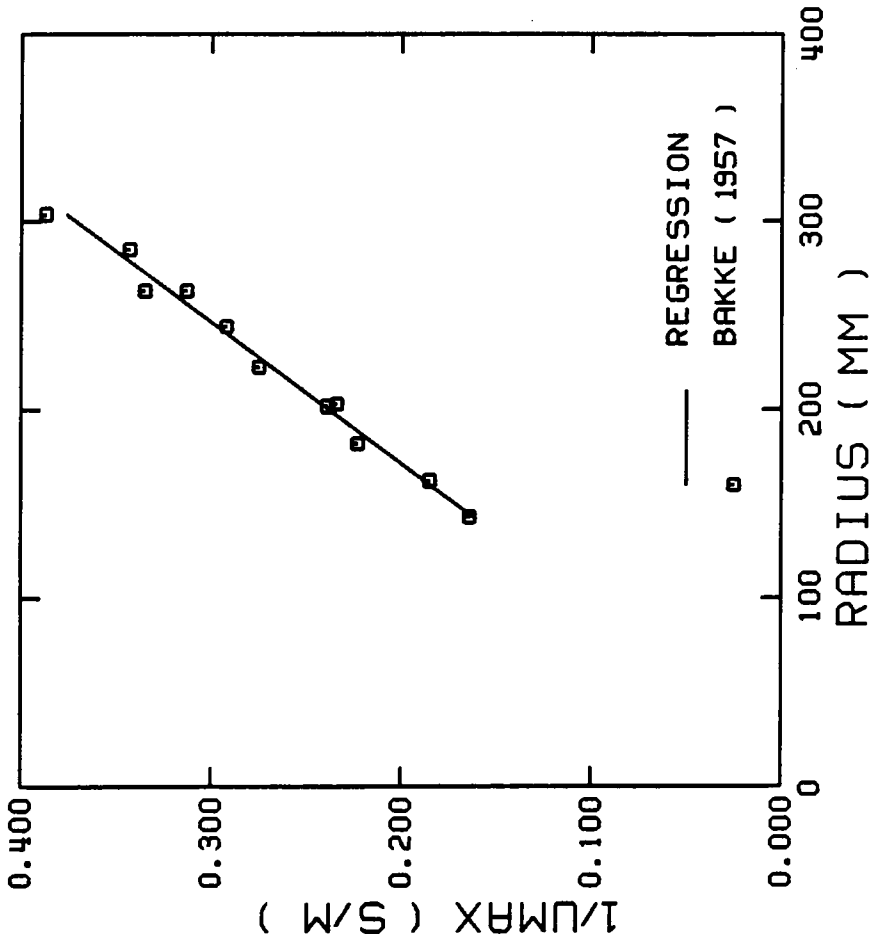


FIGURE 7. VELOCITY SCALE FOR A WALL JET FLOWING OVER A FLAT PLATE.

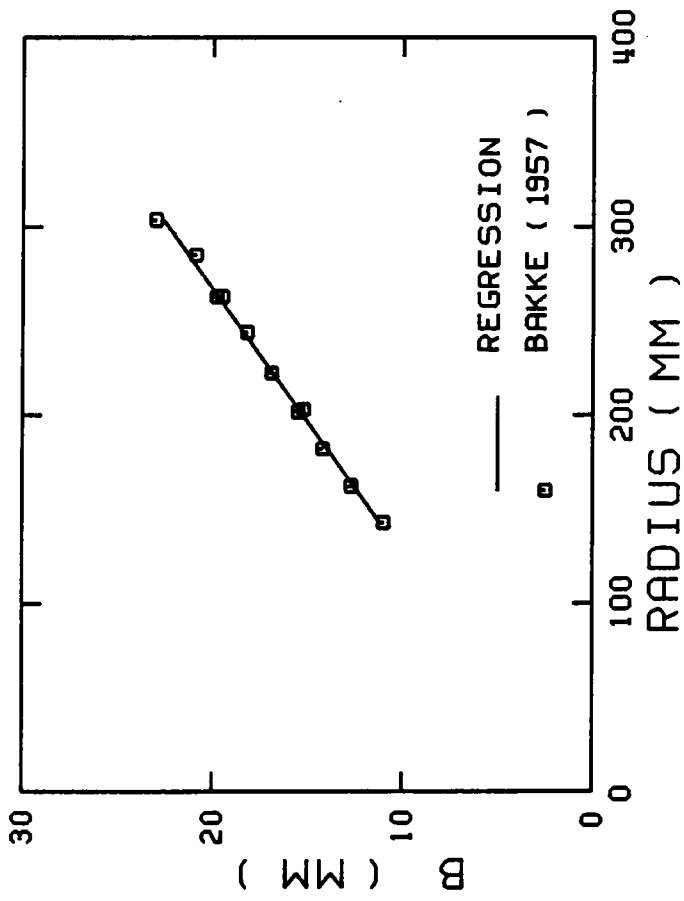


FIGURE 8. CHARACTERISTIC LENGTHS FOR A WALL JET FLOWING OVER A FLAT PLATE.

ceiling fan or orifice and decelerates slowly until it enters the impingement region where the flow is dominated by pressure. The deceleration suddenly increases as the jet enters the impingement region.

Wall Jet Obstructions. A wall jet produced by a ceiling fan is expected to exist when broilers are on the floor because the total pressure head of wall jets produced by ceiling fans was estimated to be one or two orders of magnitude larger than the drag of wall jets flowing over broilers (Timmons, 1984). Also, wall jets can flow over relatively large repeated obstructions, such as broilers (King et al., 1972 and Walker and White, 1973).

Wall Jet Interaction. Wall jet interaction occurs when an array of jets impinge on a flat plate and the resulting wall jets interact. Wall jet interaction is of interest because more than one ceiling fan is needed to properly circulate air in the 12 m by 122 m broiler houses typically used in Virginia. The jet array and single jet comparison is analogous to the multiple fan and single fan comparison according to the evidence given in the section entitled "Regions of flow". The effect of wall jet interaction on heat transfer was studied and researchers reported that Nusselt numbers along an impingement plate were approximately the same for jet arrays and single jets (Striegl and Diller, 1982). Wall jet interaction did not significantly alter the Nusselt number. Turbulence in the interaction region maintains the



Nusselt number that is present in the single jet case. Also, the impingement of two wall jets upon each other produces a pressure. The pressure causes the jets to change direction and produce an upwash. The vertical component of the velocity increases as the horizontal component decreases. Hence, a wall jet model developed for a single fan is valid for a multiple fan case because convective heat transfer from broilers located in the wall jet interaction region is expected to be enhanced by ceiling fans.

Characteristic Velocity and Data Correlation. The influence of fan speed, blade design and number of blades was combined in one term, called the characteristic velocity (UC). Characteristic velocity was defined as the maximum velocity of a free jet prior to disturbance due to turbulence. The characteristic velocity concept was developed with the aid of information on turbulence diffusion in jets. Turbulence requires several orifice diameters beyond the potential core to diffuse to the center of a round free jet where the maximum velocity exists (Gordan and Cahit, 1965). The maximum velocity, prior to the disturbance by turbulence, is approximately equal to the orifice velocity which is defined as the velocity existing at the orifice. Orifice velocity is used to correlate wall jet data for varying orifice diameters but an orifice velocity does not exist in the case of a ceiling fan (Tsuei, 1962; and Poreh et al., 1967). However, a characteristic velocity can be used to correlate the wall jet data.

CHAPTER V  
EXPERIMENTAL METHODS AND MATERIALS

Experimental Procedure

The theoretical background reported in the previous chapter was used to determine the mathematical forms of the wall jet model. Linear equations were required to predict the relationships between the inverse of the maximum velocity of the wall jet and the radial distance of the wall jet from the ceiling fan centerline ( $r$ ). These relationships for a single fan varied with characteristic velocity; however, these relationships for multiple fans varied with characteristic velocity and fan radius. Therefore, in order to correlate the linear relationships for multiple fans to one linear relationship, 1) the characteristic velocities were divided by the corresponding inverse of the maximum velocity and 2) the radial distances from the fan centerline were divided by the corresponding fan radius. Also, a linear equation was required to predict the relationship between the characteristic length and the radial distance from the fan centerline. The slope and the intercept constants were experimentally determined.

The relationship between the velocity of the wall jet ( $U$ ) and the height above the floor ( $Y$ ) was nonlinear and varied with the radial distance from the fan centerline. The velocity profiles were nondimensionalized by 1) dividing the heights from the floor by the corresponding characteristic length and 2) dividing the wall jet velocities by the corresponding maximum velocity. The nondimensional

velocity profile data was used in conjunction with the polynomial regression routine of the Statistical Analysis System (SAS) to calculate the regression coefficients.

Surface Pressure in the Impingement Region. Surface pressure in the impingement region was measured on a 3m by 3m styrofoam impingement plate with flush pressure taps. Rubber tubes linked the pressure taps to the micromanometer, which was used to measure pressures on the impingement plate to within  $\pm 0.25$  Pa. Pressure fluctuations were averaged over a one minute period.

Background: Wall Jet Measurement Procedure. Because mathematical models of wall jets produced by ceiling fans have not existed in the past and because a control case was needed, a model was developed for the simplest case, flow over a flat floor. Velocity profiles of wall jets flowing over balloons were measured to test the hypothesis that wall jets exist when balloons are located in the flow area. In order to calculate the velocity of the air impinging upon the broilers, the velocity profiles of the wall jets were measured three centimeters in front of balloons with and without paper cylinders. The paper cylinders simulated broiler necks and heads and are hereafter called paper necks. The anemometer probe was positioned with the use of a graduated radial line on the floor, a plumb bob and a level.

Fans. Wall jet data was recorded for 91.5, 83.8 and 71.1 cm radius three-bladed fans that were rated at 220, 160, and 108 W, respectively. Fan radii were measured within  $\pm 2$  mm. The fans were suspended  $2.438 \pm 0.005$  m above the floor. A constant voltage transformer was used to maintain constant fan speed within  $\pm 5$  rpm during the experiments. A speed controller was used to vary the fan speed because four fan speeds were used. To minimize the possibility of fan speed fluctuations, the fans were operated at least one hour before velocities were recorded.

Wall Jet Measurements and Balloon Orientation. Designing for the maximum flow resistance is especially important because of possible broiler mortality due to heat stress. The wall jets were measured perpendicular to the line of balloons to obtain the maximum flow resistance (Figure 9). Managerial decisions should be based on the maximum flow resistance because broilers are expected to be randomly spaced.

Wall Jet Flowing Over Smooth Floor. The control case of flow over a smooth floor (Figure 10) was needed to observe the flow resistance due to balloons with and without paper necks. The velocity measurements were recorded for 1) radial distances between 175 and 625 cm and 2) heights above the floor (Y) between 0.1 and 80 cm.

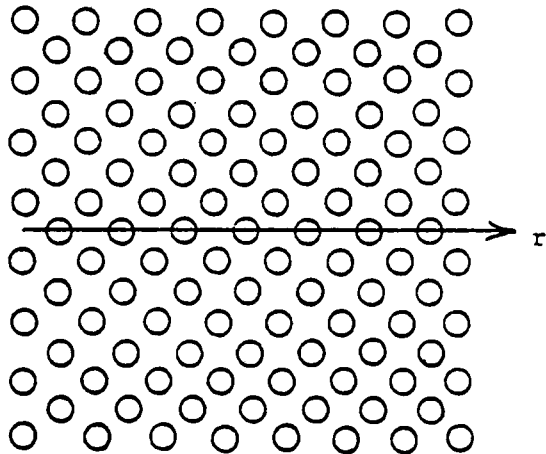


FIGURE 9. ORIENTATION OF WALL JET MEASUREMENTS WITH RESPECT TO BALLOONS.

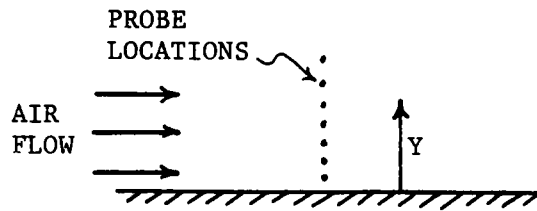


FIGURE 10. PROBE LOCATIONS ABOVE THE  
SMOOTH FLOOR.

Wall Jet Flowing Over Broilers with Necks Down. Water-filled balloons were used to physically model broilers in a restful state, sitting with necks down (Figure 11). Broilers are expected to spread out when ceiling fans are properly spaced, but they are expected to favor the floor areas where the higher velocities exist. The broilers are not expected to distribute themselves evenly along the floor. The spacing of evenly distributed broilers is approximately  $0.074 \text{ m}^2/\text{broiler}$ . Therefore, the wall jet model was developed for a uniform balloon spacing of  $0.061$  to  $0.063 \text{ m}^2/\text{balloon}$  over an area of  $19 \text{ m}^2$  (Figure 12).

The wall jet model was developed as a managerial tool to reduce broiler heat stress when broilers are most valuable, which is when they are sold at an age of approximately six weeks. Also, model development was based on six week old broilers because susceptibility to heat stress increases with broiler size. Balloon height averaged 11 cm, as given by ASAE Standard Data D321.1 (1984) for the average sitting height of six week old broilers (Figure 13).

The first experiment with the balloons involved measuring the velocity of the wall jet on the top of the balloons (Figure 13) and determining whether the wall jet was predictable. After learning that the wall jet on top of the balloon was predictable, the wall jet velocities were measured 3 cm in front of the balloon because the broiler growth model, described in the section "Background: Weight Gain of Heat Stress Broilers", predicts weight gain as a function of the average velocity impinging the broiler. The velocity of the wall jet

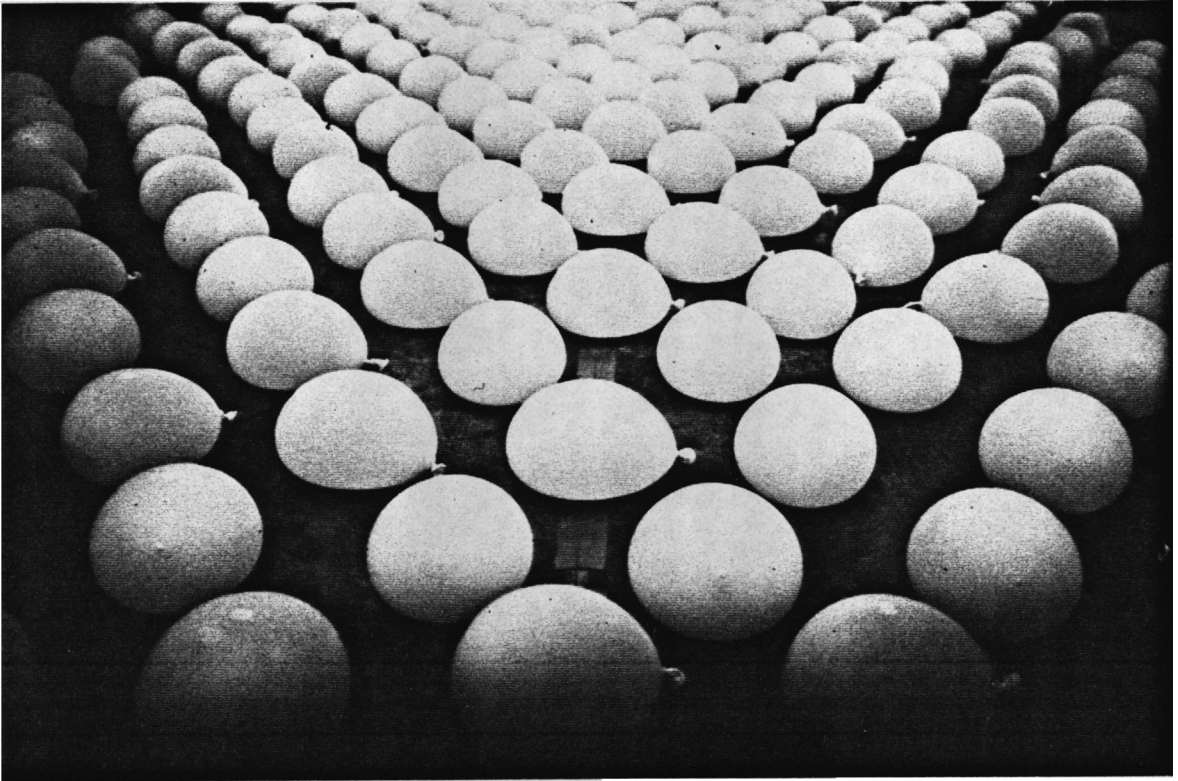


FIGURE 11. WATER BALLOONS USED TO PHYSICALLY MODEL BROILERS  
SITTING WITH NECKS DOWN.



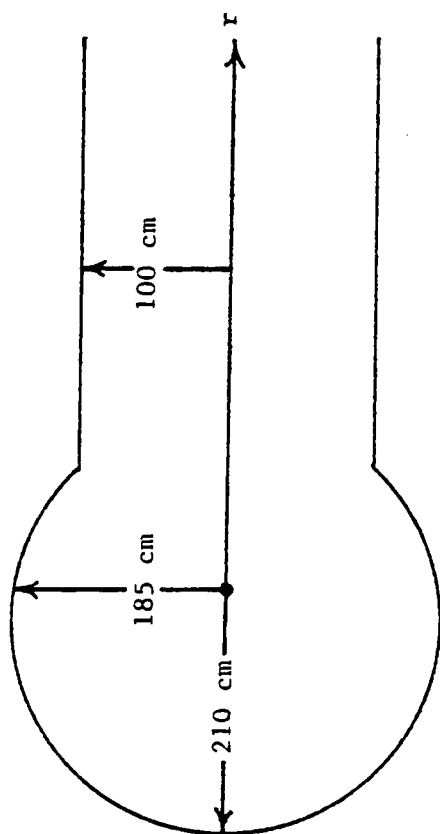


FIGURE 12. SHAPE AND SIZE OF THE FLOOR SPACE WHERE THE BALLOONS WERE LOCATED.

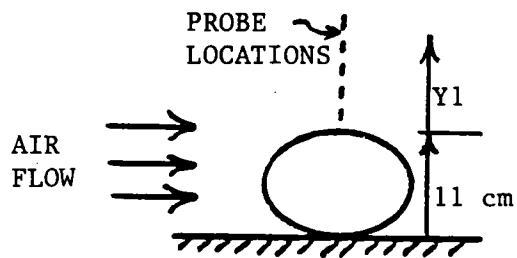


FIGURE 13. PROBE LOCATIONS OVER THE TOP OF THE BALLOONS.

was then averaged over the height of the broilers and used to predict weight gain. The velocity measurements were recorded for 1) radial distances between 155 and 441 cm and 2) heights above the balloons (Y1) between 0.1 and 70 cm.

The velocities of the wall jet were then measured 3 cm in front of a balloon at a radial distance from the fan centerline of 286.5 cm and at heights from the floor between 2 and 60 cm (Figure 14). The wall jet, measured 3 cm in front of the balloons, was the same wall jet that was previously measured on top of the balloons, hence, the decay of the maximum velocity was approximately the same for both cases. Also, the slope of the characteristic length line was equal for the top-of-the-balloon case and the front-of-the-balloon case.

Wall Jet Flowing Over Broilers with Necks Up. Water filled balloons with paper necks were used to physically model broilers in the alert state, sitting with necks up (Figure 15). The average height of six week old broilers with necks up was estimated to be 16 cm (Figure 16) (Thaxton, 1984). The velocity measurements were recorded for 1) radial distances between 155 and 444 cm and 2) heights above the floor between 0.1 and 70 cm.

Wall Jet Sensitivity to Uniform Balloon Spacing. The sensitivity of the wall jet to balloon spacing was measured for balloon spacings between 0.061 and 0.074 m<sup>2</sup> per balloon which is the largest uniform broiler spacing that is expected. Broiler houses are typically popu-

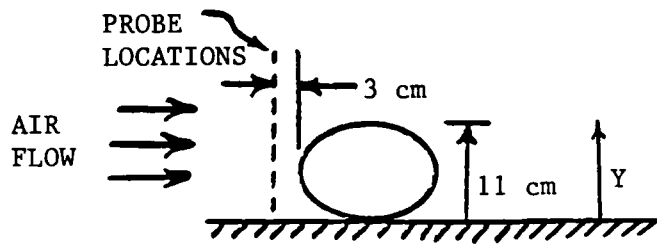


FIGURE 14. PROBE LOCATIONS 3 CM IN FRONT OF THE BALLOONS.



FIGURE 15. WATER BALLOONS WITH PAPER NECKS USED TO PHYSICALLY MODEL BROILERS SITTING WITH NECKS UP.

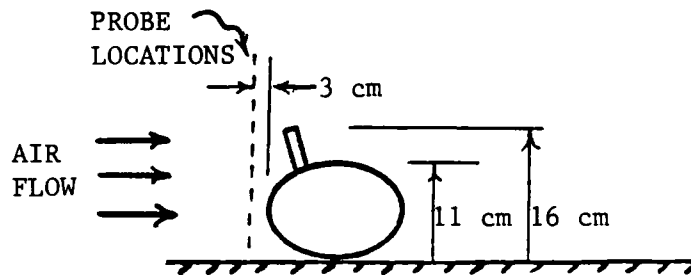


FIGURE 16. PROBE LOCATIONS 3 CM IN FRONT OF THE BALLOONS WITH NECKS.

lated so that if the broilers are evenly spaced along the floor, the broiler spacing is  $0.074 \text{ m}^2$  per broiler.

#### Wall Jet Sensitivity to Large Gaps Between Groups of Balloons.

Large groups of broilers often move and sit together in groups within a broiler house. Because of this group behavior, wall jet velocities are affected by the relatively large gaps between groups. In order to estimate the sensitivity of the wall jet to large gaps between groups of broilers, wall jet velocities were measured for a 30 and 65 cm gap spacing between groups of balloons with necks (Figure 17).

Characteristic Velocity. Characteristic velocity and fan diameter were used to correlate the ceiling fans to the wall jet velocity. The characteristic velocity was defined as the maximum velocity of the annular free jet located a distance of 30 cm below the fan blades. The distance below the blades was chosen to reduce errors due to 1) vortices near the blades and 2) periodic, maximum, momentum fluxes that cause anemometer probes to vibrate. Also, the distance between the blades was less than one-fourth of the fan diameter to ensure against turbulence disturbance.

#### Instrumentation and Data Collection

Velocity Measurements. An anemometry system was used to obtain air velocity measurements. The system was a "Model 1053B Hot Wire Anemometer" and a "Model 1125 Calibrator" made by Thermo Systems Incorporated (TSI). The system included a power supply, a constant

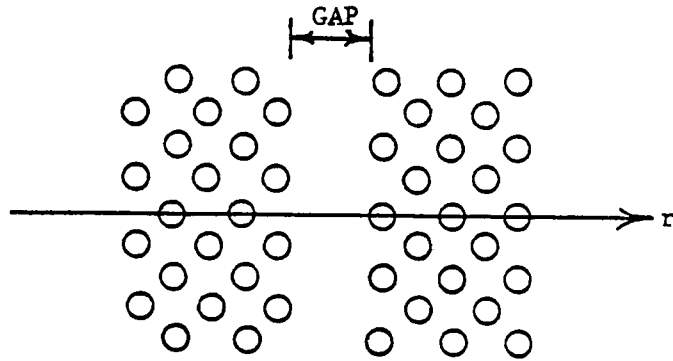


FIGURE 17. ORIENTATION OF WALL JET MEASUREMENTS WITH RESPECT TO A GAP PRODUCED BY MISSING ROWS OF BALLOONS.



temperature anemometer, a variable resistance decade, a polynomial linearizer and a metal clad sensor for low frequency (less than 10 Hz) measurements. The anemometer probe and sensor assembly was calibrated by using an air pressure source, a micromanometer and a calibrator. The calibrator included an air flow regulator, a heat exchanger and a wind chamber-nozzle assembly. The anemometer was calibrated within  $\pm 3\%$  of the true velocities.

A digital voltmeter with an integrating function was used to monitor the output voltage from the linearizer. Voltages were continuously integrated over 100 second intervals for 10 to 15 minutes. Mean velocity values were calculated by averaging the maximum and the minimum velocity values displayed over the 10 to 15 minute period. The fluctuating velocity values were assumed to be symmetrically distributed about the mean velocity (Tennekes and Lumley, 1977).

Psychrometric Properties of Air. The air velocities were corrected for air temperature and density because the anemometer was calibrated at a constant temperature and density. A motorized psychrometer was used to measure dry-bulb and wet-bulb temperatures. A psychrometric sub-routine was used to calculate air density (Wilhelm, 1976).

The calibration of the mercury thermometers in the psychrometer were checked by comparing the temperature reading of the thermometers to the readings from a K-type thermocouple. The readings from the two instruments were within  $\pm 0.6^{\circ}\text{C}$  in the range 0 to  $35^{\circ}\text{C}$ .

## Data Processing

Temperature Compensation of Velocity Data. Temperature compensation of velocity data was required because the rate of heat transfer from the anemometer sensor varied with the air temperature and air density. The bridge voltage was compensated with the following compensation factor

$$\frac{E_c}{E_e} = \left[ \frac{[A(T_s + T_c)^{0.76n + B_0}][((T_s + T_c)^{0.97 - 0.76n} / T_c^{0.17})(T_s - T_c)]}{[A(T_s + T_e)^{0.76n + B_0}][((T_s + T_e)^{0.97 - 0.76n} / T_e^{0.17})(T_s - T_e)]} \right]^{0.5} \quad (1)$$

where

$E_c$  = voltage through anemometer at calibration temperature ( $T_c$ )

$E_e$  = voltage through anemometer at environmental temperature ( $T_e$ )

$A$  = experimentally determined constant

$T_s$  = hot wire sensor temperature (K)

$T_c$  = calibration air temperature (K)

$T_e$  = environmental air temperature (K)

$n$  = experimentally determined exponent

$B_0$  = constant

Bowers (1982). Equation 1 is valid in the linear range of  $E^2$  vs  $(\rho V)^{\frac{1}{2}}$ . Most of the voltages ( $E$ ) and mass fluxes ( $\rho V$ ) were in the linear portion

of the calibration curve (Figure 18). No further temperature compensation was needed if  $Re > 44$ .

The influence of natural convection on heat transfer increased as  $\rho V$  decreased. Two algorithms were used to compensate for change in the effect of natural convection by decreasing the value of the compensation factor calculated with the use of equation 1. Both algorithms were developed from data reported by Bowers (1982). The first algorithm is proportional to the inverse of the slope of the  $E$  versus  $\rho V$  curve (Figure 19) and is expressed as

$$\left(\frac{E_c}{E_e}\right)_{NEW} = 1 + \left[\frac{E_c}{E_e} - 1\right] \left| 1 - \frac{(\partial(\rho V)/\partial E)_0}{\partial(\rho V)/\partial E} \right| \quad (2)$$

for  $Re \leq 44$  and  $E - E_0 \geq 1.875$

where

$(\partial(\rho V)/\partial E)_0$  = slope of the mass flux curve evaluated at zero flow

$\partial(\rho V)/\partial E$  = slope of the mass flux curve evaluated at  $E$

$E_0$  = voltage corresponding to zero flow

$E$  = voltage corresponding to a given flow

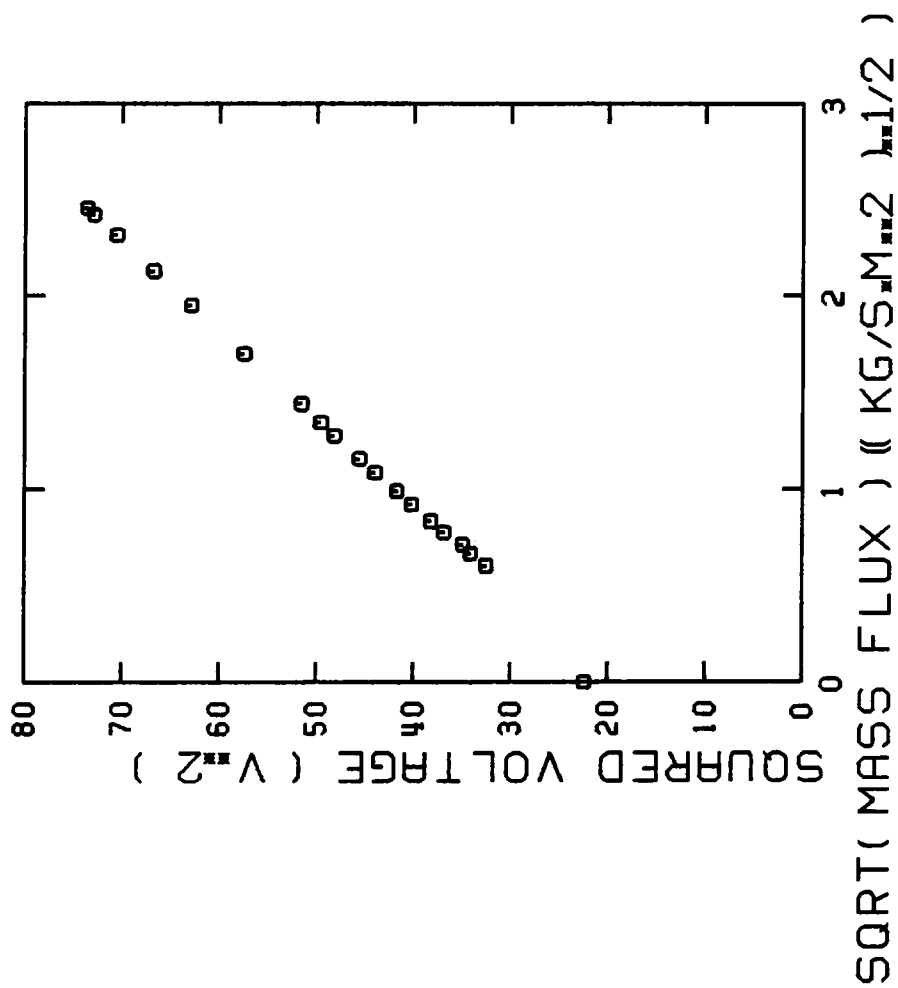


FIGURE 18. CALIBRATION CURVE FOR METAL CLAD SENSOR (MODEL 12667) OF MODEL 1053B HOT WIRE ANEMOMETER.

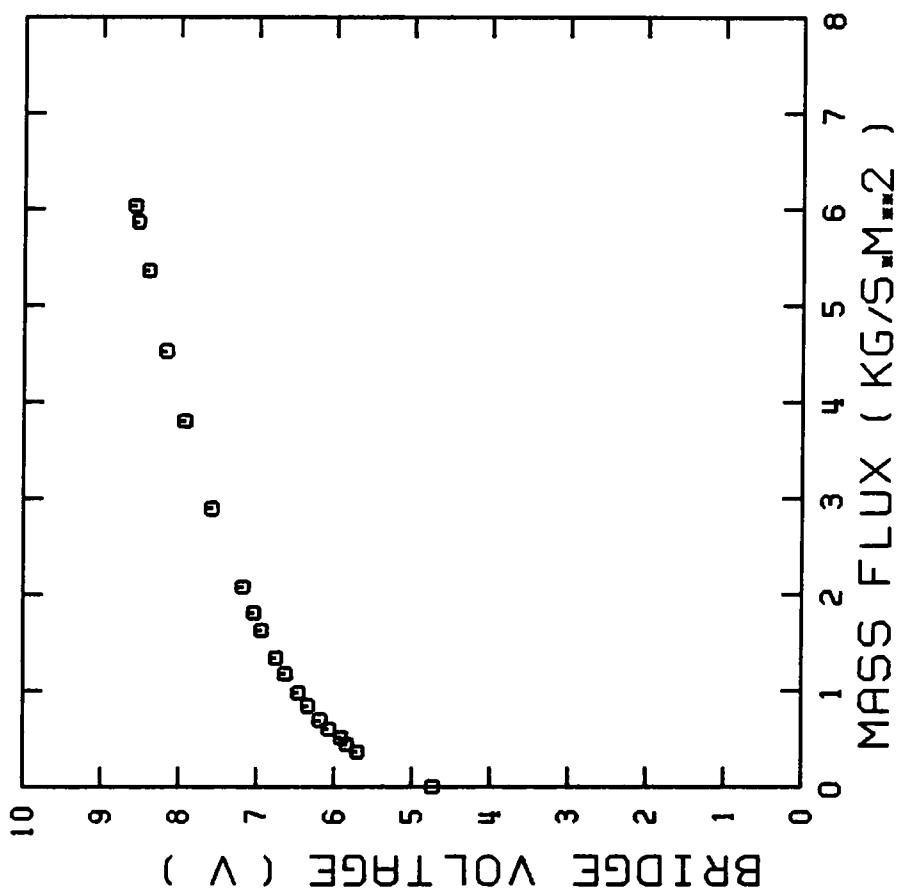


FIGURE 19. CALIBRATION CURVE FOR METAL CLAD SENSOR (MODEL 12667) OF MODEL 10538 HOT WIRE ANEMOMETER.

The second algorithm is expressed as

$$\left(\frac{E_c}{E_e}\right)_{NEW} = 1 + \left[\frac{E_c}{E_e} - 1\right] 0.2(E-E_0)^{1.80} \quad (3)$$

for  $E - E_0 \leq 1.875$ .

The compensated voltages were calculated by

$$E_c = E_e \left(\frac{E_c}{E_e}\right) \quad (4)$$

for  $Re > 44$

and

$$E_c = E_e \left(\frac{E_c}{E_e}\right)_{NEW} \quad (5)$$

for  $Re < 44$ .

The mass flux, during calibration, was calculated using the equation

$$(\rho V)_c = V_{TSI} \sqrt{\rho_c \rho_{TSI}} \quad (6)$$

where

$\rho V)_c$  = mass flux at calibration temperature

$V_{TSI}$  = velocity for standard temperature and pressure as given in the Thermo-System, Inc. (n.d.) manual (Figure 20)

$\rho_c$  = air density at calibration temperature

$\rho_{TSI}$  = air density for standard temperature and pressure as given in the Thermal-Systems, Inc. (n.d.) manual

Figure 20 was used with the TSI calibrator to determine  $V_{TSI}$  for a known pressure drop over the calibrator nozzle.

Calibration data (Figures 19 and 21) was used in conjunction with polynomial regression to develop equations of the form

$$E_e = K_1 + K_2 V_e + K_3 V_e^2 + K_4 V_e^3 + K_5 V_e^4 + K_6 V_e^5 \quad (7)$$

$$\rho V)_c = C_1 + C_2 E_c + C_3 E_c^2 + C_4 E_c^3 + C_5 E_c^4 + C_6 E_c^5 \quad (8)$$

where

$V_e$  = linearized voltage at environmental temperature ( $T_e$ )

$K_1, K_2 \dots K_6$  = coefficients

$C_1, C_2 \dots C_6$  = coefficients

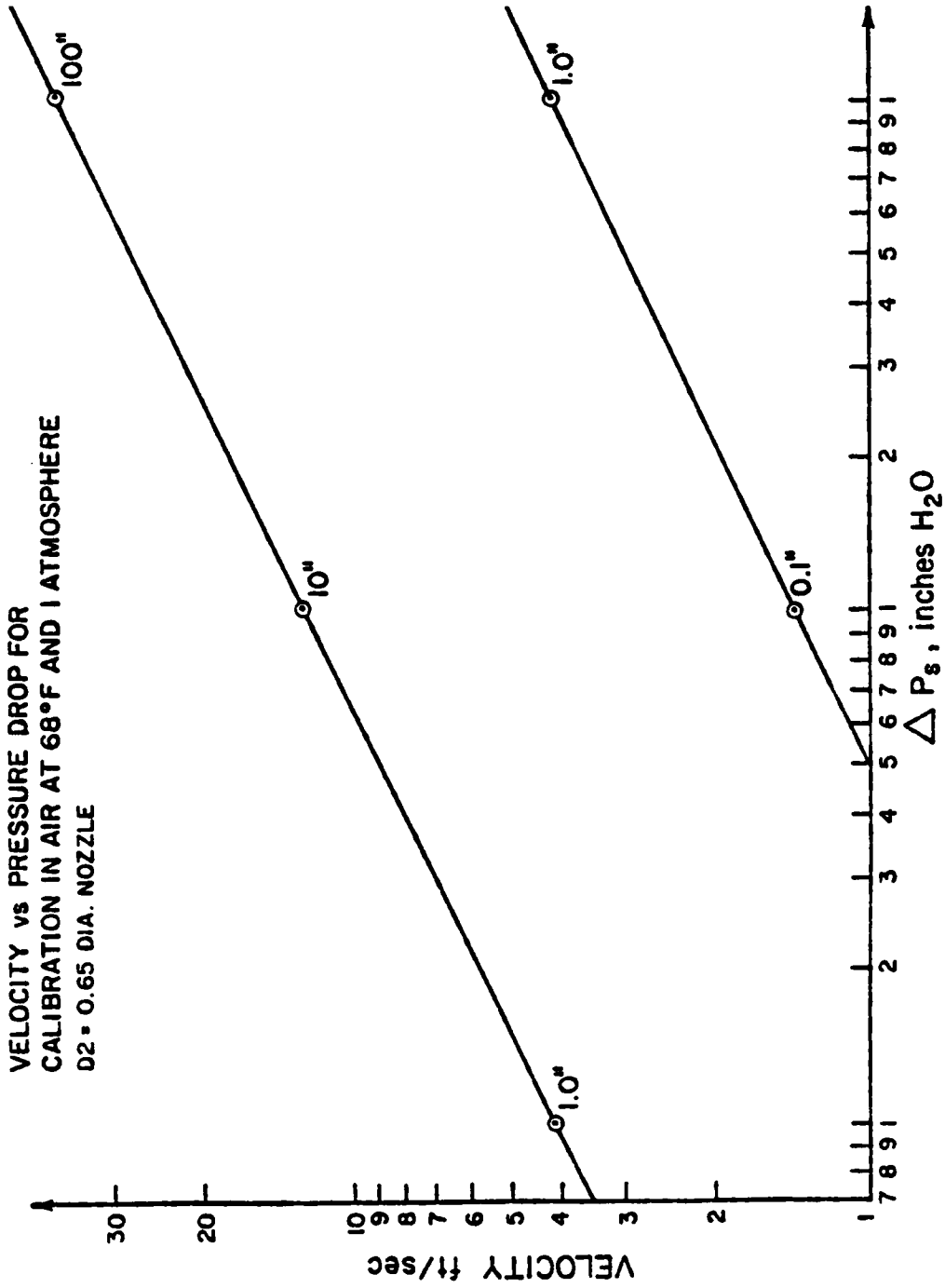


Figure 20. VELOCITY VERSUS PRESSURE DROP CURVES FOR WIND CHAMBER CALIBRATION OF SENSOR AT 68 F AND ONE ATMOSPHERE (THERMAL-SYSTEMS, INC.; n.d.).



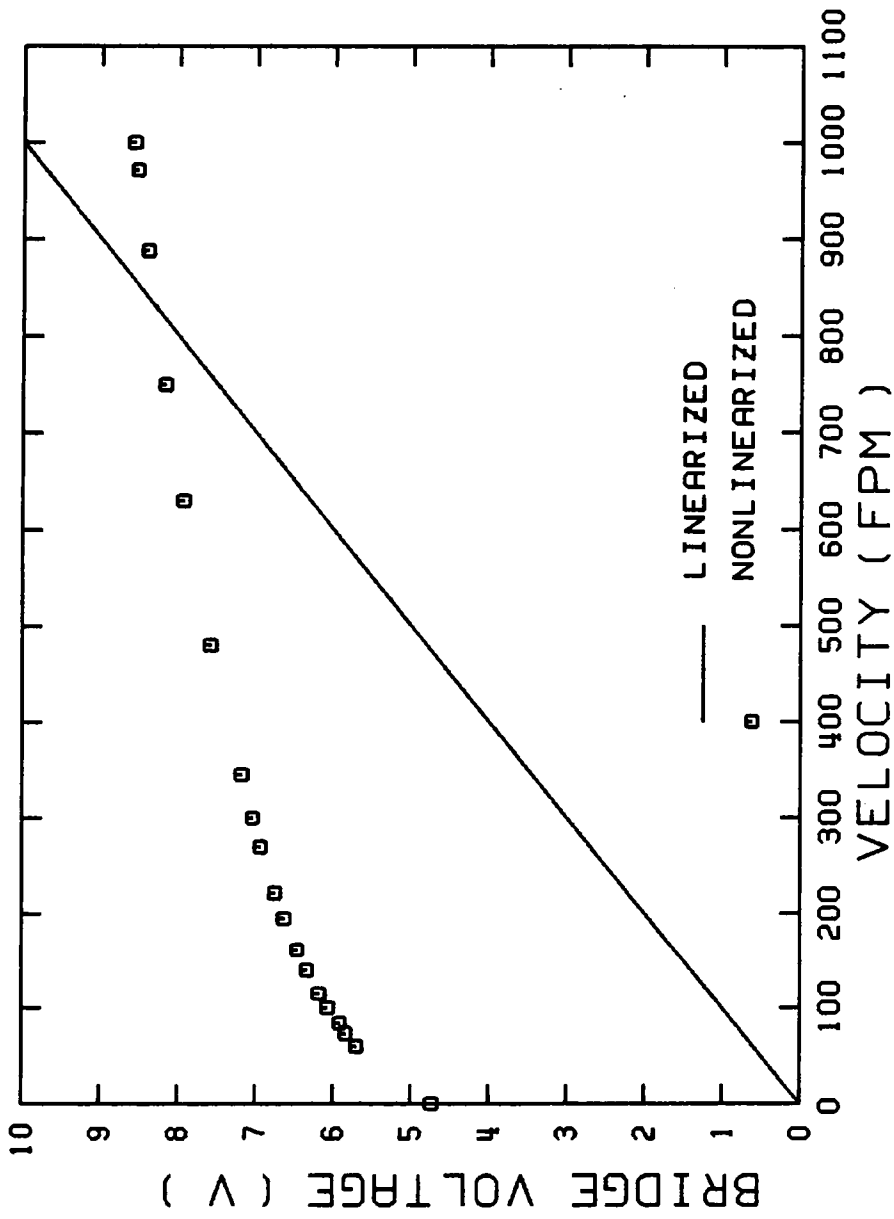


FIGURE 21. CALIBRATION CURVE FOR METAL CLAD SENSOR MODEL 12667 OF MODEL 1053B HOT WIRE ANEMOMETER.

The coefficients  $C_1, C_2 \dots C_6$  were calculated with a multiple linear regression model of the Statistical Analysis System (SAS).

Temperature and density compensation was achieved by the following procedure:

1. Use the linearized voltage at environmental temperature ( $V_e$ ) and equation 7 to calculate the anemometer voltage at environmental temperature ( $E_e$ );
2. Use the anemometer voltage at environmental temperature ( $E_e$ ) and the compensation factor to calculate the compensated anemometer voltage. If  $Re > 44$ , use equation 1. If  $Re < 44$  and  $E - E_0 \geq 1.875$ , use equation 1 and 2. If  $Re < 44$  and  $E - E_0 < 1.875$  use equation 1 and 3;
3. Set the compensated anemometer voltage equal to the calibration anemometer voltage ( $E_c$ ) because the compensated voltage is approximately equal to the anemometer voltage that would have been produced if the environmental air temperature ( $T_e$ ) during the wall jet velocity measurements had been equal to the calibration air temperature ( $T_c$ );
4. Use the compensated anemometer voltage ( $E_c$ ) and equation 8 to calculate the compensated mass flux  $(\rho V)_c$  and
5. Use the air density at environmental temperature and the compensated mass flux  $(\rho V)_c$  to calculate the compensated air velocity.

The temperature compensation method predicted the data reported by Bowers (1982) within 2.5 to 6% (Figure 22). Figure 23 illustrates a compensated and uncompensated velocity profile. The velocity corrections were between 0 to 32% of the corrected velocities.

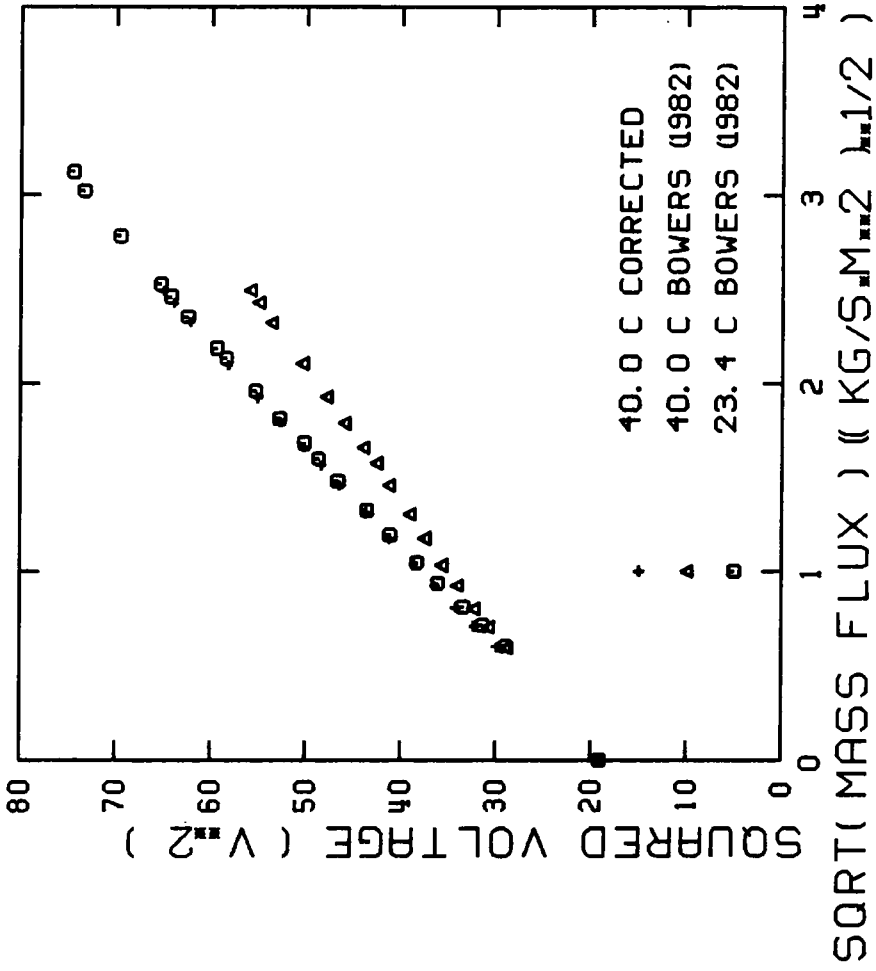


FIGURE 22. COMPARISON OF KNOWN AND CORRECTED MASS FLUX.

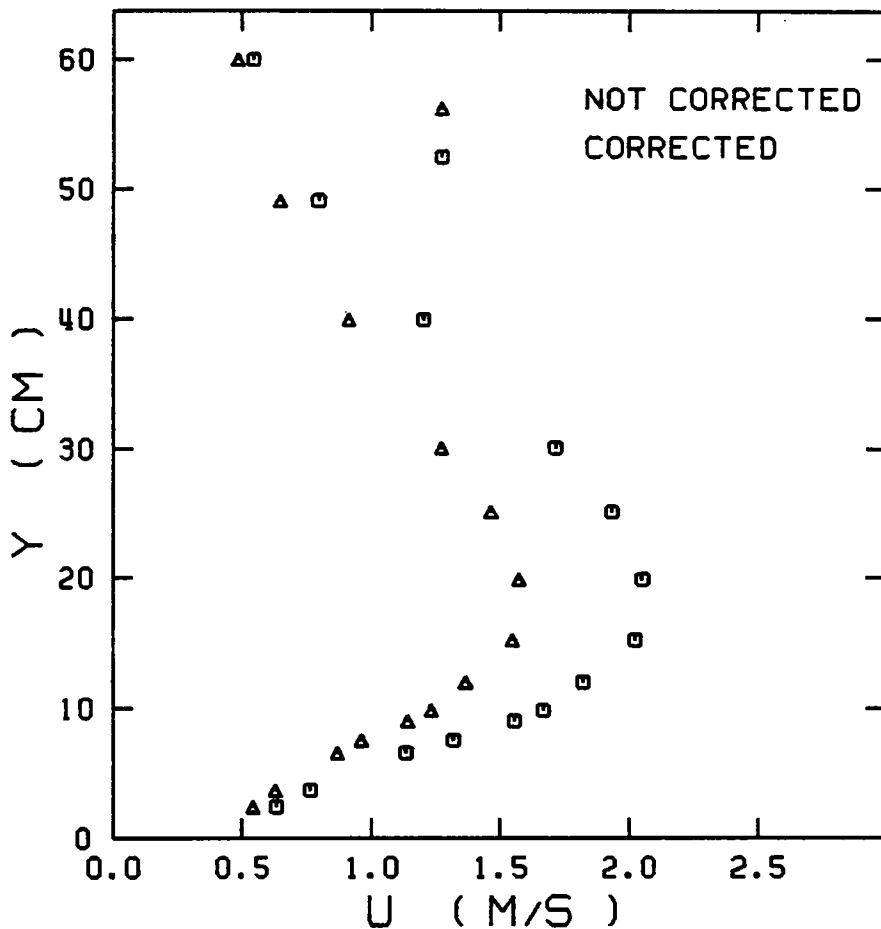


FIGURE 23. CORRECTED AND UNCORRECTED VELOCITY PROFILES OF A WALL JET AT A RADIAL DISTANCE OF 286.5 CM, MEASURED 3 CM IN FRONT OF A BALLOON AND PRODUCED BY THE 91.5 CM RADIUS FAN OPERATING AT A CHARACTERISTIC VELOCITY OF 4.922 M/S.

## CHAPTER VI

### EXPERIMENTAL RESULTS AND MODEL DEVELOPMENT

To develop a wall jet model, experimental data was required for the stagnation ring, the characteristic velocity and the air flow over broilers simulated by balloons. The wall jet model was developed so that the fan centerline corresponded to a radius equal to zero, however, the origin of the wall jet is defined as the stagnation ring. The characteristic velocity was required to correlate the wall jet with fan speed, fan diameter and blade design.

#### Stagnation Ring

The stagnation ring is defined to be the circle of maximum pressure produced on the floor by the annular free jet. The radius of the stagnation ring (Figure 24) was required to calculate the distance the wall jet had traveled. The portion of the free jet impinging on the outside of the stagnation ring produced a wall jet that flowed radially outward. The portion of the free jet impinging on the inside of the stagnation ring produced a wall jet that flowed radially inward. Also, the radius of the impingement region (Figure 24) was required to estimate the radius where wall jet acceleration ceased and where wall jet development began.

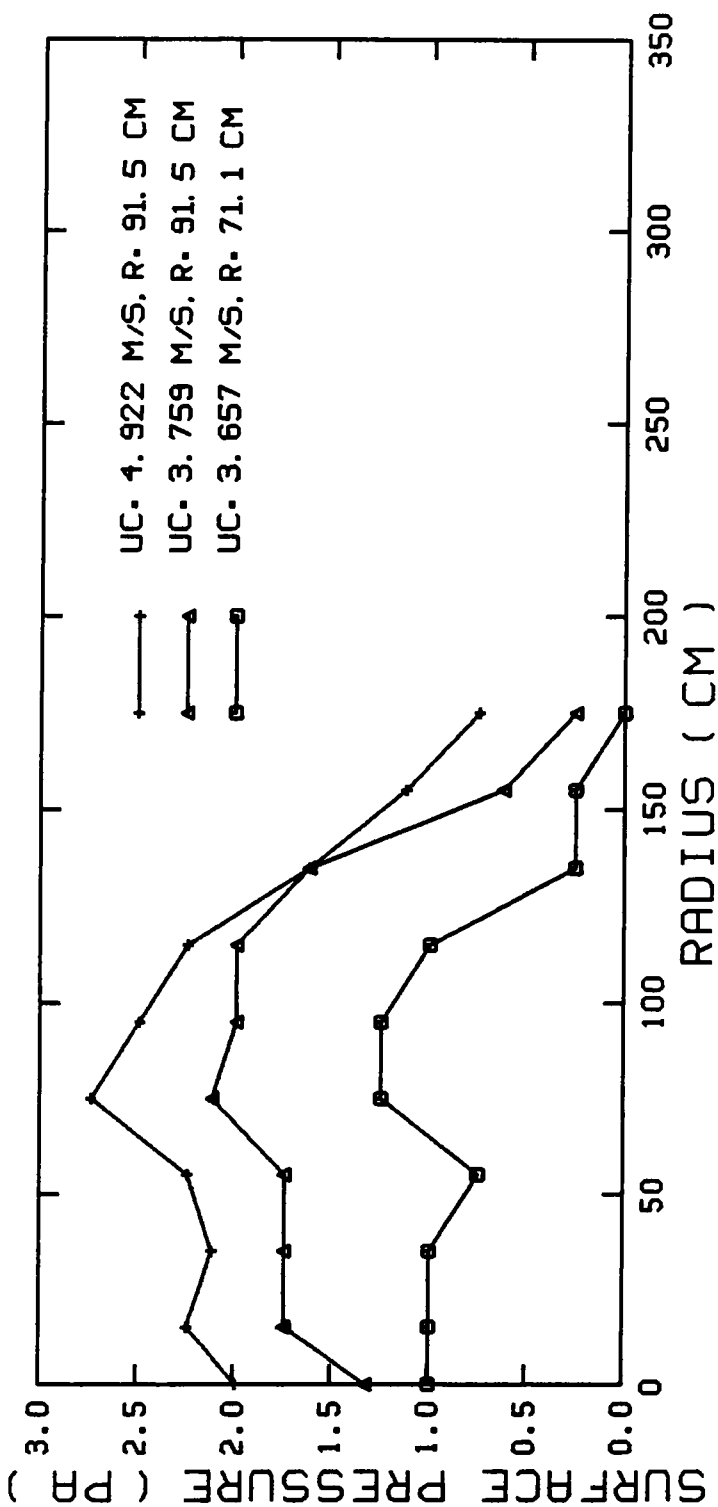


FIGURE 24. SURFACE PRESSURE ON A SMOOTH FLOOR AT VARYING RADIAL DISTANCES FROM THE FAN CENTERLINE AND WITH A FAN HEIGHT OF 2.44 M.

The radii of the stagnation rings produced by the large diameter fan operating at characteristic velocities of 4.922 and 4.074 m/s were approximately equal. Also, the radius of the stagnation ring produced by the large diameter fan operating at a characteristic velocity of 4.922 m/s was approximately equal to the radius of the stagnation ring produced by the small diameter fan operating at a characteristic velocity of 3.657 m/s. Precise differences in the stagnation ring were difficult to measure because the pressure profile produced by the small diameter fan was blunter than the pressure profile produced by the large diameter fan (Figure 24). Hence, the origin of the wall jets was approximately the same for varying fan diameters.

### Characteristic Velocity

Four characteristic velocities and the corresponding velocity profiles were measured for each of the three ceiling fans (Figure 25, 26, and 27).

### Wall Jet Model: Smooth Floor

Velocity profiles of radial wall jets flowing over a smooth floor were recorded (Figure 28). Fully developed velocity profiles were similar (Figure 29). The velocity profiles were approximately the same as the plane and radial wall jet profiles reported by Rajaratnam (1976).

Linear relationships existed between the inverse of the maximum velocity and the radial distance of the wall jet (Figure 30 and 31).

Although the linear relationships varied with velocity, the



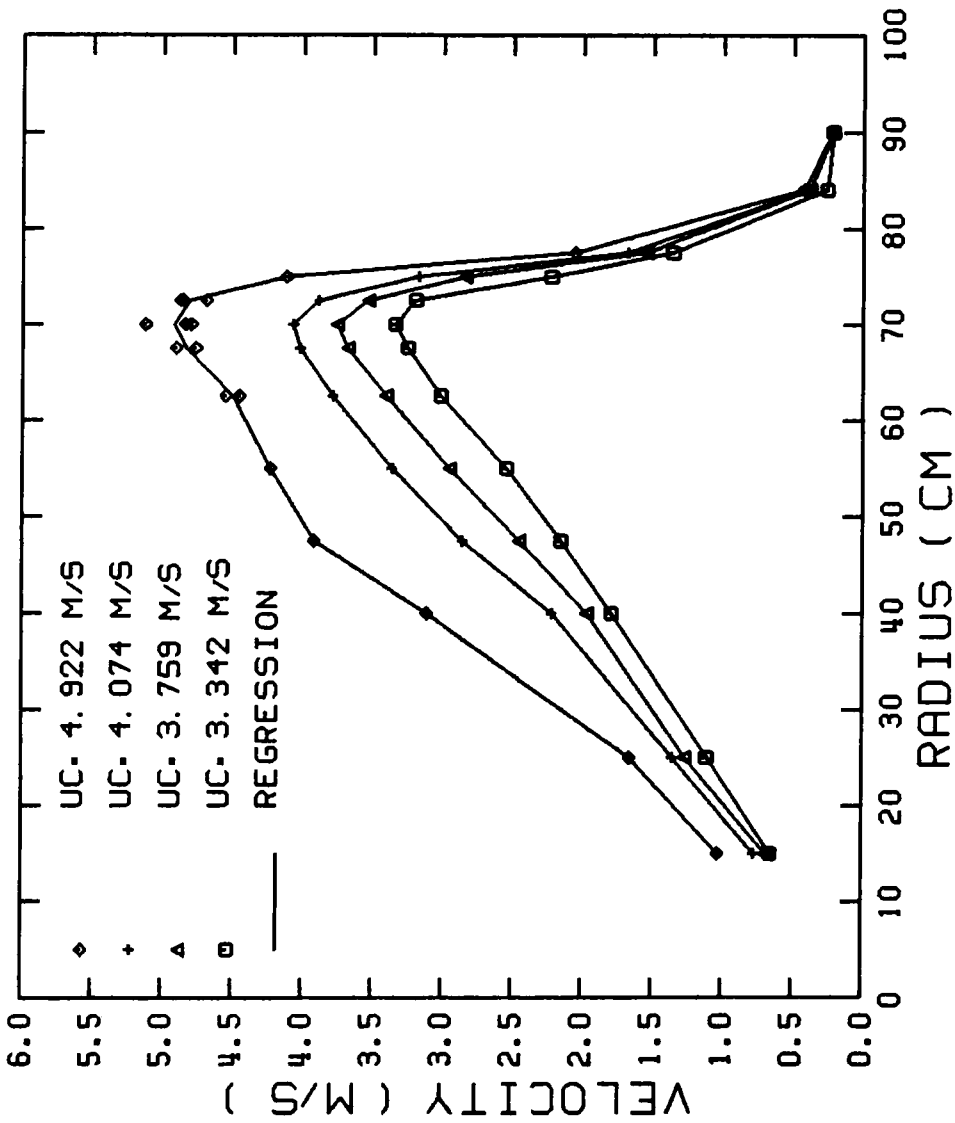


FIGURE 25. ANNULAR FREE JET, 30 CM BELOW THE BLADES, PRODUCED BY THE 91.5 CM RADIUS FAN OPERATING AT FOUR CHARACTERISTIC VELOCITIES.

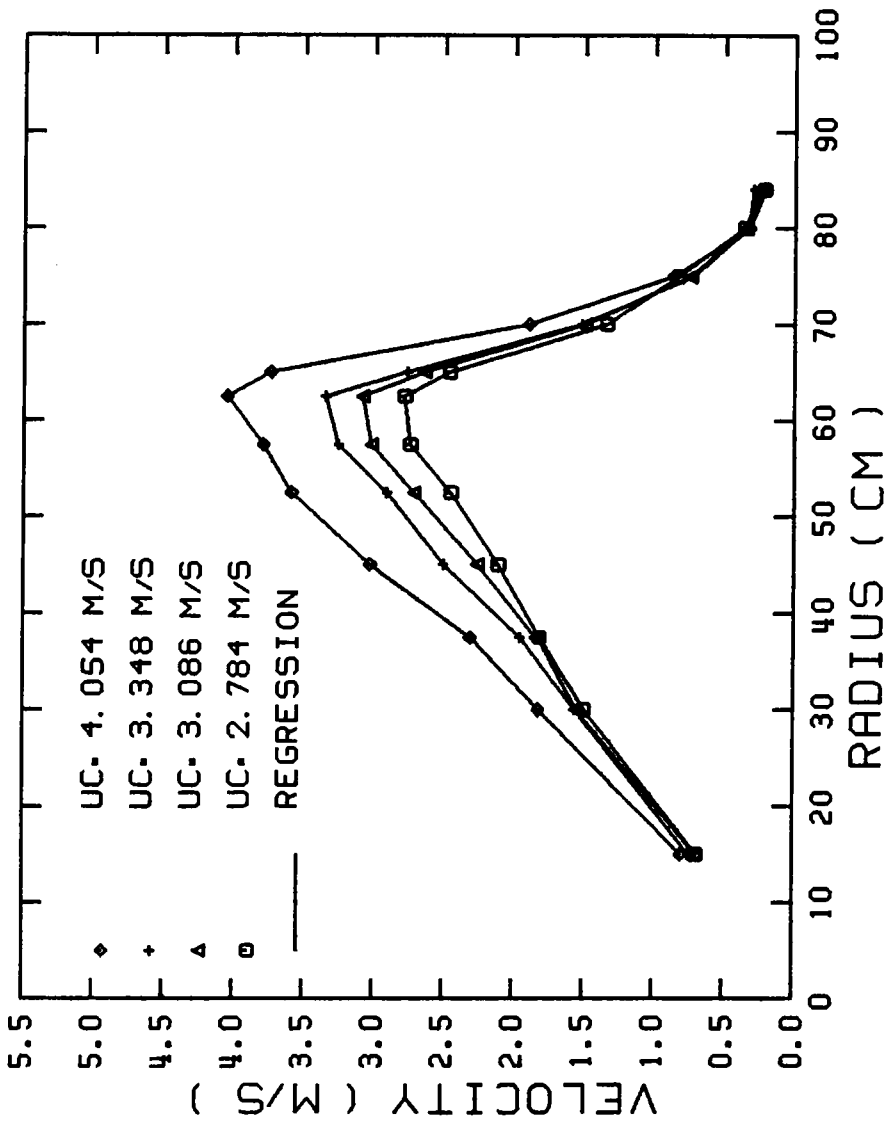


FIGURE 26. ANNULAR FREE JET 30 CM BELOW THE BLADES. PRODUCED BY THE 83.8 CM RADIUS FAN OPERATING AT FOUR CHARACTERISTIC VELOCITIES.

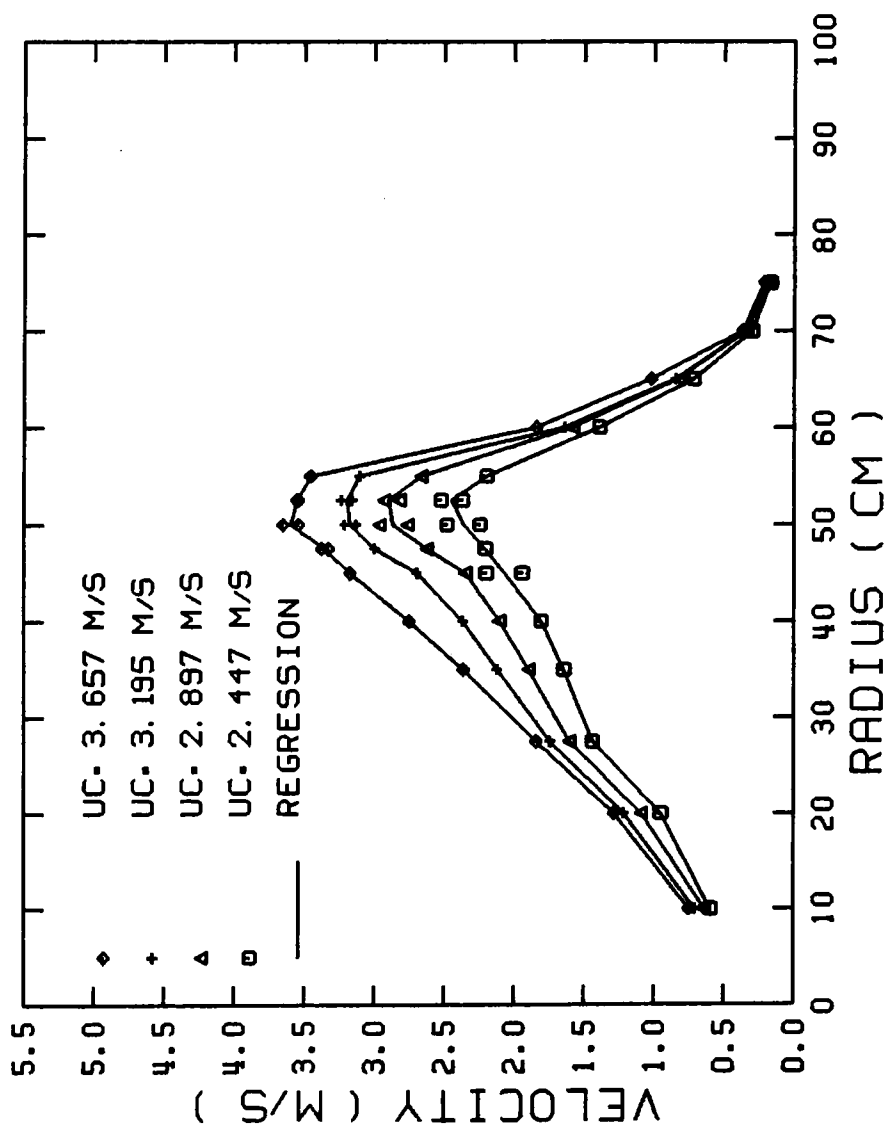


FIGURE 27. ANNULAR FREE JET, 30 CM BELOW THE BLADES, PRODUCED BY THE 71.1 CM RADIUS FAN OPERATING AT FOUR CHARACTERISTIC VELOCITIES.

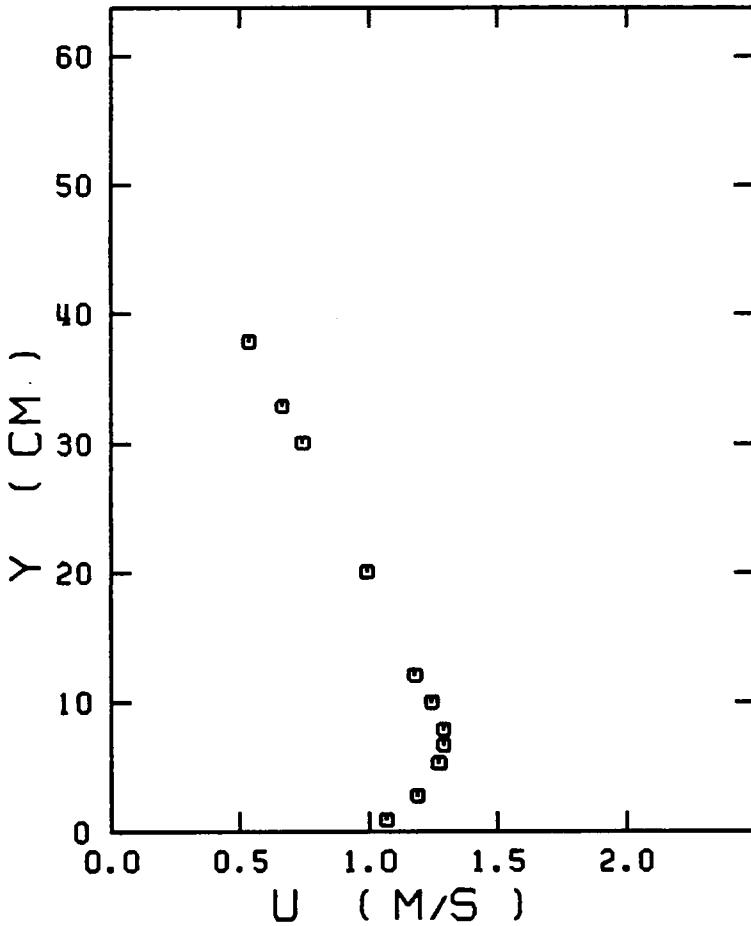


FIGURE 28. VELOCITY PROFILE OF A WALL JET AT A RADIUS OF 337 CM FLOWING OVER A SMOOTH FLOOR AND PRODUCED BY A 83.8 CM RADIUS FAN OPERATING AT A CHARACTERISTIC VELOCITY OF 3.348 M/S.

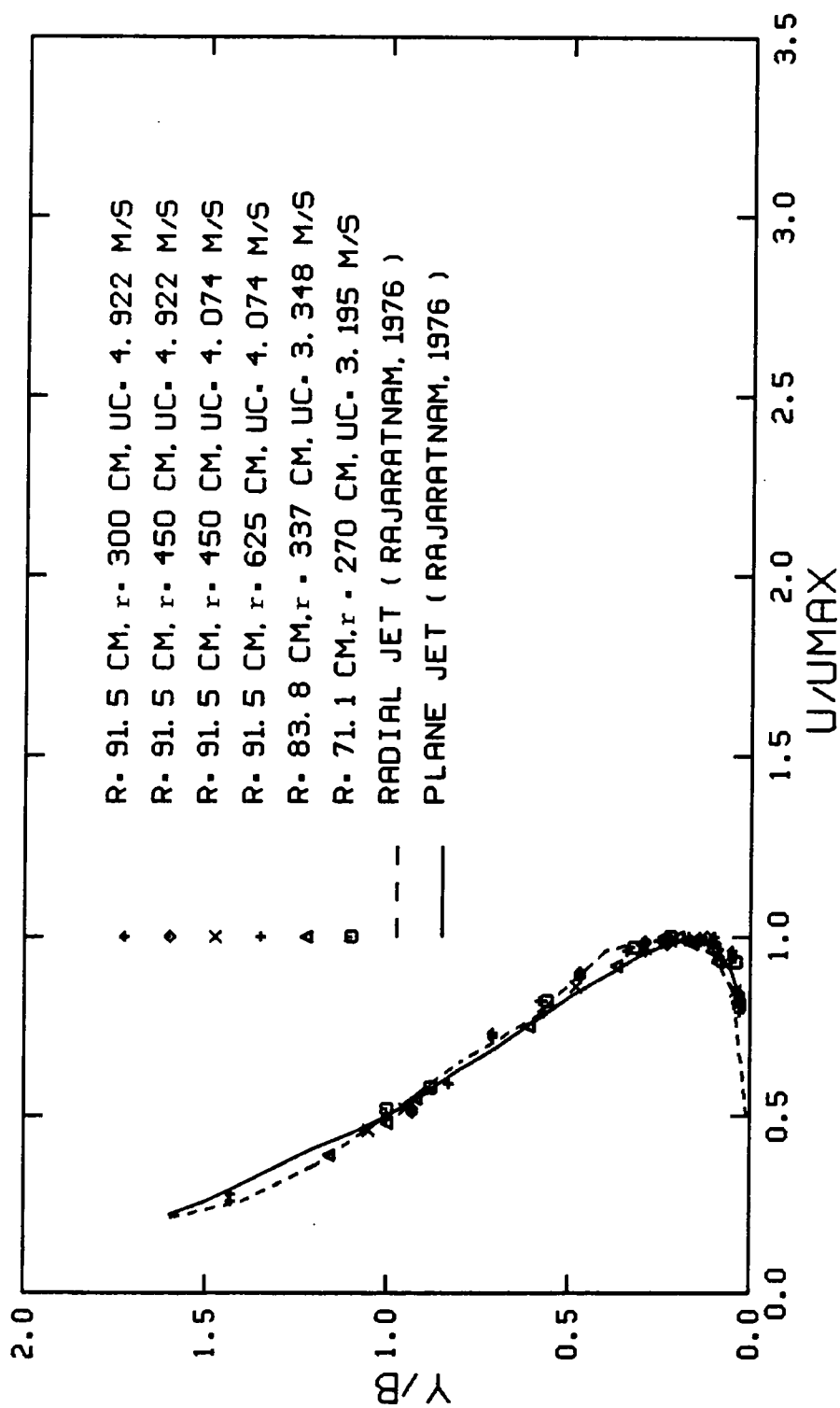


FIGURE 29. NONDIMENSIONAL VELOCITY PROFILES FOR WALL JETS FLOWING OVER A SMOOTH FLOOR.

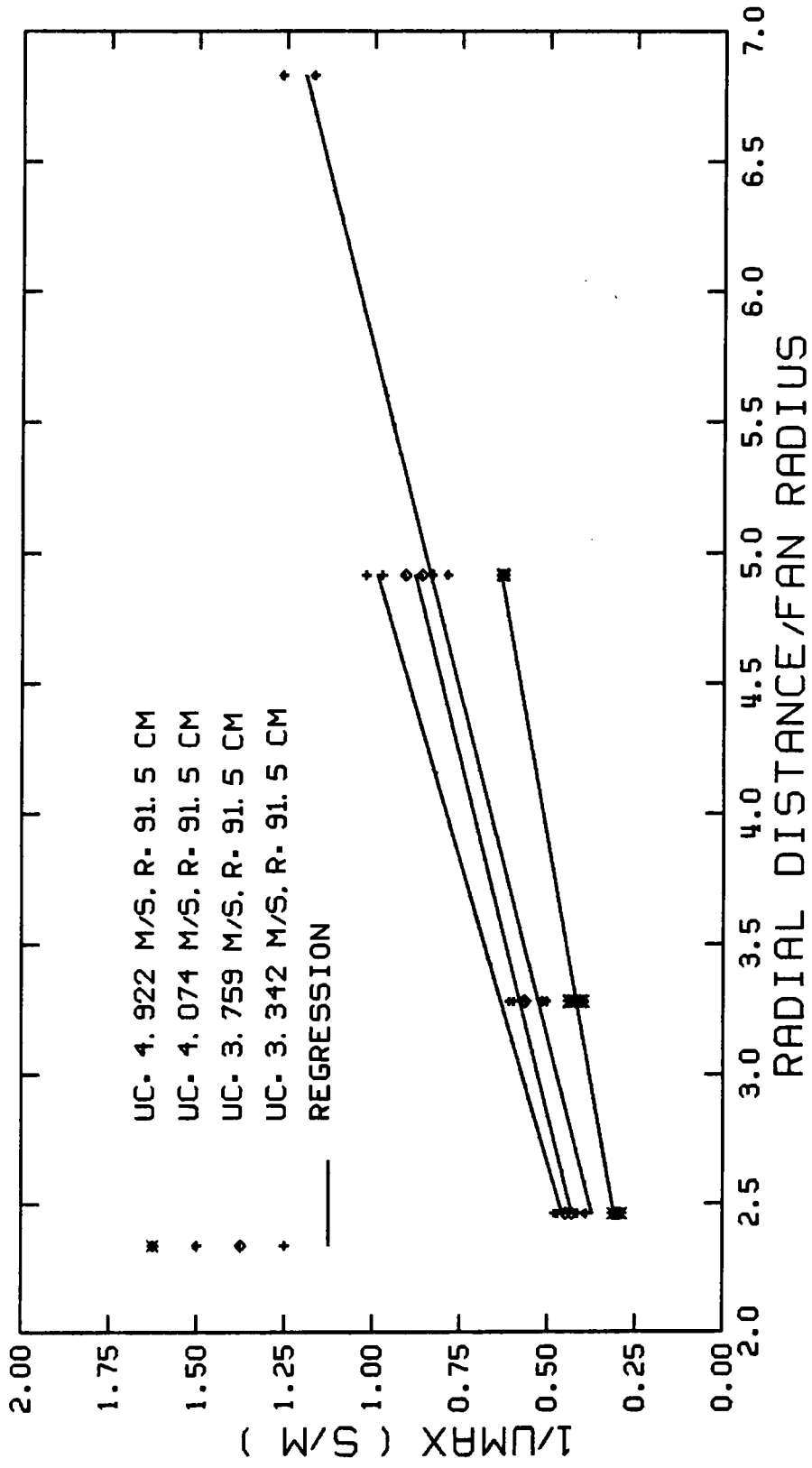


FIGURE 30. INVERSE OF THE MAXIMUM VELOCITY OF WALL JETS FLOWING OVER A SMOOTH FLOOR.

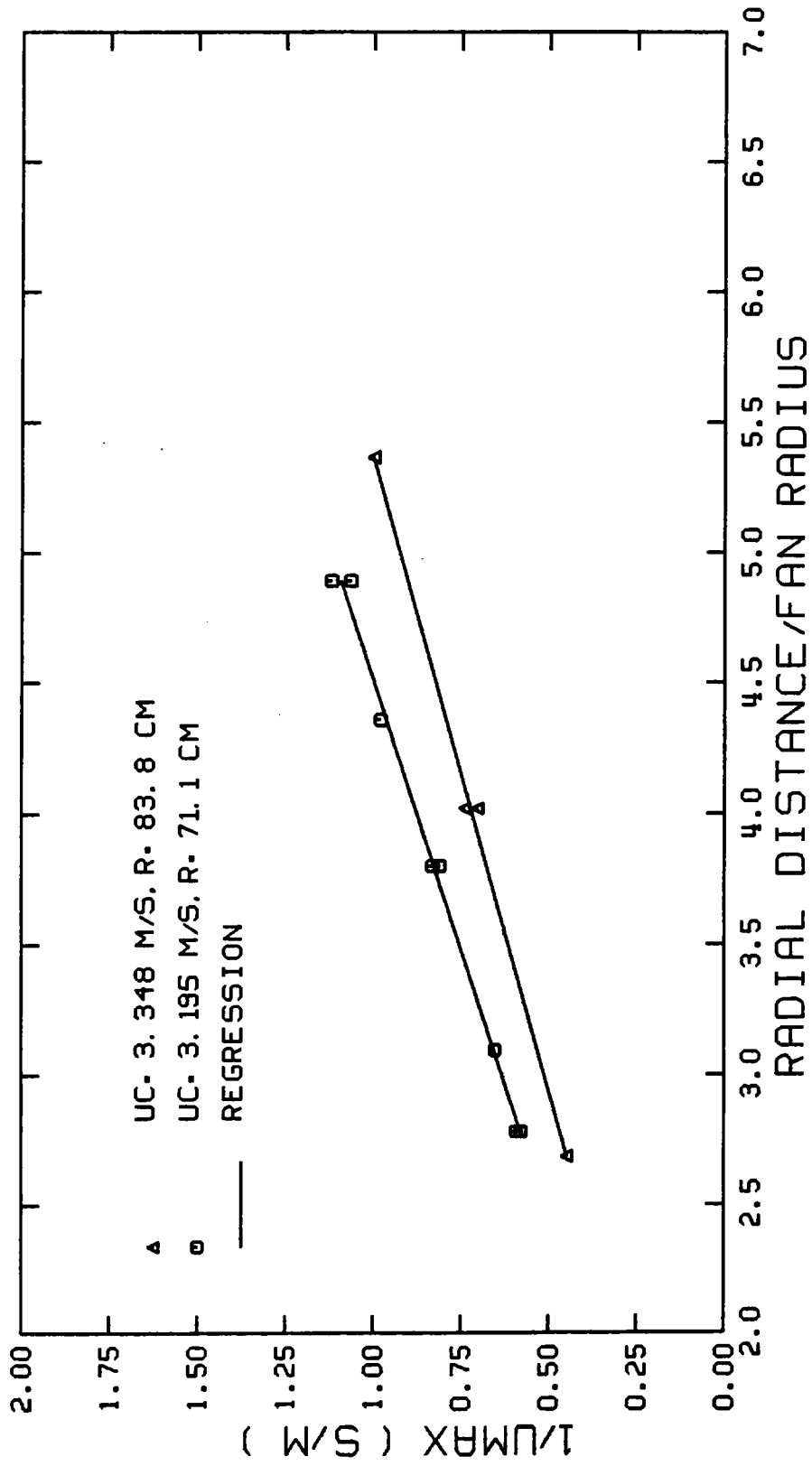


FIGURE 31. INVERSE OF THE MAXIMUM VELOCITY OF WALL JETS FLOWING OVER A SMOOTH FLOOR.

relationships were correlated to one line by using the characteristic velocities and the fan radii (Figure 32). The correlated nondimensional velocity data was expressed as

$$UC/UMAX = -0.3083 + 0.7438 (r/R) \quad (9)$$

$$2.459 \leq r/R \leq 6.831$$

where

UC = characteristic velocity (m/s)

UMAX = maximum velocity of the wall jet (m/s)

r = radial distance from the fan centerline (cm)

R = fan radius (cm).

The regression coefficient was 0.964. Also, the characteristic length was linearly related to the radial distance of the wall jet (Figure 33) and is expressed as

$$B = -0.9883 + 0.0973 r \quad (10)$$

for

$$270 \text{ cm} \leq r \leq 625 \text{ cm}$$



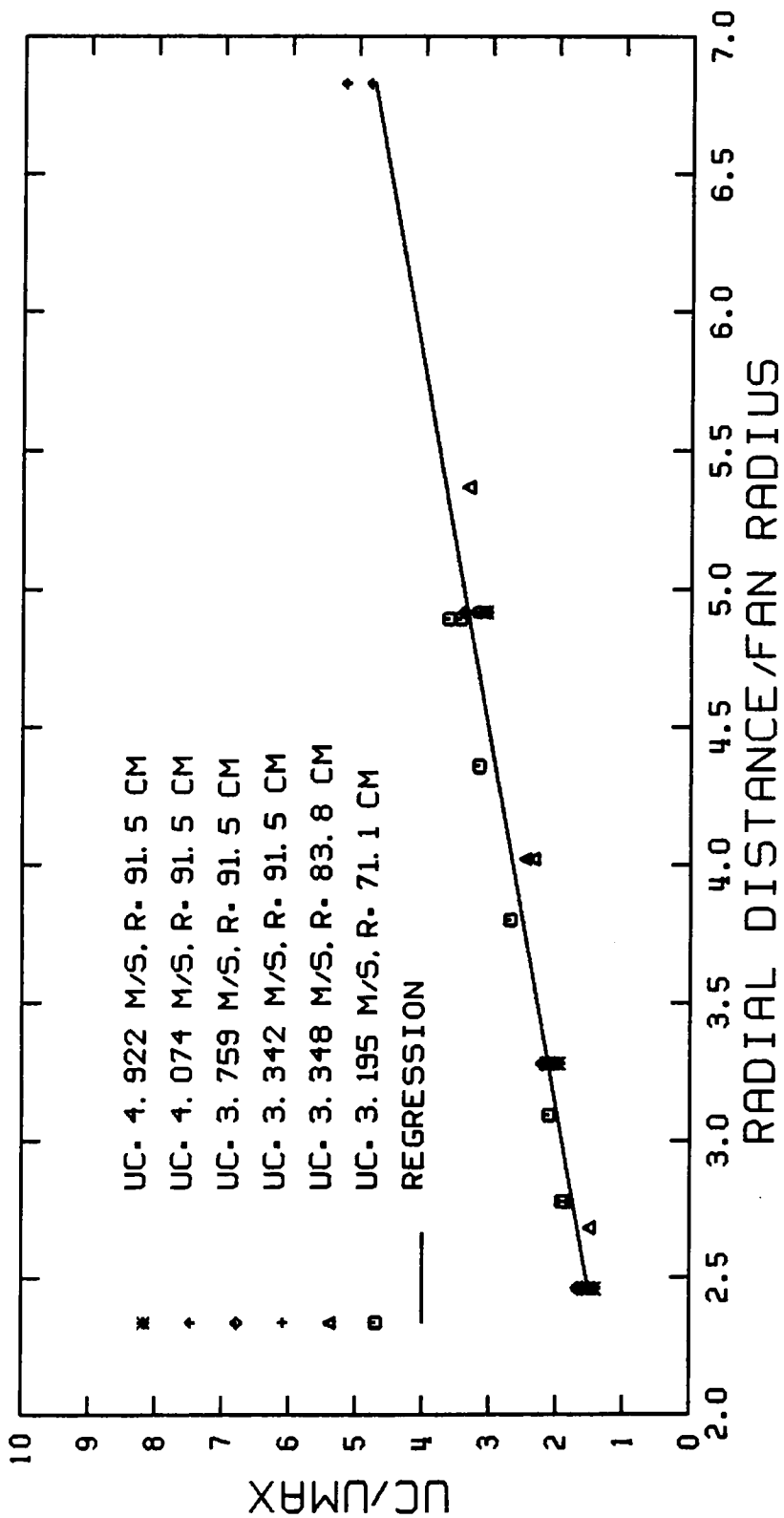


FIGURE 32. NONDIMENSIONIZED VELOCITY SCALE OF WALL JETS FLOWING OVER A SMOOTH FLOOR.

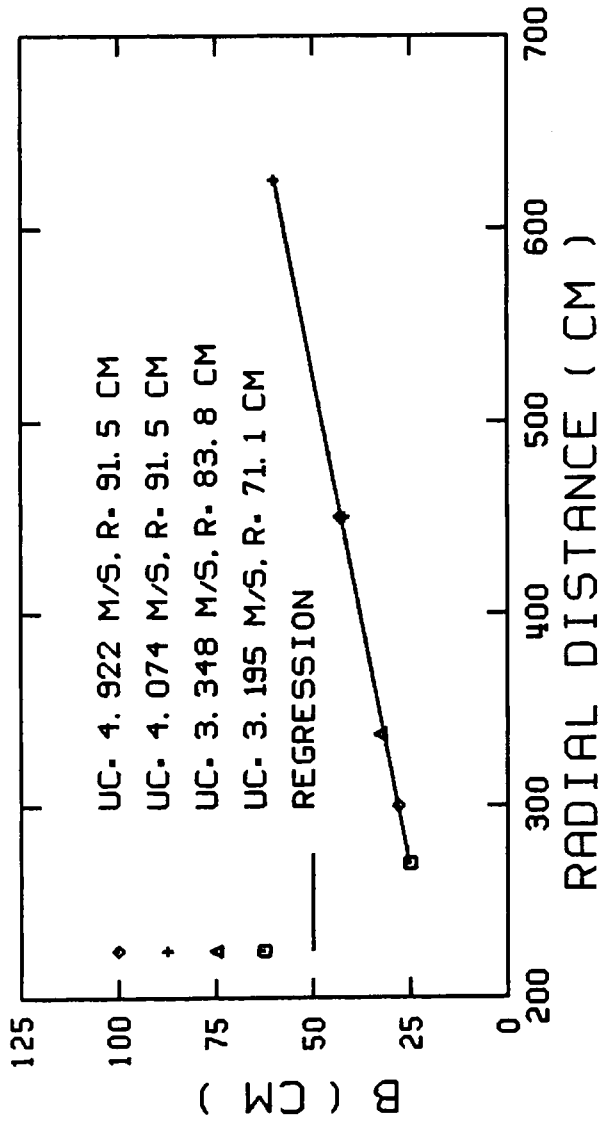


FIGURE 33. CHARACTERISTIC LENGTH OF WALL JETS FLOWING OVER A SMOOTH FLOOR.

where

B = characteristic length (cm)

The regression coefficient was 0.998.

Wall Jet Model: Broilers With Necks Down.

A well-defined, radial wall jet existed on top of the balloons (Figure 34). The fully developed velocity profiles were similar (Figure 35). Also, the velocity profiles were approximately the same as the radial wall jet profiles reported by Rajaratnam (1976).

Linear relationships existed between the inverse of the maximum velocity and the radial distance of the wall jet (Figure 36). The negative slopes in Figure 26 illustrate the acceleration of the wall jet. The correlated nondimensional velocity data (Figure 37) was expressed as

$$UC/UMAX = - 0.5465 + 1.0436 (r/R) \quad (11)$$

$$1.574 \leq r/R \leq 4.820$$

The regression coefficient value was 0.956.

Also, a linear relationship existed between the characteristic length and the radial distance of the wall jet (Figure 38). The relationship was

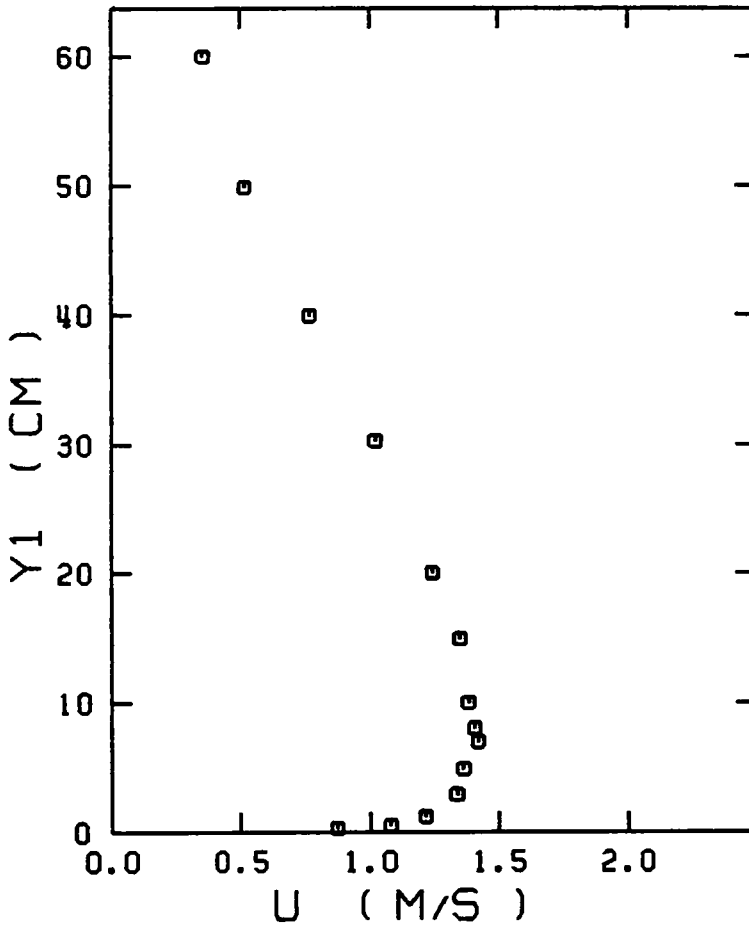


FIGURE 34. VELOCITY PROFILE OF A WALL JET AT A RADIUS OF 378 CM FLOWING OVER A BALLOON AND PRODUCED BY A 91.5 CM RADIUS FAN OPERATING AT A CHARACTERISTIC VELOCITY OF 4.074 M/S.

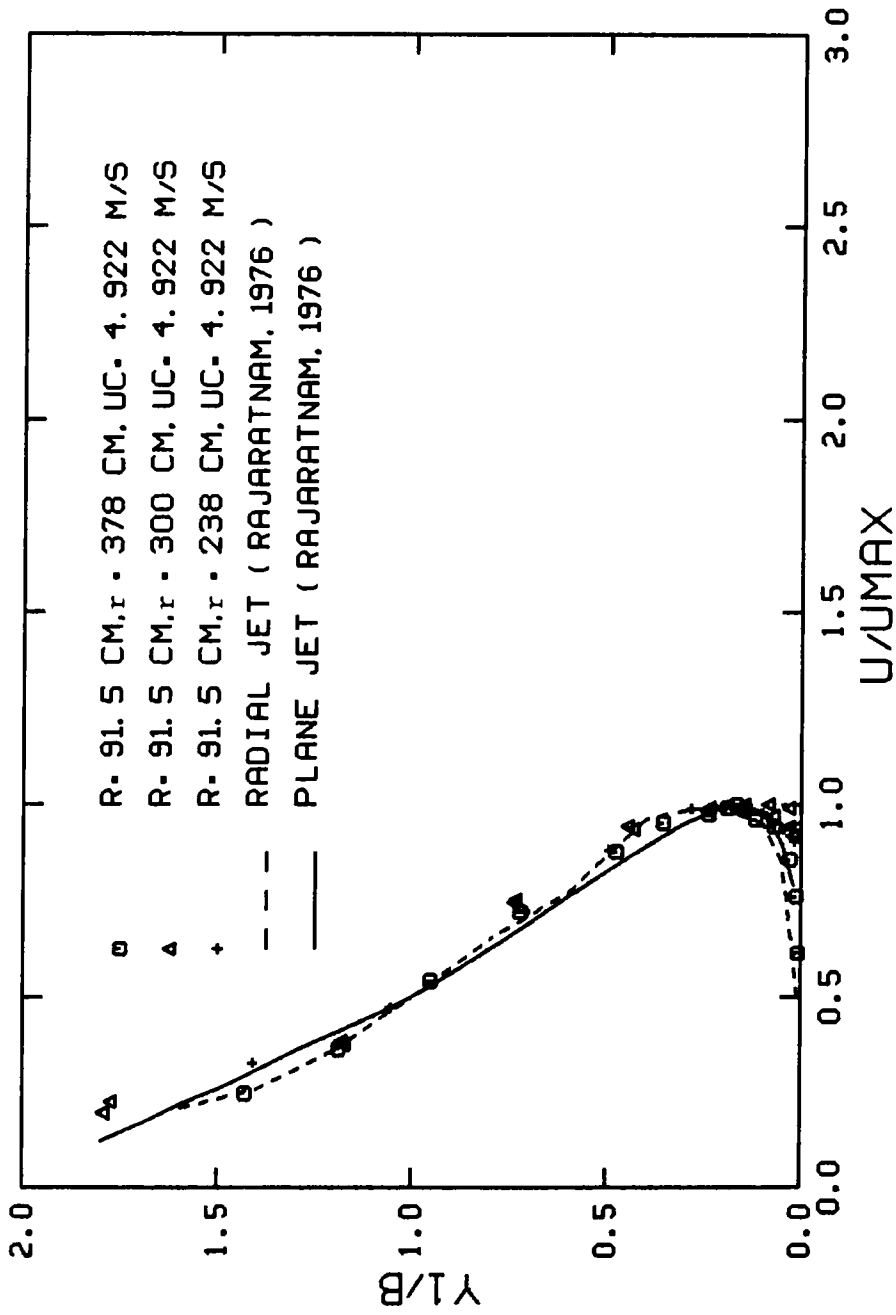


FIGURE 35. NONDIMENSIONAL VELOCITY PROFILES FOR WALL JETS FLOWING OVER BALLOONS.

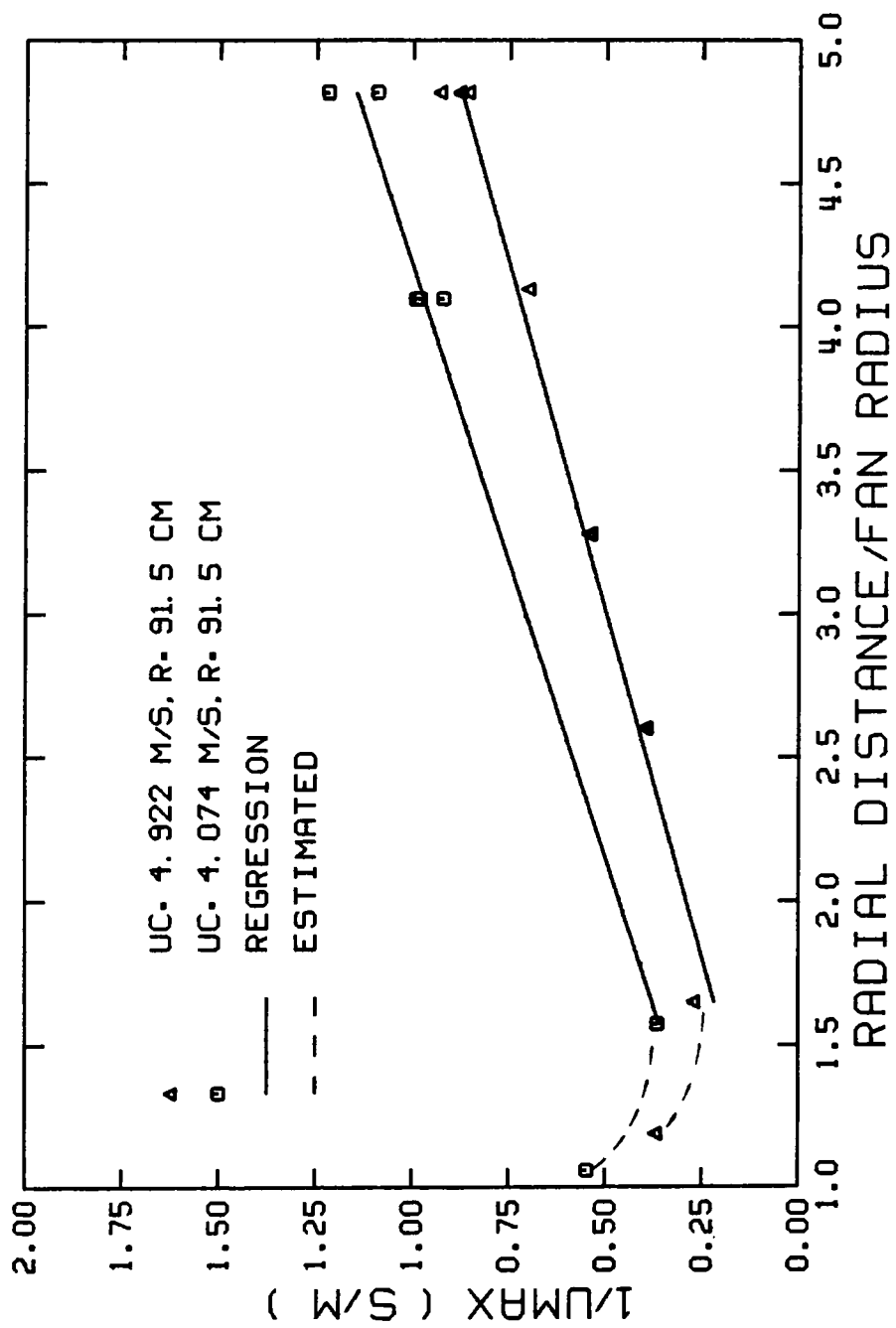


FIGURE 36. INVERSE OF THE MAXIMUM VELOCITY OF WALL JETS FLOWING OVER BALLOONS.

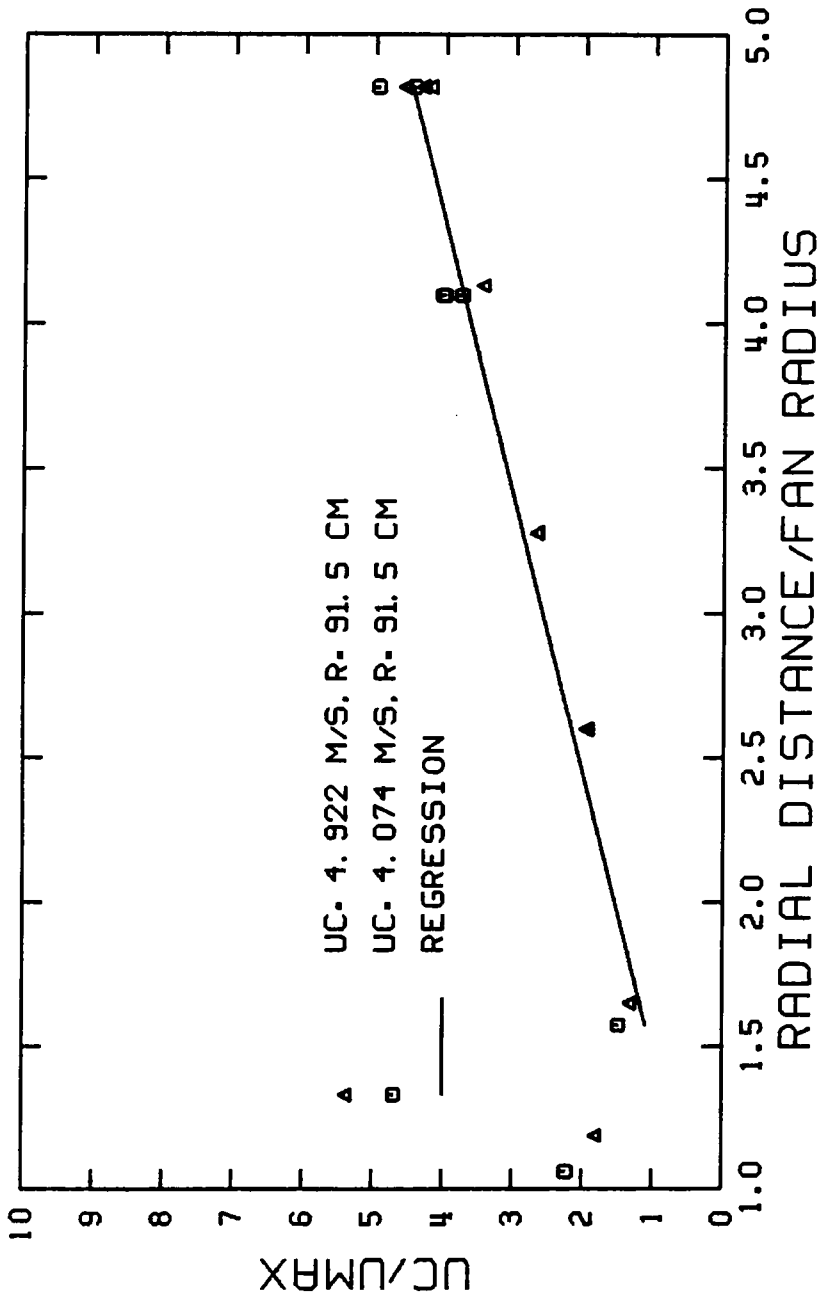


FIGURE 37. NONDIMENSIONIZED VELOCITY SCALE OF WALL JETS FLOWING OVER BALLOONS.

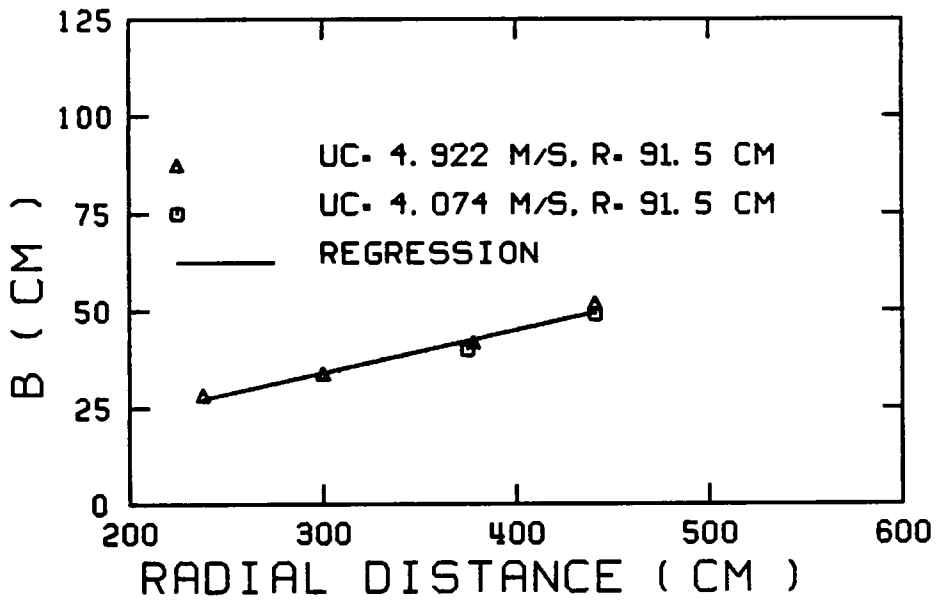


FIGURE 38. CHARACTERISTIC LENGTH OF WALL JETS FLOWING OVER BALLOONS.



$$B = 1.219 + 0.1094 r \quad (12)$$

$$238 \text{ cm} \leq r \leq 441 \text{ cm}$$

The regression coefficient was 0.970.

The velocity profiles, located 3 cm in front of the balloons (Figure 39) were assumed to be similar because the profiles on top of the balloons were similar. The similar velocity profiles (Figure 40) were described by

$$\begin{aligned} U/U_{MAX} = & 0.0054360 + 5.21108 (Y/B) - 8.7134 (Y/B)^2 \\ & + 4.83382 (Y/B)^3 - 0.83786 (Y/B)^4 \end{aligned} \quad (13)$$

$$0.05 \leq Y/B \leq 1.35$$

where

$Y$  = height above the floor (cm)

The regression coefficient value was 0.992.

The boundary layer was expressed as

$$\begin{aligned} U/U_{MAX} = & 0.207819 + 1.09956 (Y/B) + 13.016155 (Y/B)^2 \\ & - 28.18861 (Y/B)^3 \end{aligned} \quad (14)$$

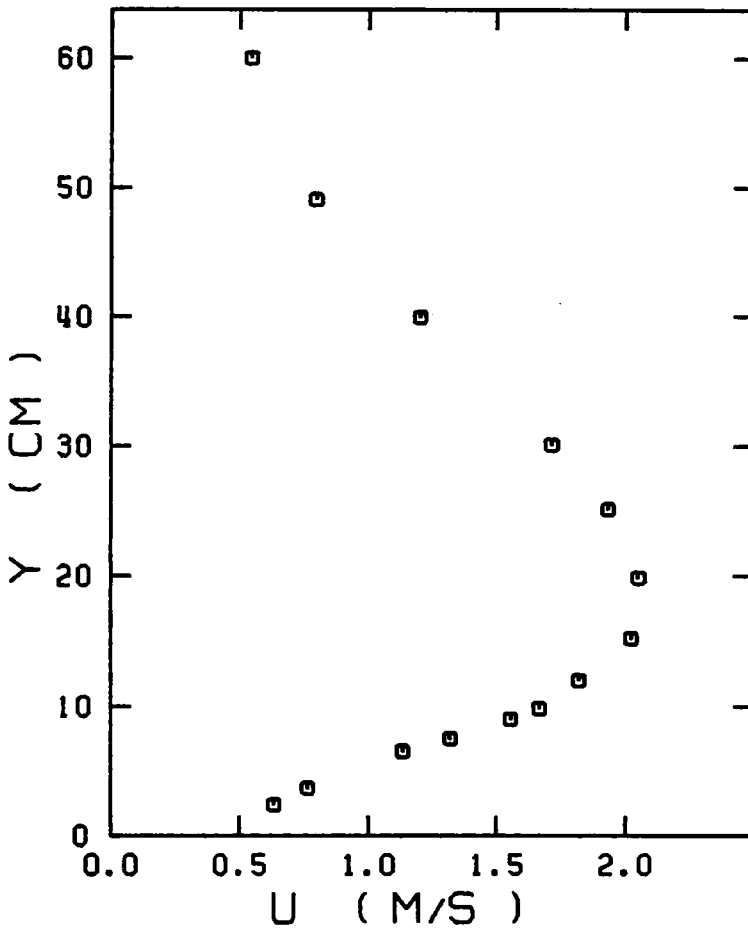


FIGURE 39. VELOCITY PROFILE OF WALL JET AT A RADIAL DISTANCE OF 286.5 CM, MEASURED 3 CM IN FRONT OF A BALLOON AND PRODUCED BY THE 91.5 CM RADIUS FAN OPERATING AT A CHARACTERISTIC VELOCITY OF 4.922 M/S.

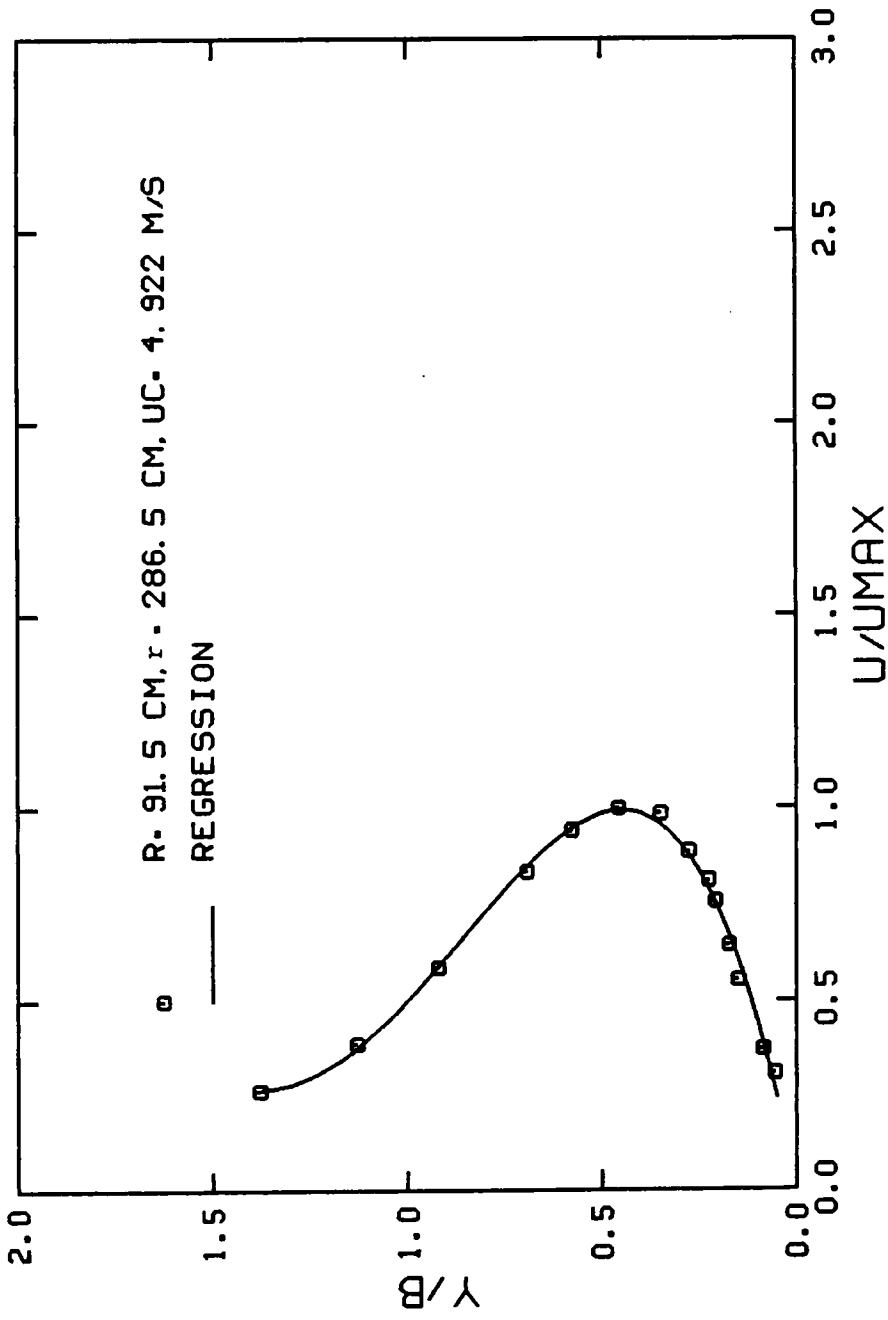


FIGURE 40. NONDIMENSIONAL VELOCITY PROFILE FOR WALL JETS 3 CM IN FRONT OF BALLOONS.

$$0.05 \leq Y/B \leq 0.35$$

The regression coefficient was 0.997.

The equation of the line representing the correlated velocity data (Figure 41) was

$$UC/UMAX = -0.5940 + 1.0514 (r/R) \quad (15)$$

$$2.174 \leq r/R \leq 4.820$$

The regression coefficient value was 0.923.

The equation of the line representing the characteristic length (Figure 42) was

$$B = 12.16 + 0.1094 r \quad (16)$$

$$238 \text{ cm} \leq r \leq 441 \text{ cm}$$

The regression coefficient was 0.970.

#### Wall Jet Model: Broilers with Necks Up

Velocity profiles of the wall jet were measured 3 cm in front of the balloons (Figure 43). The relationship between the characteristic length and the radial distance of the wall jet was piecewise linear (Figure 44), so the wall jet region was divided into two regions. In region one, the balloon heights were relatively large compared to the wall jet heights. In region two, the balloon heights were relatively

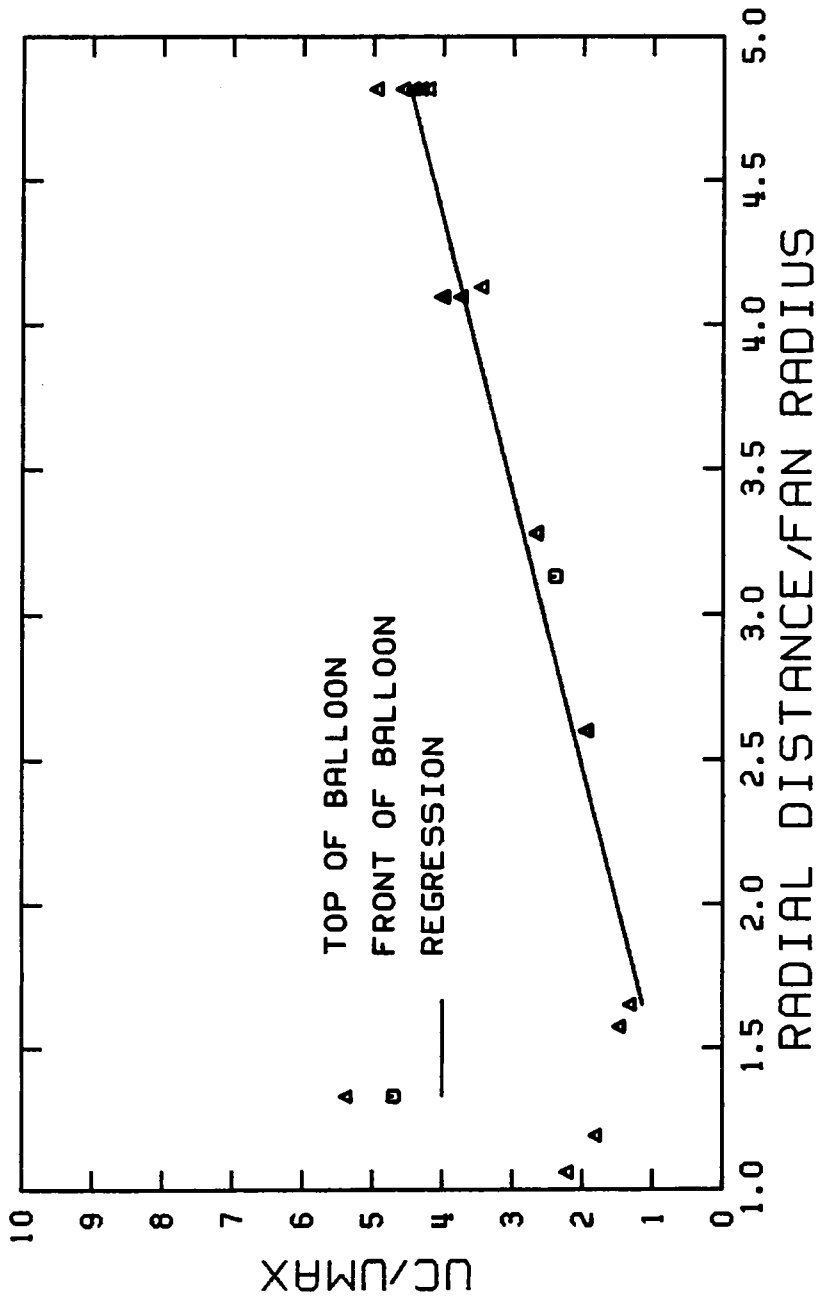


FIGURE 41. NONDIMENSIONIZED VELOCITY SCALE OF WALL JETS 3 CM IN FRONT OF BALLOONS.

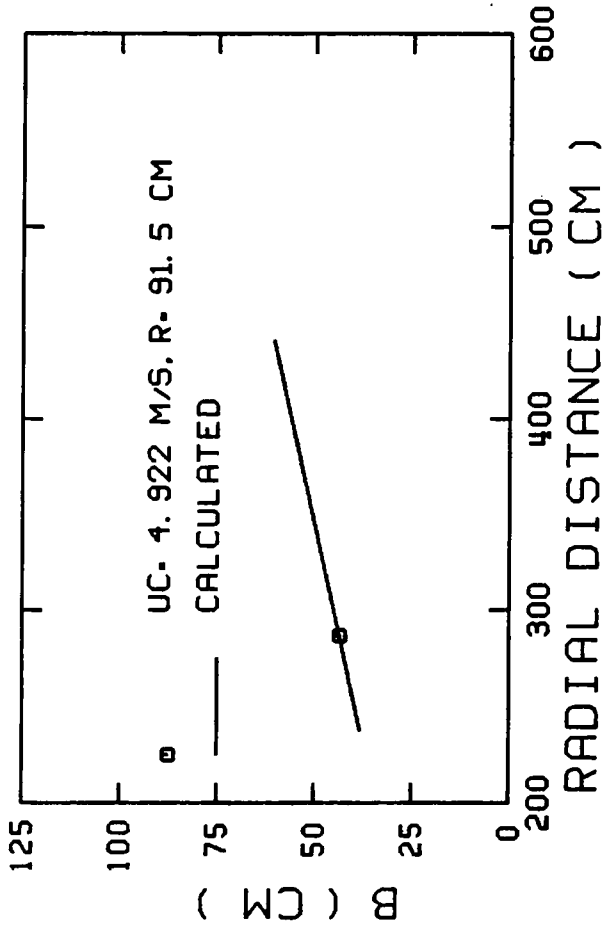


FIGURE 42. CHARACTERISTIC LENGTH OF WALL JETS 3 CM IN FRONT OF BALLOONS.

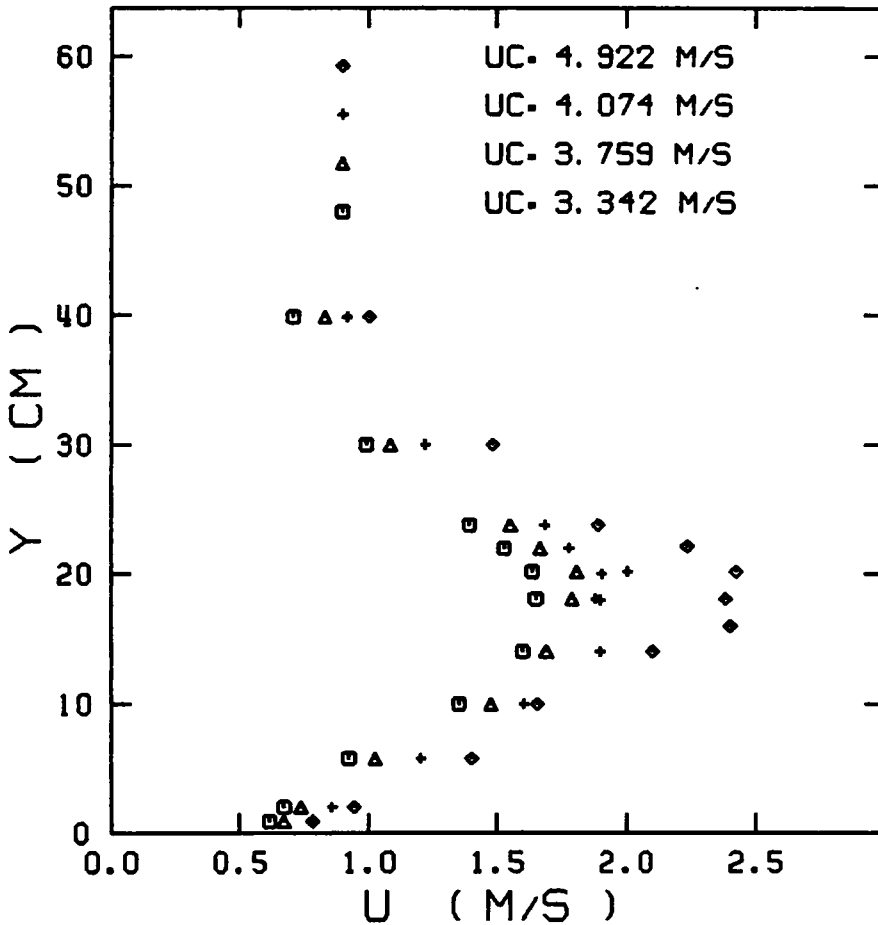


FIGURE 43. VELOCITY PROFILES OF WALL JET AT A RADIAL DISTANCE OF 204.5 CM, 3 CM IN FRONT OF A BALLOON WITH A NECK AND PRODUCED BY THE 91.5 CM RADIUS FAN OPERATING AT FOUR CHARACTERISTIC VELOCITIES.

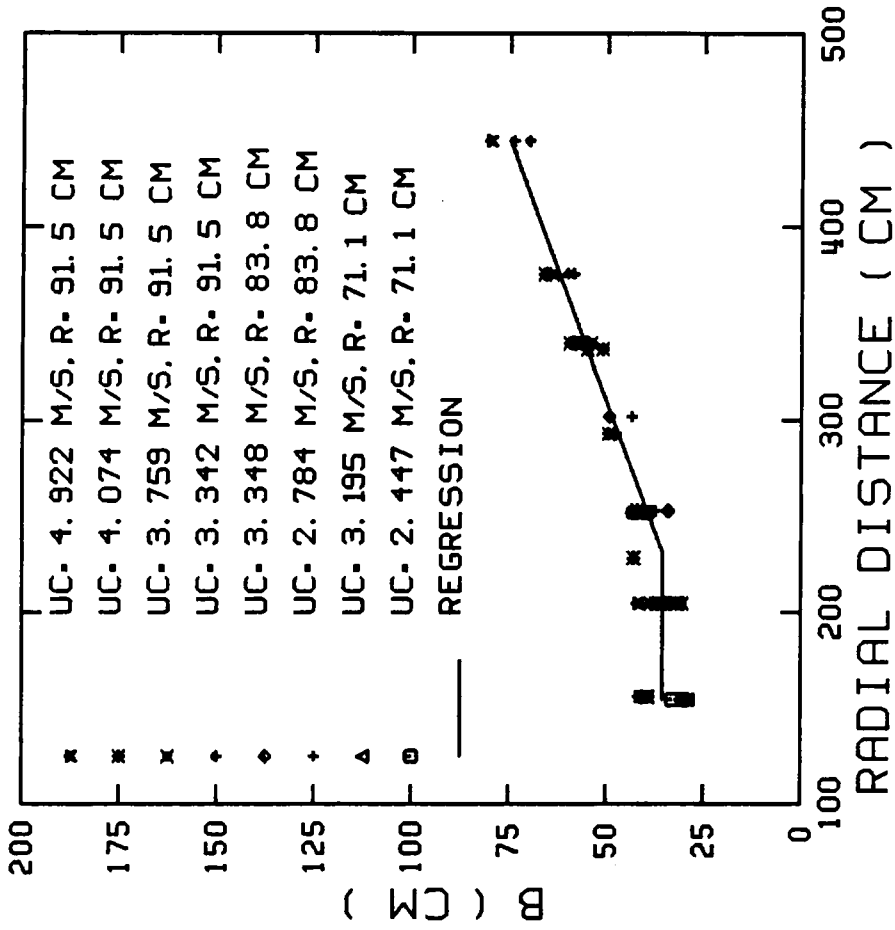


FIGURE 44. CHARACTERISTIC LENGTH OF WALL JETS FLOWING OVER BALLOONS WITH NECKS.



small compared to the wall jet heights. The regression equation for the characteristic length in region one was

$$B = 35.4 \quad (17)$$

$$154.6 \text{ cm} \leq r \leq 231 \text{ cm}$$

The regression equation for the characteristic length in region two was

$$B = -7.5636 + 0.185968 r \quad (18)$$

$$231 \text{ cm} \leq r \leq 444.4 \text{ cm}$$

The regression coefficient was 0.933.

The fully developed velocity profiles were similar in region one (Figure 45) and region two (Figure 46). The regression equation for the velocity profiles in region one was

$$U/UMAX = 0.346368 + 2.32708 (Y/B) - 0.81648 (Y/B)^2 - 3.76467 (Y/B)^3 + 2.38781 (Y/B)^4 \quad (19)$$

$$0 \leq Y/B \leq 1.2$$

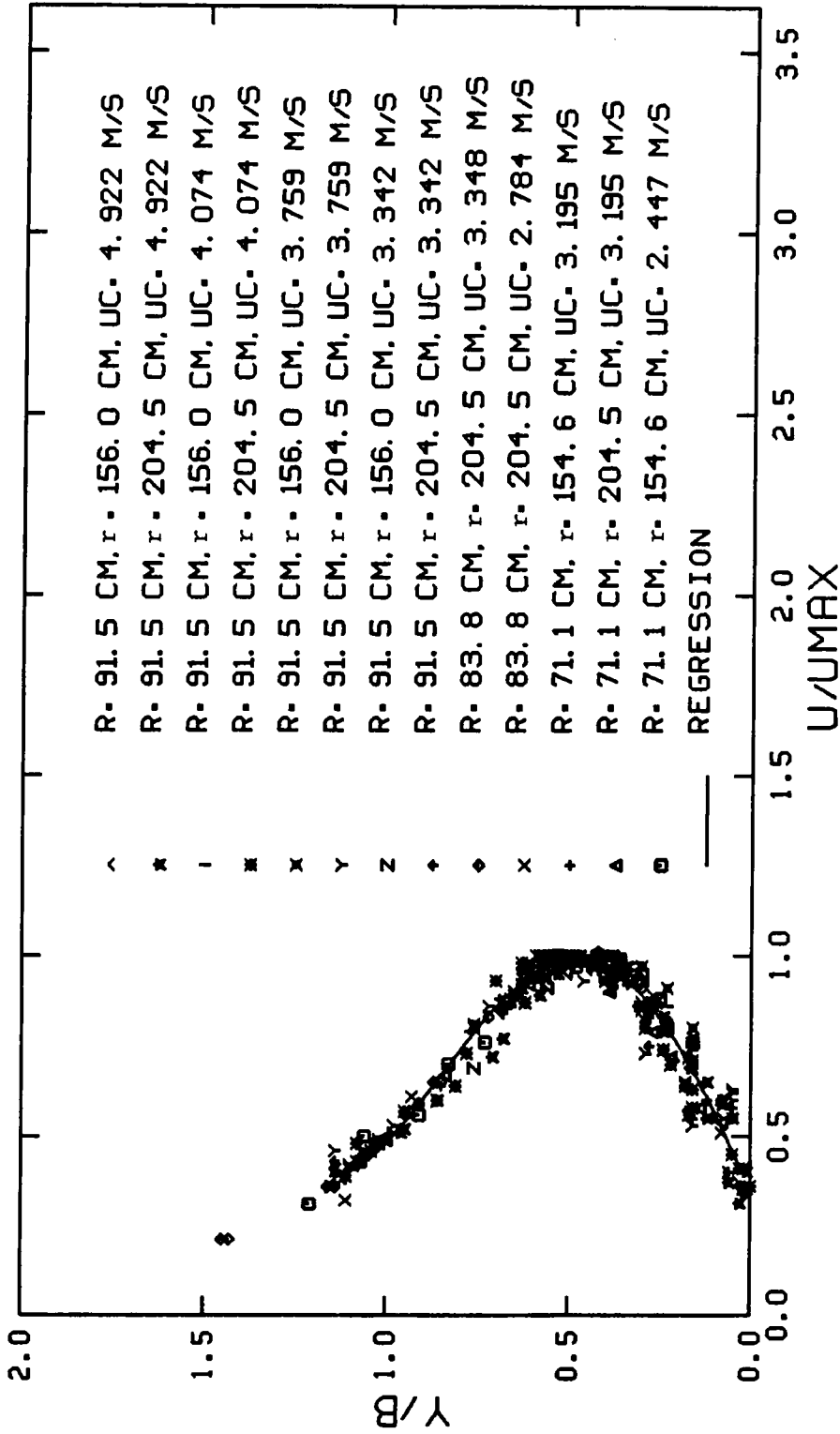


FIGURE 45. NONDIMENSIONAL VELOCITY PROFILE FOR WALL JETS, IN REGION ONE, FLOWING OVER BALLOONS WITH NECKS.



$$154.6 \text{ cm} \leq r \leq 204.5 \text{ cm}$$

The regression coefficient was 0.950

The boundary layer in region one was expressed as

$$\begin{aligned}
 U/UMAX &= 0.354282 + 2.22311 (Y/B) - 0.95922 (Y/B)^2 \\
 &- 1.8649 (Y/B)^3 \qquad \qquad \qquad (20)
 \end{aligned}$$

$$0 \leq Y/B \leq 0.55$$

$$154.6 \text{ cm} \leq r \leq 204.5 \text{ cm}$$

The regression coefficient was 0.932.

The regression equation for the velocity profiles in region two was

$$\begin{aligned}
 U/UMAX &= 0.245509 + 1.45446 (Y/B) + 6.49506 (Y/B)^2 \\
 &- 20.429 (Y/B)^3 + 17.6758 (Y/B)^4 \qquad \qquad \qquad (21) \\
 &- 4.95253 (Y/B)^5
 \end{aligned}$$

$$0 \leq Y/B \leq 1.2$$

$$204.5 \text{ cm} \leq r \leq 444.4 \text{ cm}$$

The regression coefficient value was 0.961

The regression equation for the boundary layer in region two was

$$U/UMAX = 0.252024 + 1.46263 (Y/B) + 4.52167 (Y/B)^2 - 9.1767 (Y/B)^3 \quad (22)$$

$$0 \leq Y/B \leq 0.50$$

$$204.5 \text{ cm} \leq r \leq 444.4 \text{ cm}$$

The regression coefficient was 0.948

Linear relationships existed between the inverse of the maximum velocity and the radial distance of the wall jet (Figures 47, 48 and 49). The equation of the line representing the correlated velocity data (Figure 50) was

$$UC/UMAX = -0.24201 + 1.02182 (r/R) \quad (23)$$

$$2.174 \leq r/R \leq 4.857$$

The regression coefficient was 0.970.

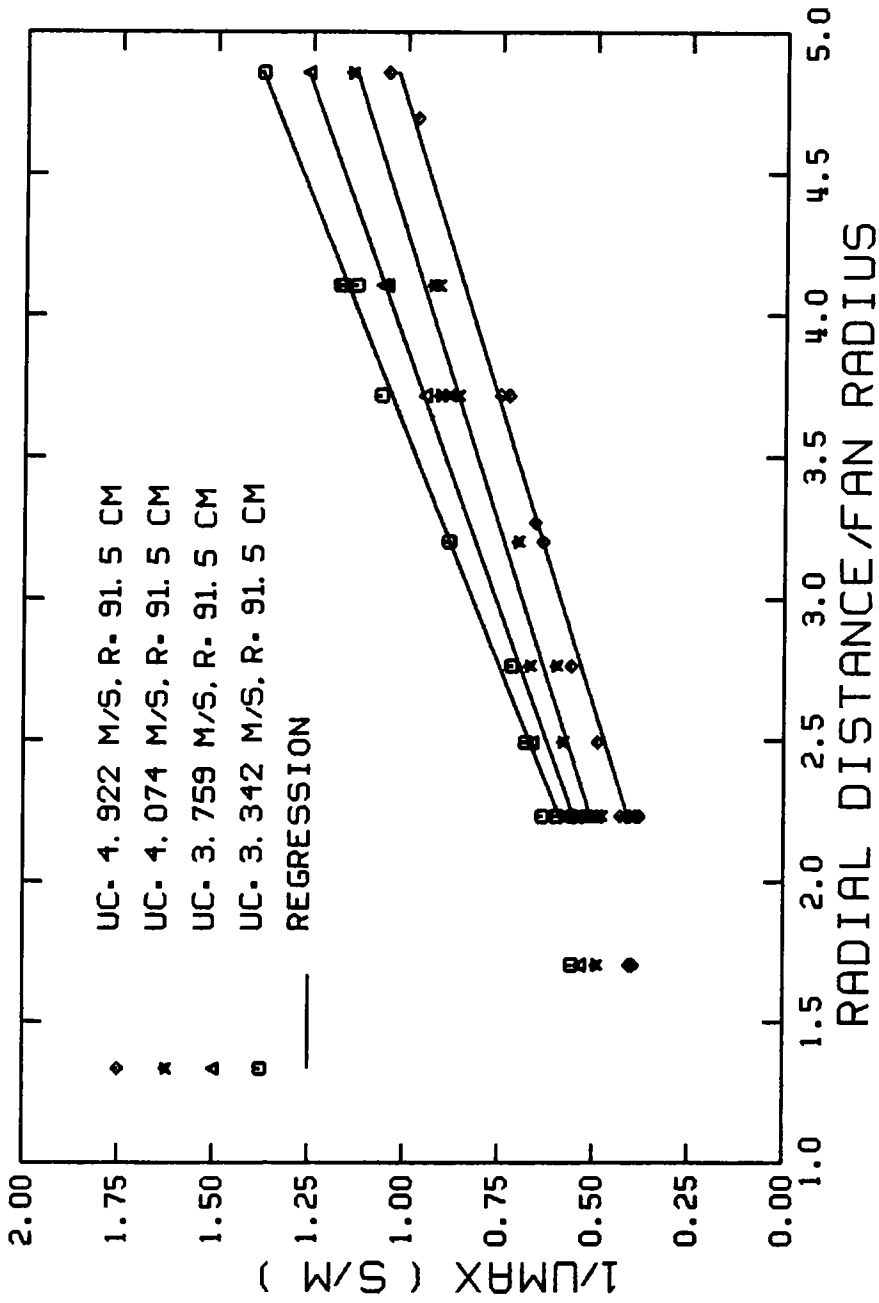


FIGURE 47. INVERSE OF THE MAXIMUM VELOCITY OF WALL JETS FLOWING OVER BALLOONS WITH NECKS AND PRODUCED BY A 91.5 CM RADIIUS FAN OPERATING AT FOUR CHARACTERISTIC VELOCITIES.

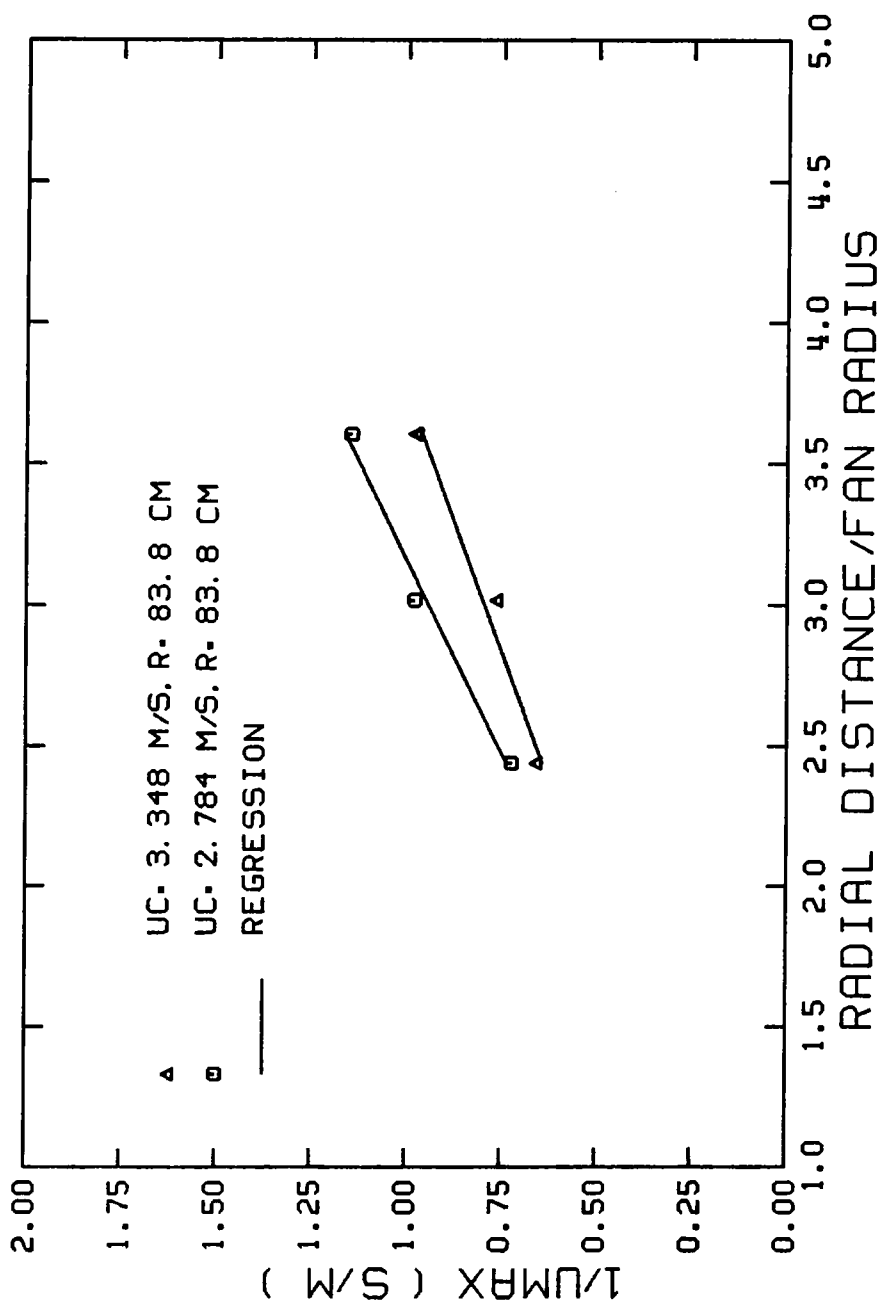


FIGURE 48. INVERSE OF THE MAXIMUM VELOCITY OF WALL JETS FLOWING OVER BALLOONS WITH NECKS AND PRODUCED BY A 83.8 CM RADIUS FAN OPERATING AT TWO CHARACTERISTIC VELOCITIES.

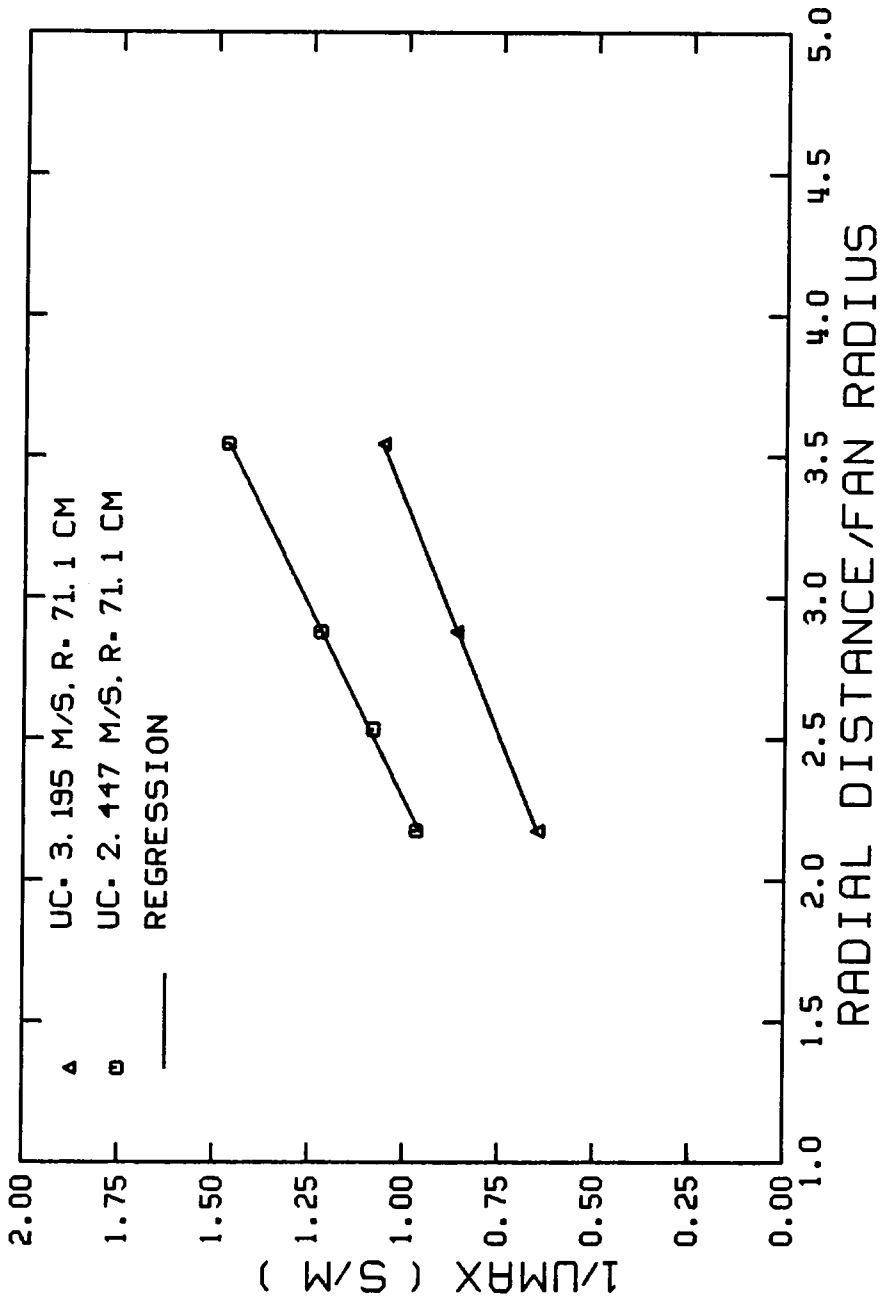


FIGURE 49. INVERSE OF THE MAXIMUM VELOCITY OF WALL JETS FLOWING OVER BALLOONS WITH NECKS AND PRODUCED BY A 71.1 CM RADIUS FAN OPERATING AT TWO CHARACTERISTIC VELOCITIES.



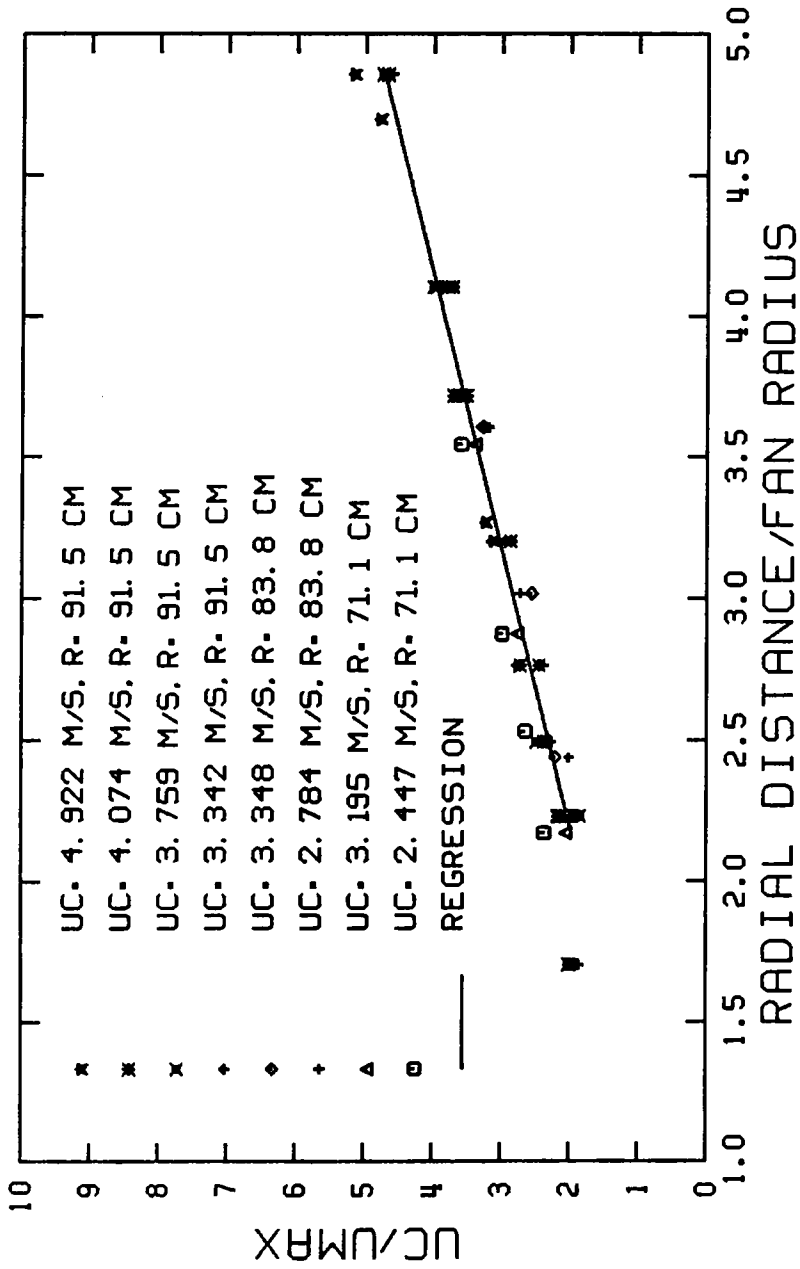


FIGURE 50. NONDIMENSIONIZED VELOCITY SCALE OF WALL JETS FLOWING OVER BALLOONS WITH NECKS.

### Model Sensitivity to Balloon Spacing

Sensitivity of the wall jet model to uniform balloon spacing was measured. Maximum velocities, characteristic lengths and nondimensional velocity profiles did not change significantly for uniform balloon spacings of 0.061 and 0.074 m<sup>2</sup> per balloon (Figures 51, 52, and 53).

### Model Sensitivity to Large Gaps Between Groups of Balloons

Sensitivity of the wall jet to relatively large gaps between groups of balloons was calculated using velocity profiles for gap spacings of 0, 30 and 65 cm (Figure 54). Maximum velocities, characteristic lengths and nondimensional velocity profiles did not change significantly for the three gap spacing (Figures 55, 56, and 57). The largest difference in the velocity profiles from the 0 and 30 cm gap spacings was 2%. The largest difference in the velocity profiles from 0 to 65 cm gap spacings was 9%.

### Velocity Decay

The velocity of the wall jets flowing over the balloons with necks was lower than the velocity of the wall jets flowing over the balloons without paper necks (Figure 58). Also, the velocity of the wall jets flowing over the balloons without necks was lower and decayed quicker than the velocity of the wall jets flowing over a smooth floor (Figure 58).

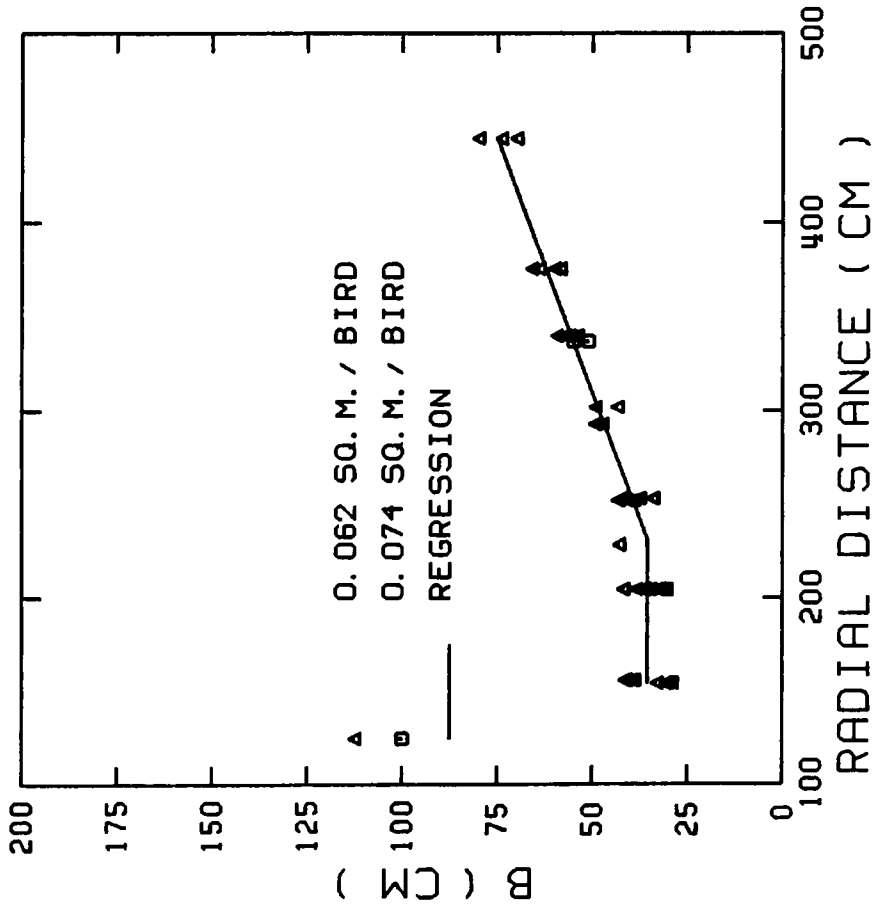


FIGURE 51. CHARACTERISTIC LENGTH OF WALL JETS FLOWING OVER BALLOONS ( WITH NECKS ) AT TWO BALLOON SPACINGS.

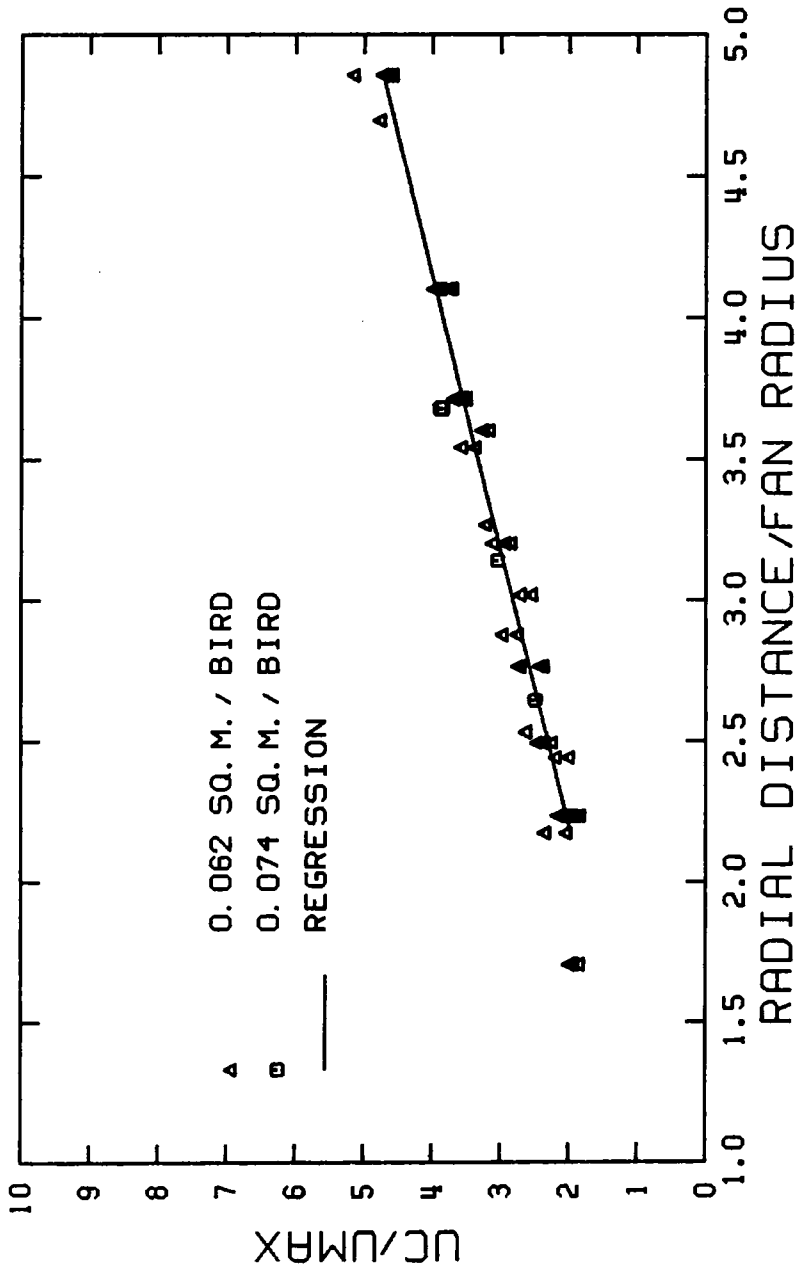


FIGURE 52. NONDIMENSIONIZED VELOCITY SCALE OF WALL JETS FLOWING OVER BALLOONS (WITH NECKS) AT TWO BALLOON SPACINGS.

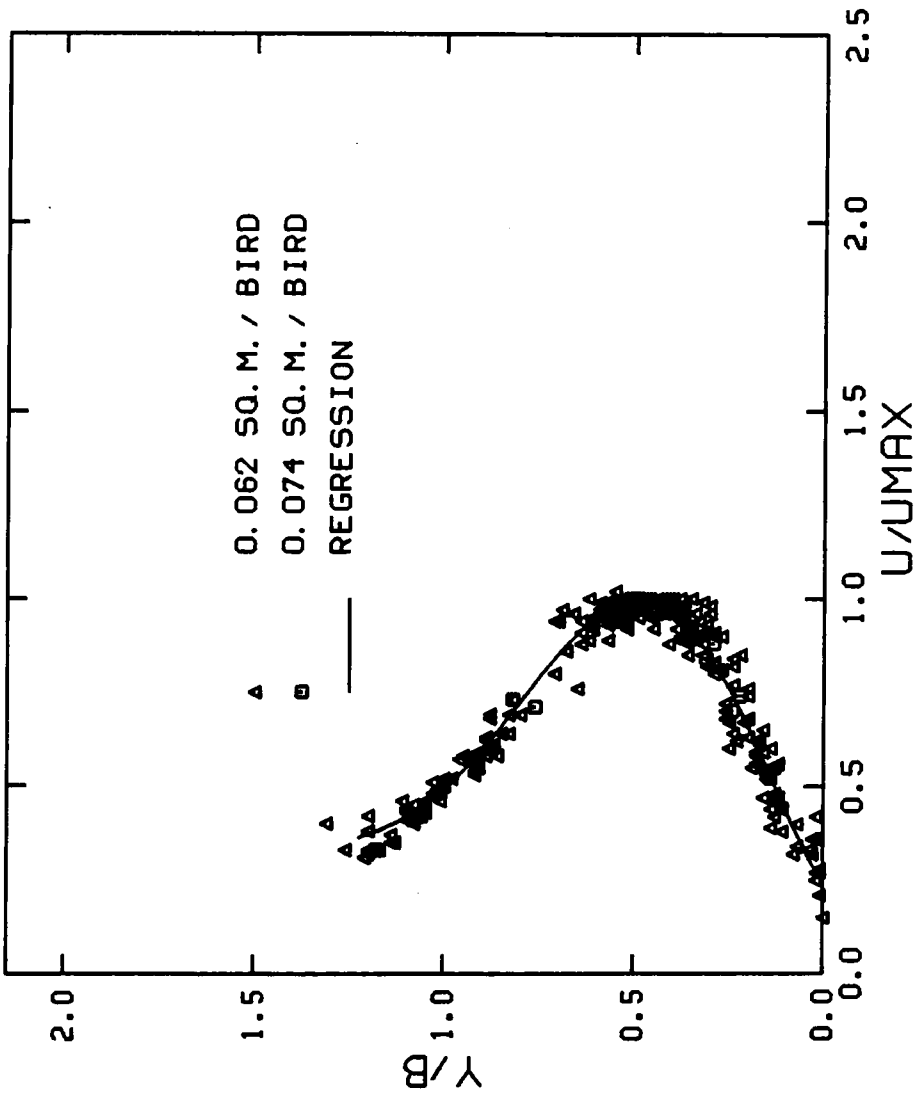


FIGURE 53. NONDIMENSIONAL VELOCITY PROFILE FOR WALL JETS FLOWING OVER BALLOONS ( WITH NECKS ) AT TWO BALLOON SPACINGS.

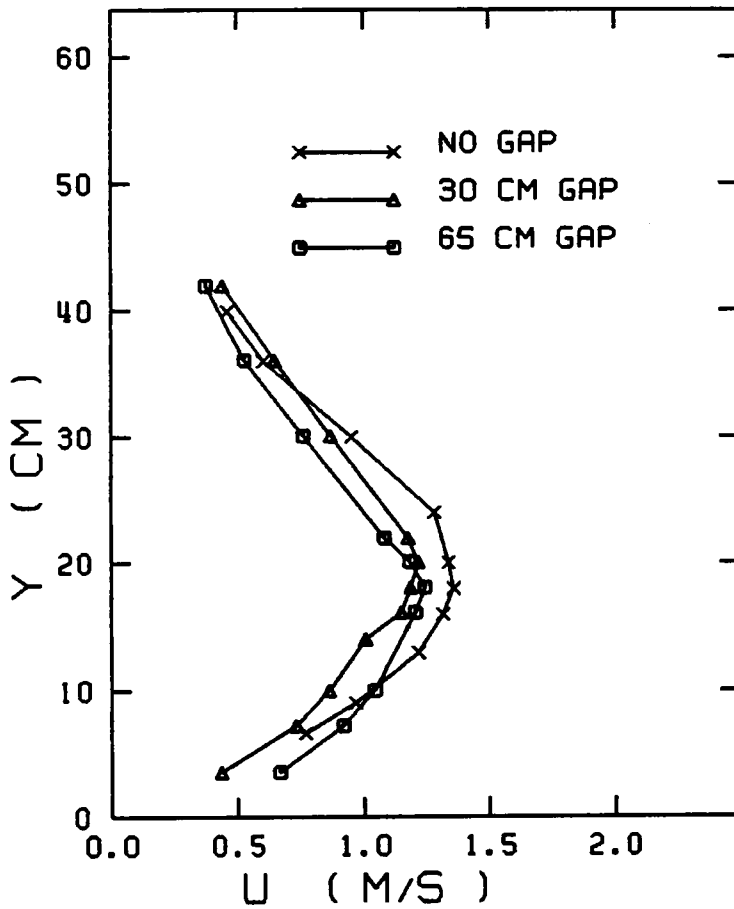


FIGURE 54. WALL JET VELOCITY PROFILES  
 FOR TWO GAP SPACINGS  
 ( CHARACTERISTIC VELOCITY -  
 3.348 M/S, R = 838 CM,  
 r = 253 CM )

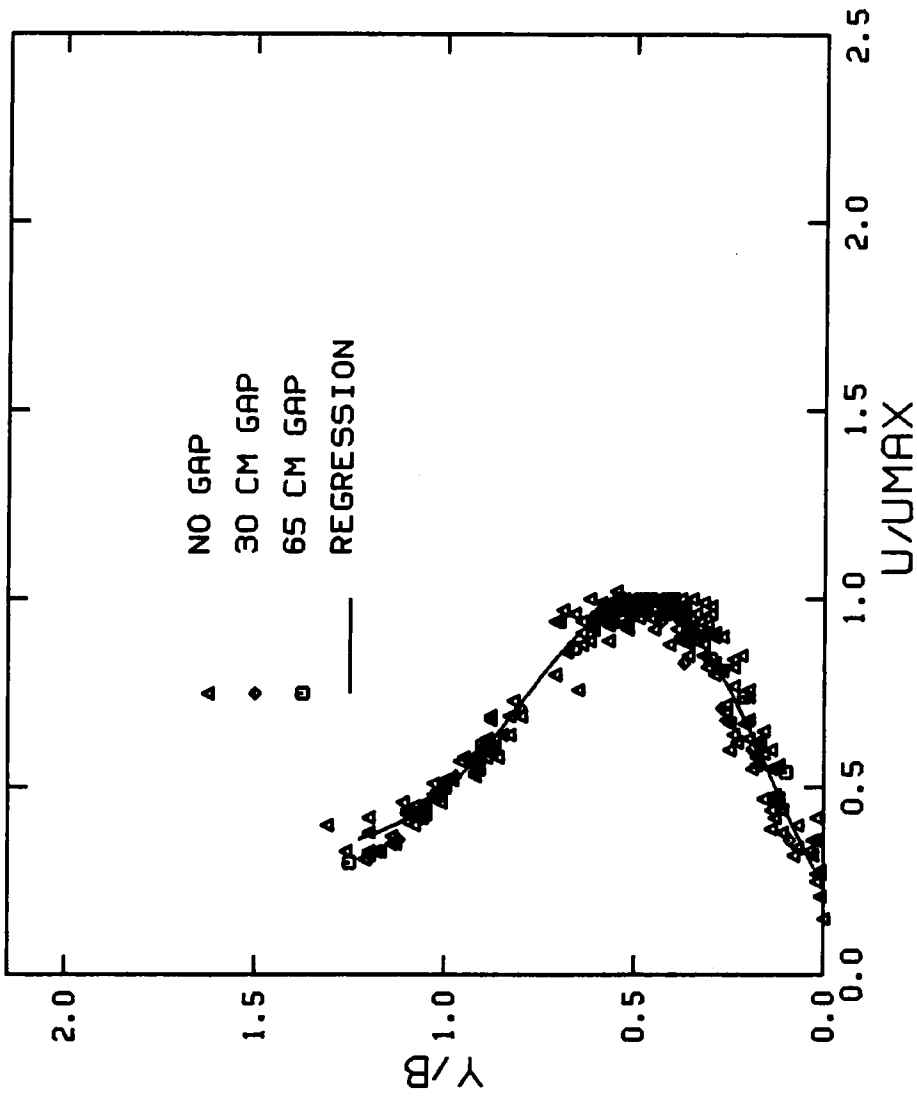


FIGURE 55. NONDIMENSIONAL VELOCITY PROFILE FOR WALL JETS FLOWING OVER BALLOONS ( WITH NECKS ) AT TWO GAP SPACINGS.

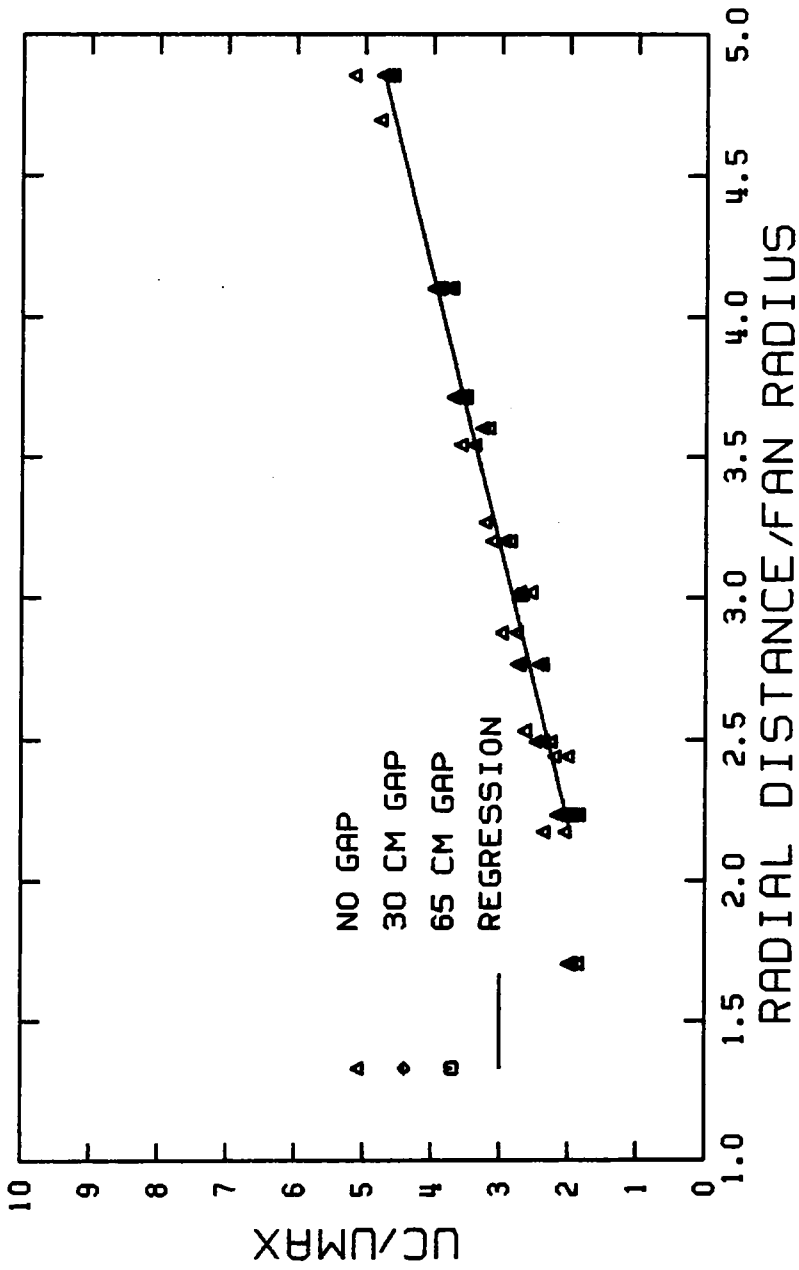


FIGURE 56. NONDIMENSIONIZED VELOCITY SCALE OF WALL JETS FLOWING OVER BALLOONS ( WITH NECKS ) AT TWO GAP SPACINGS.



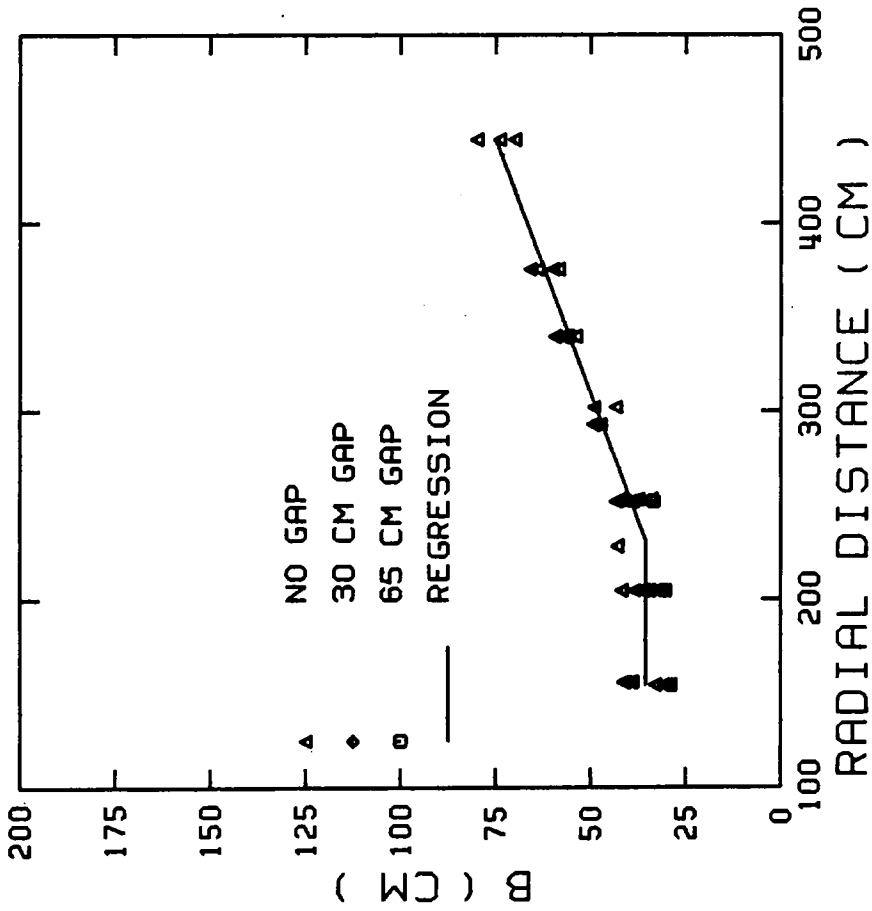


FIGURE 57. CHARACTERISTIC LENGTH OF WALL JETS FLOWING OVER BALLOONS ( WITH NECKS ) AT TWO GAP SPACINGS.

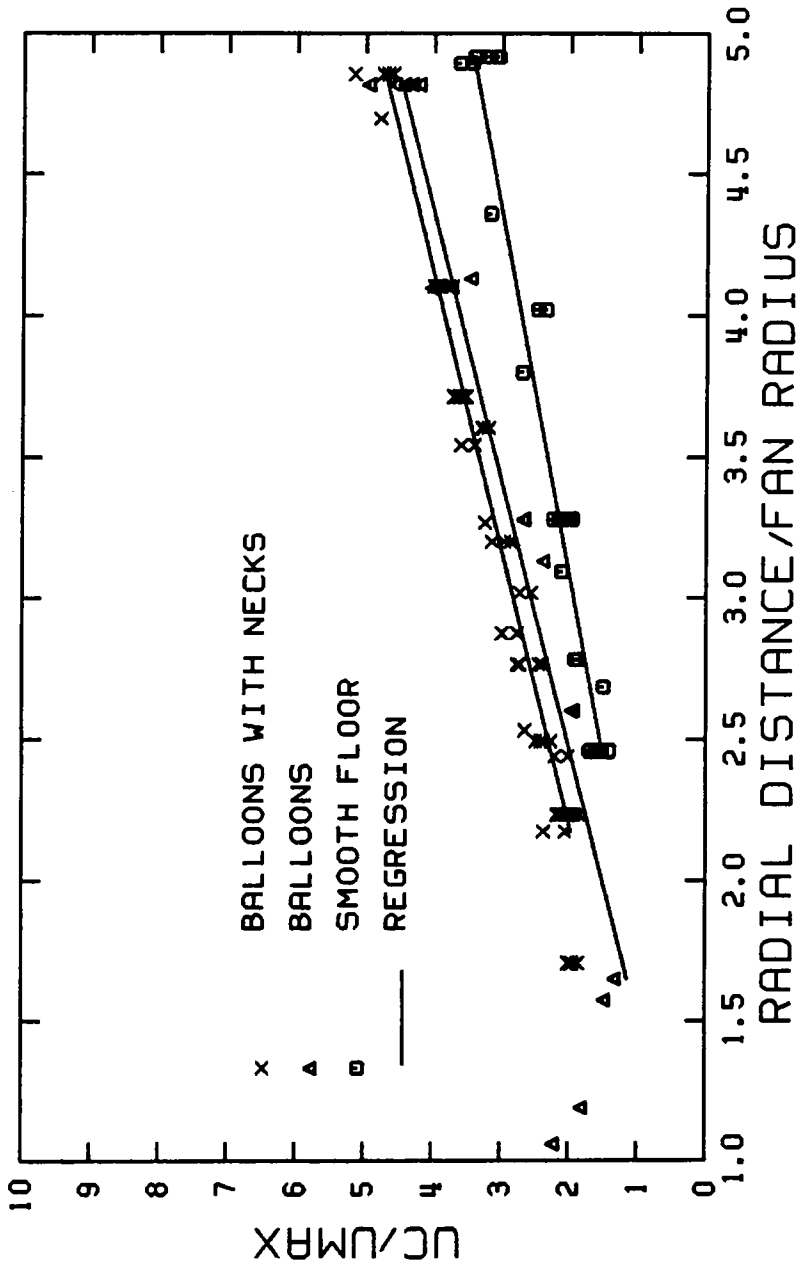


FIGURE 58. COMPARISON OF NONDIMENSIONALIZED VELOCITIES OF WALL JETS.

## CHAPTER VII

### APPLICATION

Two computer routines were developed to aid poultry production managerial decisions. The computer routines include the summer routine and the winter routine. Flowcharts for these routines are given in Figures 59 and 60 and are listed in Appendices A and B, respectively. The summer routine (Figure 59) contains a composite model that interfaces the wall jet model with the broiler growth model. The composite model predicts the air velocity in the space occupied by the broilers and predicts the corresponding weight gain. The winter model (Figure 60) predicts the air velocity one centimeter above litter to aid in litter management decisions.

#### Summer Routine

Background: Weight Gain of Heat Stressed Broilers. Weight gain of heat stressed broilers increases as air velocity increases. Drury (1966) reported the relationship between weight gain of heat stressed broilers and air velocity (Figure 61). Seven week old, commercial crossbred, male broilers were tested for two weeks in a diurnally cycled hot environment. Air dry-bulb temperature was cycled  $28.3 \pm 7.2$  C and dewpoint temperature was maintained at  $18.3 \pm 2.2$  C. Air temperature and relative humidity were chosen to simulate the conditions on a hot day in the Southeast. Daily weight gain per bird was related to air

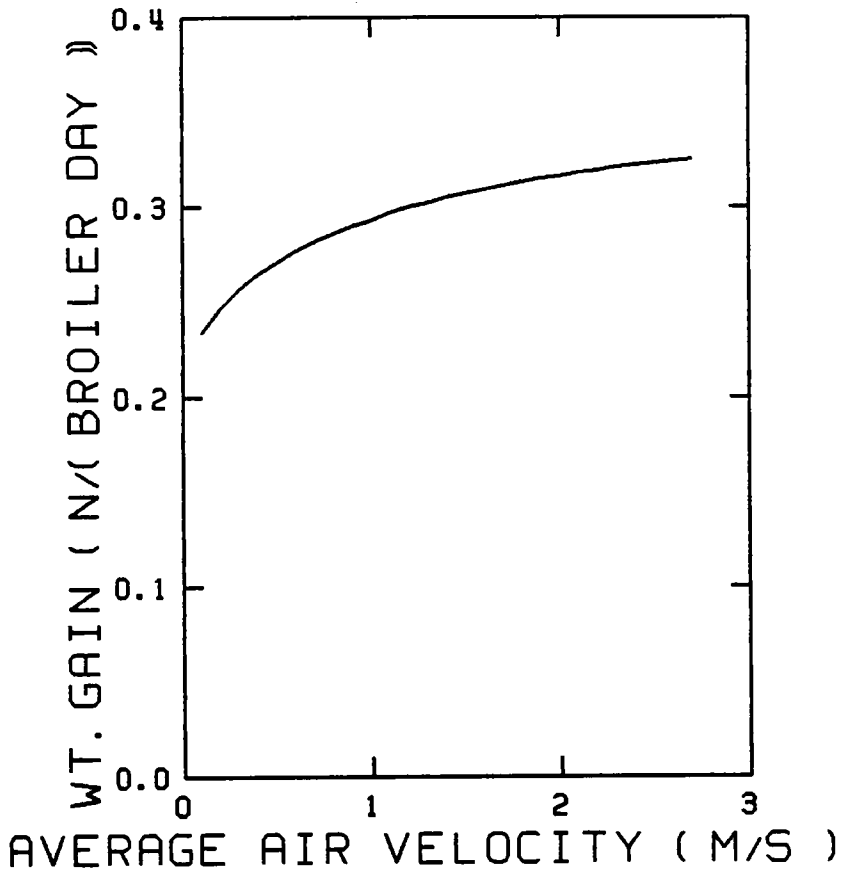


FIGURE 61. AIR VELOCITY EFFECT ON GROWTH OF 7 WEEK OLD MALE BROILERS TESTED FOR 2 WEEKS IN A DIURNALLY CYCLING HOT, HUMID ENVIRONMENT ( DRURY, 1966 )

velocity by

$$\text{Gain} = 0.1967 + 0.126064 V^{\frac{1}{2}} - 0.029267 V \quad (24)$$

$$0.11 \leq V \leq 2.69 \quad \text{m/s}$$

where

Gain has the units of N/(day broiler) and

V is the average air velocity impinging the broilers (m/s)

Equation 24 is ASAE Standard Data D270.4 (1984).

Appetite depression is relieved by an increase in air velocity (Drury, 1966). Therefore, as appetite depression is relieved, weight gain approaches to a value that is normal for unstressed broilers.

Equation 24 predicted the weight gain of 7 week old broilers in 1966. However, broiler weight gain doubled in the period from 1964 to 1983 (Figure 62) (Roberts, 1964). Therefore, 7 week old broilers in 1966 were approximately the same size as 4 week old broilers in 1985. Heat stress increases with broiler size because the ratio of surface area to basal metabolism decreases as broiler size increases (Esmay, 1978). Assuming the data for 1964 can be extrapolated for 7 week old broilers, 4 week old broilers in 1985 experience heat stress similar to 7 week old broilers in 1966. Likewise, 4 week old broilers in 1985 experience appetite depression and weight loss similar to 7 week old

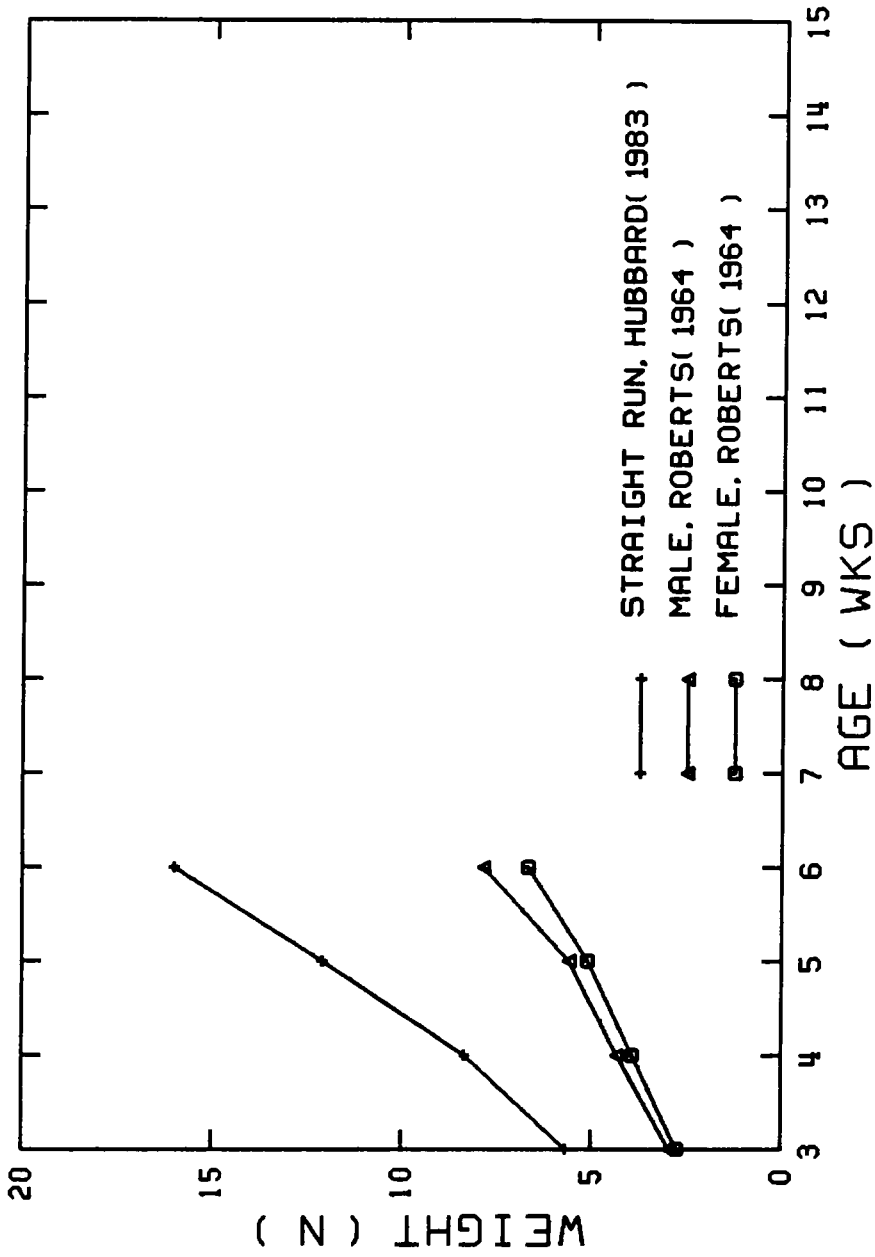


FIGURE 62. BROILER GROWTH AT VARYING AGES MEASURED IN 1964 AND 1983.

broilers in 1966. Because ceiling fan operation is typically begun at the beginning of the third week, the broiler growth model developed by Drury (1966) is applicable for 3.5 to 4 week old broilers in 1985.

Ceiling fans should not be operated when air temperatures exceed 40.6° C. Although air velocities up to 2.9 m/s reduce adverse physiological responses of broilers at air temperatures up to 40.6°C (Drury and Siegel, 1966; Siegel and Drury, 1968a), high air velocities are detrimental to broilers when air temperatures exceed 40.6°C (Siegel and Drury, 1968b).

Summer Routine Development. The summer routine was developed using the boundary layer equations 14, 20 and 22 to model the air flow impinging broilers. An average air velocity term was developed to express the average air velocity impinging broilers with necks down. The term was developed by integrating equation 14 from  $Y = 0.05$  to  $Y = 11$  cm.

Two average air velocity terms were developed to express the average air velocity impinging broilers with necks up. The two average air velocity terms correspond to the two regions described in the section "Wall Jet Model: Broilers with Necks Up". The two average velocity terms for broilers with necks up were developed by integrating equations 20 and 22 from  $Y = 0.05$  to  $Y = 16$  cm. The average velocity terms were substituted into the broiler growth model (equation 24). The resulting expression for broiler weight gain is a function of the

characteristic velocity, the fan radius and the radial distance from the fan centerline.

There were three regions of air flow in the space occupied by the balloons: 1) the potential flow region, 2) the transition region, and 3) the fully developed region. The transition region and the fully developed region correspond to region one and two described in the section "Wall Jet Model: Broilers with Necks Up".

Characteristics of the potential flow region included a constant characteristic length and a decaying exponential function of  $UC/UMAX$  that is expressed as

$$UC/UMAX = 3.629 \text{ EXP } (-0.543 (r/R)) \quad (25)$$

$$0 \leq r/R \leq 2.174$$

for the necks down case and

$$UC/UMAX = 4.606 \text{ EXP } (-0.483 (r/R)) \quad (26)$$

$$0 \leq r/R \leq 2.174$$

for the necks up case.

Characteristic lengths do not exist in potential flow, but a constant characteristic length was assumed as an approximation. The coefficients of the exponential function were graphically estimated for the case of necks up. The estimate was based on data from the case of necks down (Figure 41). Characteristics of the transition region included a



constant characteristic length and a linear function of UC/UMAX. Characteristics of the fully developed region included a linear function of the characteristic length and a linear function of UC/UMAX.

The daily additional weight gain was defined as the weight gain influenced by a ceiling fan minus the weight gain for zero velocity. The daily addition weight gain due to a ceiling fan of given radius and characteristic velocity was

$$\frac{\text{additional weight gain}}{\text{day}} = \int \frac{\text{additional weight gain}}{\text{broiler} \cdot \text{day}} \cdot (\text{number of broilers}) \, dr \quad (27)$$

The total daily addition weight gain influenced by a ceiling fan was predicted by summing the integrals from the potential flow region, the transition region and the fully developed region. Numerical integration was used because of the complex forms of the three integrands. The integrands were graphically smooth and were approximately quadratic in the range of velocities used in the study (Figure 61). The integrands were integrated using Simpson's rule, which is precise for quadratic integrands (Dorn and McCracken, 1962).

The summer routine allows the input of several fan characteristics, such as fan diameter, characteristic velocity, energy consumption and fan cost. The routine varies each fan characteristic and fan spacing separately. The routine predicts the optimum fan diameter, characteristic velocity and fan spacing for the given floor area. The

criterion for the optimum solution was the minimum break-even period which was based on a before-tax analysis. FORTRAN coding and user manual for the summer routine is in Appendix A. The summer routine is entitled BROILER 1.

As an example of a summer application consider 1) a 12 m by 122 m or 1464 m<sup>2</sup> broiler house, 2) two flocks of birds, 3) bird spacings of 0.068 and 0.074 m<sup>2</sup>/broiler, and the data in Table 1. The program output is in Table 2.

The summer routine will also compare the benefits of ceiling fans with the benefits of an alternative air circulator. As an example, consider the data in Table 1 and eleven alternative air circulator that 1) cost \$380 per circulator, 2) have a ten year salvage value of \$40 per circulator, 3) consume 746 W per circulator and 4) produce an average air velocity of 0.508 m/s at bird level. The output is in Table 3.

The optimum combination of fan spacing, fan diameter and characteristic velocity is applicable to broiler houses built in the future because the house dimensions can be chosen in accordance with the optimum fan spacing. However, in the case of limited truss spans or existing broiler houses, the optimum solution is site specific. Table 4 can be used to obtain a site specific optimum combination for existing building. The table contains a list of the combinations of fan spacing, fan diameter and characteristic velocity and the corresponding break-even periods. The site specific optimum combination is characterized by the most feasible fan spacing with the minimum break-even period.

Table 1. Data for the Summer Routine Example Problem

Fan Diameter, m	1.83	1.68	1.42			
Fan Cost, \$/Fan	339	249	189			
Salvage Value, \$/Fan	40	30	20			
Characteristic Velocity, m/s						
High	4.922	4.054	3.657			
Medium High	4.074	3.348	3.195			
Medium	3.759	3.086	2.897			
Low	3.342	2.784	2.447			
Energy Consumption, W						
High	220	160	108			
Medium High	125	90	72			
Medium	98	70	54			
Low	69	52	32			
Fan Spacing, m	5	6	7	8	10	12
Cost of Electricity, \$/KWh	0.07					
Necks Down (1) or Up (2)	2					
Broiler Value, \$/N	0.11					
Interest Rate, decimal	0.08					

Table 2. Output for Summer Routine Example Problem:  
Ceiling Fans Compared to No Fans (Zero Air Flow)

\*\*\* 2 Flocks of Heat Stressed Broilers \*\*\*

Break-even period = 0.3 years

Purchase of ceiling fans is \$1890

Yearly Benefit = \$5,962.

Average Velocity Impinging Broilers = 0.852 m/s

Characteristic Velocity = 3.657 m/s

Broiler Spacing = 0.068 sq m/broiler

Fan Spacing = 12.00 m

Fan Diameter = 1.422 m

Yearly value of addition weight gain = \$6,038

Yearly cost of electricity = \$76.

Number of ceiling fans needed = 10

You cannot buy a fraction of a ceiling fan therefore 24.00  
sq m of floor area has not been accounted for

Table 3. Output for Summer Routine Example Problem:  
Ceiling Fans Compared to Alternative Air Circulators

Ceiling fans compared to alternative air circulators

Immediate benefit

Break-even period is zero

\*\*\* 2 Flocks of Heat Stressed Broilers \*\*\*

Benefit after ten years = \$6,483

Purchase of ceiling fans is cheaper by \$22.

Yearly benefits (not including purchase savings) = \$646.

Average velocity impinging broilers = 0.902 m/s

Yearly value of addition weight gain = \$235

Yearly monetary saving for electricity = \$411

You cannot buy a fraction of a ceiling fan therefore 56.00

sq m of floor area has not been accounted for

Table 4. Output for Summer Routine Example: Combinations of Fan Characteristics and the Predicted Results

Break-even Period (yr)	Initial Investment (\$)	Additional Weight Gain (N)	Averaging Impinging Velocity (m/s)	Characteristic Velocity (m/s)	Uniform Broiler Spacing (m <sup>2</sup> /broiler)
Fan Spacing (m)	Fan Diameter (m)	Value of Addition Weight Gain (\$)	Electrical Cost (\$)	Number of Fans (fan)	Unaccounted Floor Area (m <sup>2</sup> )
2.0	19662.	9927.	1.517	4.922	0.068
5.0	1.83	10828.	900.	58.	14.0
2.2	19662.	9049.	1.517	4.922	0.074
5.0	1.83	9950.	900.	58.	14.0
1.4	13560.	9595.	1.451	4.922	0.068
6.0	1.83	10216.	621.	40.	24.0
.	.	.	.	.	.
.	.	.	.	.	.
.	.	.	.	.	.
.	.	.	.	.	.

Insights for Summer Ceiling Fan Applications. Weight gain increases as the characteristic velocity increases. However, the rate of change of weight gain is lower than the rate of change of characteristic velocity. The difference in the rate of increase is due to the location of broilers in the boundary layer. Velocity profiles in the boundary layer converge to zero as  $Y$  approaches zero. The height of the boundary layer increases as the radial distance of the wall jet increases. Hence, the rate of change of weight gain with respect to characteristic velocity decreases as the radial distance of the wall jet increases. Therefore, the influence of fan speed on weight gain decreases as fan spacing increases.

Weight gain increases are predicted to be larger when broilers have their necks down than when broilers have their necks up because air velocity is higher for the neck down than the neck up case (Figure 58)

The summer routine depends partly on the data for the alternative air circulators. The data is used for the comparison of ceiling fans to the alternative air circulators. The comparison will be biased if improper data is used to describe the air flow due to alternative air circulators. Studies, similar to this study, can provide the proper data to describe the air flow resulting from alternative air circulators.

Reduction of risk due to broiler mortality is not included in the ceiling fan benefits predicted by the summer routine. However, benefits due to the reduction of risk could be included in the summer routine. A statistical study involving the frequency of occurrence of mass broiler

death due to heat stress would be required. The risks due to heat stress are analogous to the risks due to flooding. A ten year mass broiler death would be reported in a similiar manner as a ten year flood.

Ceiling fan applications in broiler houses in Virginia are predicted to be beneficial, assuming the input data in the summer routine example problem is valid for most broiler houses in Virginia (Table 2). The predicted yearly benefit is \$5,962 per house. The expected managerial decision based on this prediction is to use ceiling fans. Inclusion of the benefits due to risk reduction will increase the predicted yearly benefit presently calculated by the routine and cause the optimum fan spacing to decrease.

### Winter Routine

Background: Litter Conditions. Harris et al. (1977) reported that the amount of moisture in four week old litter decreased as ventilation increased. Air exchange and air circulation enhance litter drying, however, air exchange in the winter is constrained by the cost associated with the heat loss. Air circulation is especially important in the winter because it mixes warm and cool air in broiler houses. The warmer air increases the vapor pressure difference between the litter and the air.

An increase in air velocity near the litter increases the shear stress at the air-litter interface. Mass transfer is increased by increases in shear stress at the interface. Hence, the diffusion of



moisture in litter is increased by increasing air velocity near the litter.

Winter Routine Development. The winter routine is similar to the summer routine except that the emphasis is on the rate of water vapor transfer from the litter to the air. Hence, the program predicts the air velocity one centimeter above the litter for varying radii. Management can use the velocity predictions to choose the fan spacing and the operating speed needed to produce the recommended minimum velocity. HP-41C coding and the user manual for the winter routine are in Appendix B.

The winter routine was developed for  $r \leq 204.5$  cm and  $r/R \leq 2.174$ . The fully developed wall jet region was used because large values of  $r$  are required to calculate fan spacing. The winter routine was developed using boundary layer equations 14 and 22. Characteristic length,  $UC/UMAX$  and  $U/UMAX$  expressions were also used. A value of one was substituted for the variable  $Y$ .

Insights for Winter Ceiling Fan Applications. Air velocities one centimeter about the litter are nearly independent of whether the broilers neck are up or down because velocities in the boundary layer converge to zero as  $Y$  approaches zero. The winter routine did not require an optimization routine to predict the type of fan and number of fans to buy because ceiling fans will be selected and bought for summer applications. Also, summer air circulation will require more ceiling

fans than winter air circulation, so additional fans will not have to be bought for winter circulation.

As an example of a winter application consider a radial distance of 400 cm, a fan radius of 91.5 and a characteristic velocity of 4.990 m/s. The program output is in Table 5.

Table 5. Output for Winter Routine Example Problem:  
r = 400 CM, R = 91.5 CM and UC = 4.990 M/S

## XEQ "NECKDN"

RADIUS CM	400.00	RUN
FANRAD CM	91.50	RUN
UC M/S	4.990	RUN
M/S = 0.29		

## XEQ "NECKUP"

RADIUS CM	400.00	RUN
FANRAD CM	91.50	RUN
UC M/S	4.990	RUN
M/S = 0.33		

CHAPTER VIII  
CONCLUSIONS, SAFETY AND FUTURE WORK

Conclusions

Based on the results of this study of wall jet models for ceiling fan applications in broiler houses, the following conclusions were drawn:

1. A wall jet model was developed to predict the velocity of the wall jet impinging upon broilers located at varying radii from the fan centerline. The velocity changes due to broiler spacing and relatively large gaps between groups of broilers were negligible, hence, the wall jet model is a general model.
2. The wall jet model was interfaced to a broiler growth model that predicts the weight gain of heat stressed broilers as a function of air velocity.
3. A computer routine was developed to predict the optimum combination of fan diameter, fan speed and fan spacing for a given broiler house.
4. A computer routine was developed to predict the wall jet velocity one centimeter above litter.

Future Work

Based upon both the results of this study and the experiences gained in working with ceiling fans, the following suggestions for future work are offered: 1) ceiling fan safety tests, 2) development of fan standards, 3) future ceiling fan concepts, 4) development of an updated broiler growth model for heat stressed broilers, 5) ceiling fan applications for air exchange, and 6) the inclusion of the reduction of risk in the summer routine.

Safety. Producers often climb ladders to adjust the cables supporting waterers and feeders. Therefore, head and limb injuries, due to ceiling fans, were of concern. The 91.5 cm radius fan rotated at 310 rpm while operating on high speed. The corresponding tip velocity was 3.0 m/s. A perfectly elastic collision between the tip of the blade and a human head would produce a force of approximately 20 kN. Assuming an impact area of 0.10 m x 0.002 m, the resulting pressure would be  $1.45 \times 10^5$  kPa. The previous estimates were based on the following assumptions: 1) the blades decelerated linearly, so the average tip velocity was 15 m/s, 2) the blade traveled 5 cm during deceleration, 3) the blade thickness was 0.002 m, and 4) the length of the impact area was 0.10. Safety tests are needed to measure the actual impact forces due to ceiling fans.

Fan Standards. Ceiling fan standards can be simplified because ceiling fan performance depends on only two fan characteristics, the fan radius and the characteristic velocity. In contrast, existing standards require several velocity measurements (Home Ventilating Institute, 1982). Existing standards for ceiling fan performance are based on the volumetric air flow through a horizontal plane 3 feet above the floor when 8 or 10 foot ceiling heights are used. Velocity measurements are recorded at angles of 0, 90, 180 and 270 degrees for radial distances of 0, 10.2, 20.3, 30.5 cm, etc. until the velocities are less than 0.2 m/s.

Future Ceiling Fan Concept. Ceiling fans produce wall jets that flow radially inward and produce an upwash. The momentum of the upwash is exchanged with the momentum of the annular free jet traveling downward. The momentum exchange reduces fan performance. Extensions supporting the blades from the motor (Figure 63) would: 1) allow the outward radial wall jet to cover a larger floor area, 2) allow the inner radial wall jet to be used effectively to cool broilers and 3) reduce the upwash. Length of the extensions will depend on the velocity decay of the inner wall jet. The velocity decay of the inner wall jet can be estimated with the wall jet model. Also, the wall jet model will be useful to predict the outer wall jet. The wall jet produced by the 91.5 cm radius fan, operating at high speed, was used as an example. The maximum velocity of the wall jet flowing over the balloons with paper necks at a radius of 4.62 m was 1 m/s. Hence a single fan with 4.62 m extensions will circulate air over broilers in a floor area of 270 m<sup>2</sup>, with a minimum velocity of 1 m/s, assuming the characteristics of the inner radial wall jet are approximately equal to the characteristics of the outer radial wall jet. If the previous assumption is true, a fan with extensions will circulate air in a floor area four times larger than the floor area ventilated by a fan without extensions. The power requirement of the motor will be larger, however, the motor rpm will need to be reduced to prevent excessive tip velocities.

The wall jet model relates  $UC/UMAX$  to  $r/R$  (Figure 53). The relationship is a special case of  $UC/UMAX$  versus  $(r - L)/R$ , where  $L$  equals

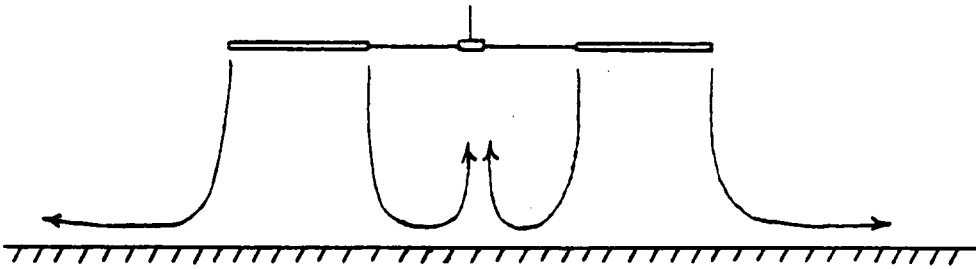


FIGURE 63. CEILING FAN WITH BLADE EXTENSIONS AND RESULTING AIR FLOW PATTERNS.

the extension length. The extension length is zero for present ceiling fans.

The fan blade extension concept is unfeasible for most broiler house applications because of space constraints due to cables hanging from the ceiling. However, this concept is an example of how the wall jet model can be used for future innovation.

Updated Broiler Growth Model. An updated broiler model for heat stressed broilers would increase the accuracy of the summer routine predictions, because heat stress is more severe for present day commercial broilers than for commercial broilers used in 1966 (Weaver, 1985).

Ceiling Fan Applications for Air Exchange. Ceiling fan applications can be designed to exchange air for oxygen replenishment and heat and odor removal. Heat removal by air exchange is often required in open-wall broiler houses for summer weather conditions because of the heat load caused by solar energy. In order to achieve air exchange, broiler houses must have open-walls at floor level (Figure 64). The wall jet model can be used to predict the required height of the floor level open-walls and the flow rate of the wall jet existing the broiler house. A screen would be required to contain the broilers and protect them from predators. Proper designs for floor level open-walls may require an obstruction of the line-of-sight between broilers and predators.



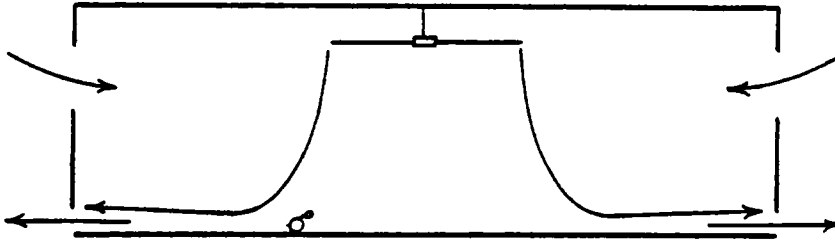


FIGURE 64. CEILING FAN APPLICATION FOR AIR CIRCULATION AND AIR EXCHANGE.

Inclusion of the Reduction of Risk in the Summer Routine.

Inclusion of the reduction of risk of broiler mortality may decrease the value of the predicted optimum fan spacing. Further discussion of the reduction of risk is given in "Insights for Summer Ceiling Fan Applications".

## LITERATURE CITED

- Anderson, D. P., C. W. Beard and R. P. Hansen. 1964. The adverse effects of ammonia on chickens, including resistance to infection with Newcastle Disease. *Avian Diseases* 8(3):369-379.
- ASAE. 1984. Standards - 1984. American Society of Agricultural Engineers, St. Joseph, Mi.
- Bakke, P. 1957. An experimental investigation of a wall jet. *Journal of Fluid Mechanics* 2(5):467-472.
- Baughman, G. R. 1984. Personal communication. Biological and Agricultural Engineering Department, North Carolina State University, Raleigh, N.C.
- Bowers, C. G. 1982. Buoyancy and radiation effects on low velocity flows in an asymmetrically heated channel. Ph.D. Thesis, Virginia Polytechnic Institute and State University, Blacksburg, VA.
- Bradshaw, P. and E. M. Love. 1961. The normal impingement of a circular air jet on a flat surface. Aeronautical Research Council, London, R and M, 3205: 1-8.
- Charles, D. R. and C. G. Payne. 1966. The influence of graded levels of atmospheric ammonia on chickens. *British Poultry Science* 7(3):177-187.
- Conley, W. 1980. Computer optimization techniques. Petrocelli Books, Inc. USA.
- Deaton, J. W., N. F. Reece, and T. H. Vandaman. 1978. The effect of temperature and density on broiler performance. *Poultry Science* 47(1):293-300.

- Dorn, W.S. and D.D. McCracken. 1972. Numerical methods with FORTRAN IV case studies. John Wiley and Sons, Inc. USA.
- Drury, L. N. 1966. Air velocity and broiler growth in a diurnally cycled hot environment. TRANSACTIONS of the ASAE 9(3):329-332.
- Drury, L. N. and H. S. Siegel. 1966. Air velocity and heat tolerance of young chickens. TRANSACTIONS of the ASAE 9(4):583-585.
- Esmay, M. L. 1978. Principles of animal environment, AVI Publishing Company, Inc., Westpoint, CT.
- Gardon, R. and J. Akfirat Cahit. 1965. The role of turbulence in determining the heat transfer characteristics of impinging jets. International Journal of Heat and Mass Transfer 8(10):1261-1272.
- Harris, G. C., G. S. Nelson, T. A. Cole, K. R. Shelby, J. A. Benson and D. R. Ingram. 1977. Effects of ventilation on litter condition and performance of broilers brooded at high density to 4 weeks of age. Poultry Science 56(5):1720.
- Holman, J. P. 1978. Experimental methods for engineers. McGraw-Hill, Inc., USA.
- Home Ventilating Institute. 1982. Ceiling fan test standard and certification procedure. Home Ventilating Institute, Rolling Meadows, IL.
- Hubbard. 1983. Management guide for the hubbard broilers. Hubbard Farms, Inc., Walpole, NH.
- Hughes, H. A. 1985. Personal Communication. Agricultural Engineering Department. Virginia Polytechnic Institute and State University, Blacksburg, VA.

- Hughes, H. A. and J. Wu. 1985. Ceiling fans for broiler houses. ASAE Paper No. 85-4023, ASAE, St. Joseph, MI 29085.
- Joiner, W. P. and T. M. Huston. 1957. The influence of high environmental temperature on immature domestic fowl. Poultry Science 36(5):973-978.
- Kempster, H. L. 1938. The influence of summer temperatures on the rate of growth of chickens. Poultry Science 17(4):259-263.
- Kling, H. F. and C. L. Quarles. 1974. Effect of atmospheric ammonia and the stress of infectious bronchitis vaccination on Leghorn males. Poultry Science 53(3):1161-1167.
- King, F. C. Jr., G. M. White and J. N. Walker. 1972. The effect of surface obstructions on air wall jets. TRANSACTIONS of the ASAE 15(2):361-365.
- Maki, H., H. Ito and F. Saigo. 1980. Studies on the flow of axisymmetric radialwise wall jet on the impinged wall by the annular impinging jet. Bulletin of the JSME 23(176):217-223.
- Poreh, M. Y. G. Tsuei and J. E. Cermak. 1967. Investigation of a turbulent radial wall jet. TRANSACTIONS of the ASME, Series E, Journal of Applied Mechanics 34:457-463.
- Quarles, C. L. and H. F. King. 1974. Evaluation of ammonia and infectious bronchitis vaccination stress on broiler performance and carcass quality. Poultry Science 53(4):1592-1596.
- Rajaratnam, N. 1976. Turbulent jets. Elsevier Scientific Publishing Company, Amsterdam, The Netherlands.

- Reece, F. N. 1981. Use of solar energy in broiler production. *Poultry Science* 60(5):911-916.
- Reece, F. N., B. D. Lott and J. W. Deaton. 1981. Low concentrations of ammonia during brooding decrease broiler weight. *Poultry Science* 60(5):937-940.
- Roberts, C. W. 1964. Estimation of early growth rate in the chicken. *Poultry Science* 43(1):238-252.
- Sammelwitz, P.H. 1967. Adrenocortical hormone therapy of induced heat stress mortality in broilers. *Poultry Science* 46(5):1314.
- Siegel, H. S. and L. N. Drury. 1968a. Physiological responses of chickens to variations in air temperature and velocity. *Poultry Science* 47(4):1120-1127.
- Siegel, H. S. and L. N. Drury. 1968b. Physiological responses to high lethal temperature and air velocity in young fowl. *Poultry Science* 47(4):1230-1235.
- Striegl, S.A. 1982. The effect of entrainment on jet impingement heat transfer. M.S. Thesis, Virginia Polytechnic Institute and State University, Blacksburg, VA.
- Striegl, S. A. and T. E. Diller. 1984. An analysis of the effect of entrainment temperature on jet impingement heat transfer. *TRANSACTIONS of the ASME, Series C, Journal of Heat Transfer* 106 (4):804-810.
- Tani, I. and Y. Komatsu. 1964. Impingement of a round jet on a flat surface. *Proc. 11th Congr. Appl. Mech., Munich*, pp. 465-468.

- Tennekes, H. and J. L. Lumley. 1972. A first course in turbulence. 4th Printing, MIT Press, Cambridge, MA.
- Thaxton, P. J. 1984. Personal Communication. Poultry Science Department, North Carolina State University, Raleigh, N.C.
- Thermo-Systems, Inc. 1982. Personal communication. St. Paul, MN.
- Thermo-Systems, Inc., n.d. Instruction manual for model 1125 calibrator. St. Paul, MN.
- Timmons, M. B. 1984. Internal air velocities as affected by the size and location of continuous inlet slots. TRANSACTIONS of the ASAE 27(5):1514-1517.
- Timmons, M. B. and G. R. Baughman. 1983. Operational characteristics of overhead fans. ASAE Paper No. 83-4512, ASAE, St. Joseph, MI. 49085.
- Tsuei, Y. G. 1962. Axisymmetric boundary layer of a jet impinging on a smooth plate. Ph.D. Thesis, Colorado State University, Fort Collins.
- Walker, J. N. and G. M. White. 1973. Influence of ceiling surface irregularities of air jets. TRANSACTIONS of the ASAE 16(1):145-147.
- Weaver, Jr. W. D. 1985. Personal Communication. Poultry Science Department. Virginia Polytechnic Institute and State University, Blacksburg, VA.
- Wilhelm, L. R. 1976. Numerical calculation of psychrometric properties in SI units. TRANSACTIONS of the ASAE 19(2):318-323.

## APPENDIX A

### SUMMER ROUTINE: BROILER1 USER MANUAL

BROILER1 calculates the optimum combination of characteristic velocity, fan spacing, fan diameter and number of fans for the given data. The routine will compare 1) three fan diameters with the corresponding fan costs, 2) four characteristic velocities per fan, 3) four power requirements per fan, 4) six fan spacings and two broiler spacings. BROILER1 also compares the break-even periods and monetary benefits of ceiling fans with alternative air circulators. A listing of the variable names are given in Table 6.

Input descriptions are of the form

Row number: Description of input variable, units, format

The inputs for BROILER1 are

- Row 1: Three fan diameters, m, (3F10.0)
- Row 2: The corresponding fan costs \$/fan,(3F10.0)
- Row 3: The corresponding fan salvage values after 10 yrs,  
\$/fan, (3F10.0)
- Row 4: Four characteristic velocities for fan 1, m/s, (4F10.0)
- Row 5: Four characteristic velocities for fan 2, m/s, (4F10.0)
- Row 6: Four characteristic velocities for fan 3, m/s, (4F10.0)
- Row 7: Four input power requirements corresponding to the four  
characteristic velocities of fan 1, W/fan, (4F10.0)
- Row 8: Four input power requirements corresponding to the four  
characteristic velocities of fan 2, W/fan (4F10.0)



- Row 9: Four input power requirements corresponding to the four characteristic velocities of fan 3, W/fan, (4F10.0)
- Row 10: Six fan spacings, m, (6F10.0)
- Row 11: Two broiler spacings,  $m^2$ /broiler, (2F10.0)
- Row 12: A) The estimated average air velocity impinging broilers when the alternative air circulators are used, m/s  
 B) Broiler house floor area,  $m^2$   
 C) Broiler value, \$/N  
 D) Alternative air circulator salvage value after 10 yrs., \$/circulator  
 E) Code 1 for necks down or  
 Code 2 for necks up  
 (4F10.0,I1)
- Row 13: A) Cost of electricity, \$/kWh  
 B) Interest rate of alternative investment, decimal  
 C) Number of heat stressed flocks, flocks/year  
 D) Cost of alternative air circulator, \$/circulator  
 E) Number alternative air circulators  
 F) Input power requirement of the alternative air circulator, W/circulator (6F10.0)

Multiple broiler house predictions are calculated by inputting the total floor area and the total number of alternative air circulators.

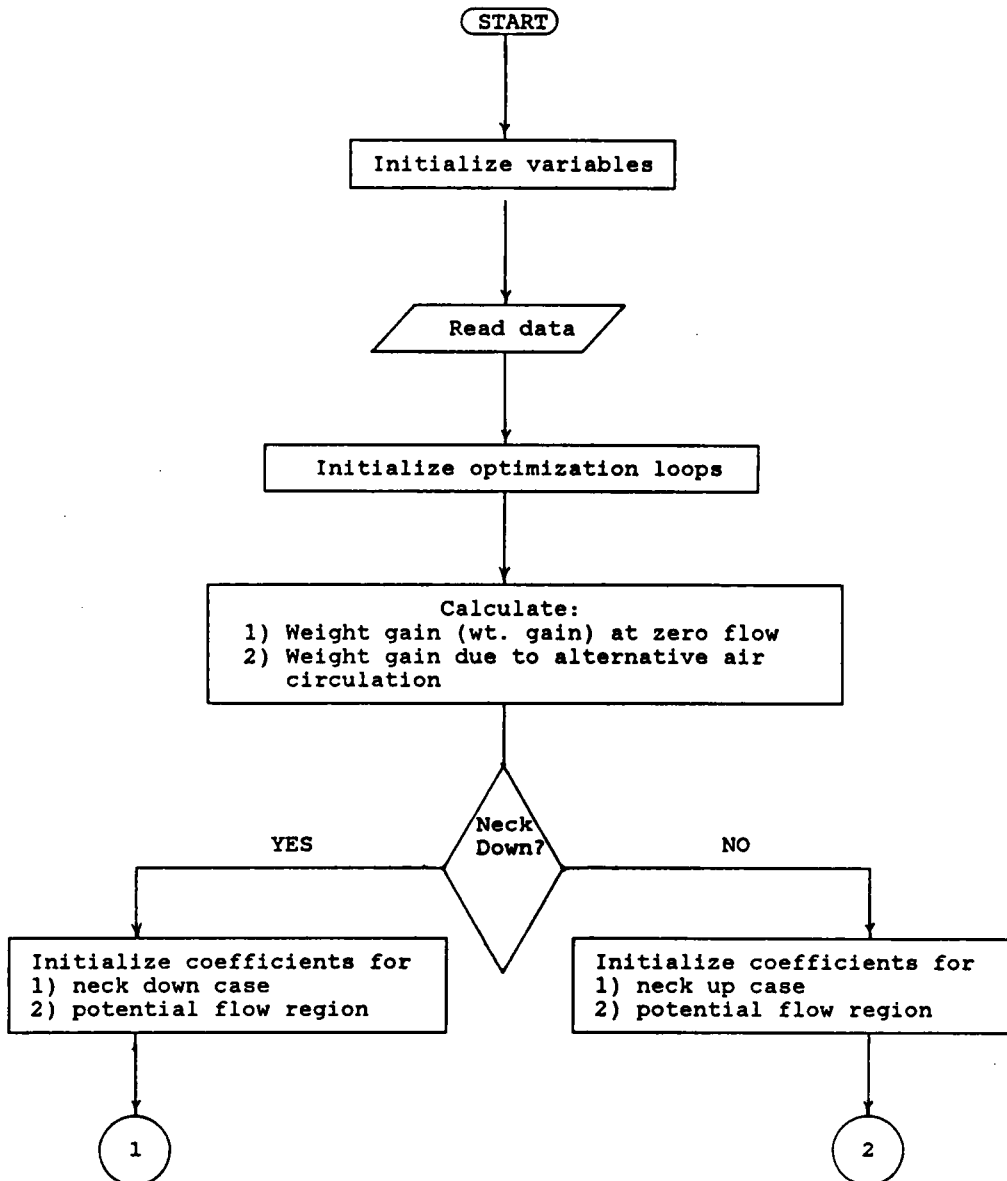
Fortran coding for the summer routine is in Table 7. Definitions of the variables in the summer routine are listed below.

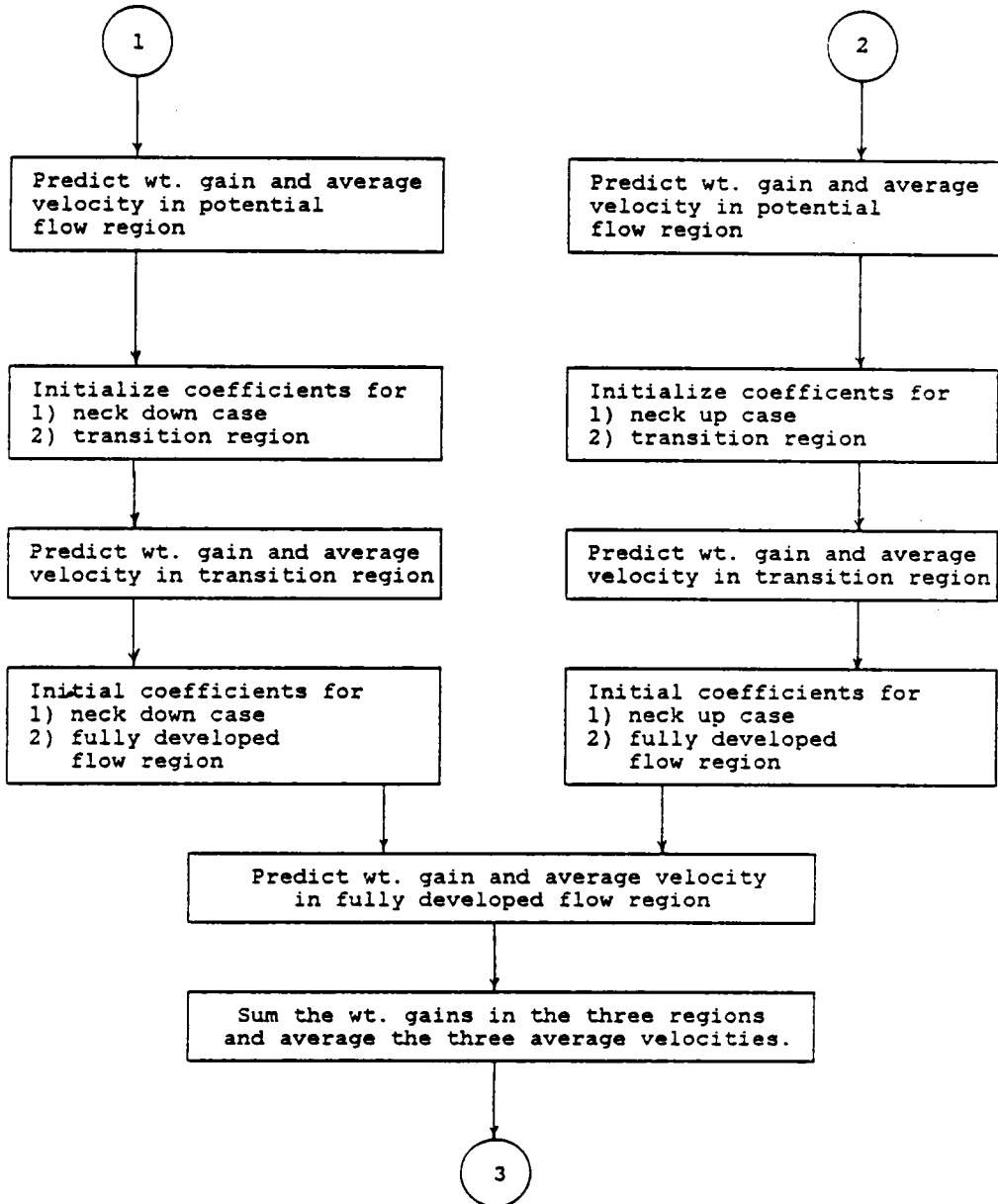
TABLE 6. Listing of Variable Names for BROILER1

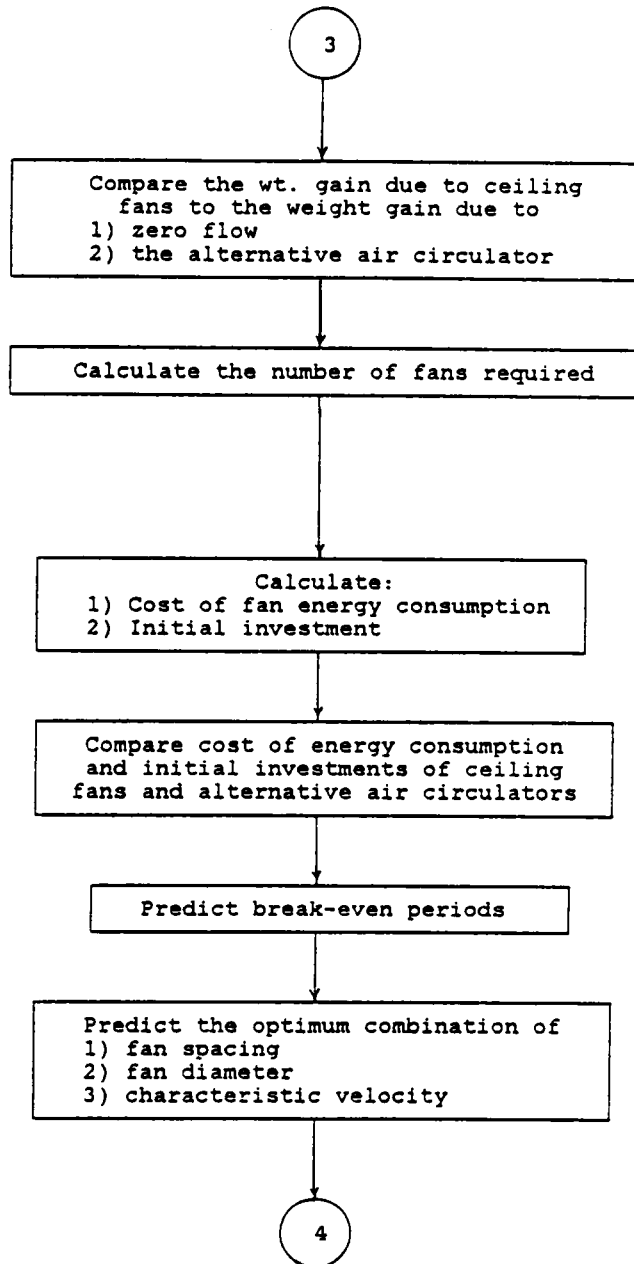
AREA	=	floor area
B	=	characteristic length
BBMIN	=	minimum break-even period
BCOST	=	cost of alternative air circulator
BDIFF	=	difference in initial investments
BELEC	=	total kilowatt - hours used by alternative air circulators
BENMAX	=	maximum monetary benefit for a 10 yr period
BEP	=	break-even period
BMIN	=	minimum break-even period
BNUM	=	number of alternative air circulators
BPOW	=	cost of energy consumed by alternative air circulators
BSAL	=	salvage value of alternative air circulator after 10 yr
BVAL	=	broiler value
BWATTS	=	energy consumption of an alternative air circulator
CORNER	=	daily weight gain in the corners of the imaginary square ventilated by a ceiling fan
DAYS	=	number of days the fans are operated
DELEC	=	difference in energy cost between ceiling fans and alternative air circulators
DURA	=	estimated life of ceiling fans
ECOST	=	cost of energy consumed by ceiling fans
ELECOS	=	cost of electricity

EXTRA	=	the floor area ventilated by the remaining fraction of a ceiling fan
FANRAD	=	ceiling fan radius
FAREA	=	area of the imaginary square ventilated by a ceiling fan
FCOST	=	ceiling fan cost
FNUM	=	number of ceiling fans minus the fraction
FPY	=	number of heat stressed flocks per year
GAIN01	=	difference in monetary value of weight gain due to ceiling fans and alternative air circulators
GAIN1	=	GAIN01 - DELEC
GAIN11	=	yearly, monetary advantage of weight gain due to ceiling fans compared to alternative air circulators
GAIN02	=	difference in monetary value of weight gain due to ceiling fans compared to no fans (zero air flow)
GAIN2	=	GAIN02 - ECOST
GAIN22	=	yearly, monetary advantage of weight gain due to ceiling fans compared to zero air flow
INT	=	interest rate of an alternative investment
INVEST	=	initial investment of ceiling fans
NODE	=	integer code for necks up or down
R1 and R2	=	limits of integration
SAL	=	total salvage value of alternative air circulators after 10 yr
SALV	=	total salvage value of ceiling fans after 10 yr
SALVAG	=	ceiling fan salvage value after 10 yr

SPACE	=	broiler spacing
SPARE	=	daily weight gain in the floor area not accounted for by the circle and the corners that form the imaginary square ventilated by a fan
TCBLOW	=	initial investment of alternative air circulators
TOTKWH	=	total kilowatt - hours used by ceiling fans
UAVE	=	average of the average air velocity impinging broilers in the three flow regions
UAVEA	=	average velocity in the potential flow region
UAVEB	=	average velocity in the transition region
UAVED	=	average velocity in the fully developed flow region
UC	=	characteristic velocity of ceiling fan at a given fan speed
UGUESS	=	estimated velocity impinging broiler due to an alternative air circulator
WATTS	=	ceiling fan energy consumption
WGUESO	=	daily weight gain for zero air flow
WGUESS	=	daily weight gain due to the alternative air circulator
WTD	=	total, daily weight gain influenced by ceiling fans
WTDA	=	daily weight gain, in the potential flow region, influenced by ceiling fans
WTDB	=	daily weight gain, in the transition region, influenced by ceiling fans
WTDD	=	daily weight gain, in the fully developed flow region, influenced by ceiling fans







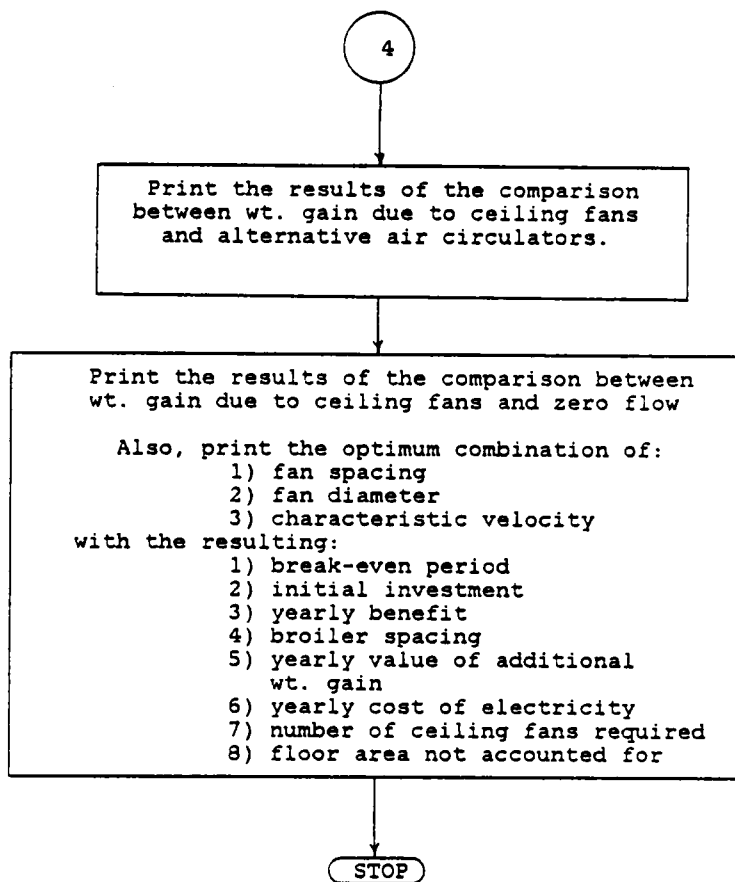


FIGURE 59. FLOWCHART FOR SUMMER ROUTINE BROILER1.



TABLE 7. FORTRAN CODING FOR SUMMER ROUTINE (BROILER1).

```

C*****
C*** BROILER FORTRAN *
C*** BY NEAL BLACKWELL 9/85 *
C*****
C*** BROILER FORTRAN CALCULATES THE OPTIMUM CEILING FAN *
C*** PARAMETERS FOR A GIVEN FLOOR AREA AND PREDICTS THE *
C*** RESULTING WEIGHT GAIN, ENERGY CONSUMPTION, *
C*** INITIAL INVESTMENT, BREAK-EVEN PERIOD, ETC. *
C*****
      IMPLICIT REAL *4(A-M,O-Z)
      REAL FANRAD(3),SPACE(2),B(6),WATTS(12),FCOST(3),SALVAG(3)
      COMMON A1,Y1,C1,M,UC(12)
C*****
C*** INITIALIZE VARIABLES *
C*** *
      A1=0.196672
      Y1=0.126064
      C1=0.029267
      DAYS=21.
      DURA=10.
      BENMAX=0.0
      BMIN=99.
      BMIN=99.
      NEY1=0
      NEY2=0
      NEY3=0
C*****
C*** READ INPUT DATA *
C*** *
      READ(1,100)(FANRAD(N1),N1=1,3)
      READ(1,100)(FCOST(N1),N1=1,3)
      READ(1,100)(SALVAG(N1),N1=1,3)
100  FORMAT(3F10.0)
      READ(1,101)(UC(N2),N2=1,12)
      READ(1,101)(WATTS(N2),N2=1,12)
101  FORMAT(4F10.0,/,4F10.0,/,4F10.0)
      READ(1,102)(B(N3),N3=1,6)
102  FORMAT(6F10.0)
      READ(1,103)(SPACE(N4),N4=1,2)
103  FORMAT(2F10.0)
      READ(1,104)JUGUESS,AREA,BVAL,BSAL,NODE
      #,ELECOS,INT,FPY,BCOST,BNUM,BWATTS
104  FORMAT(4F10.0,I1,/,6F10.0)
C*****
C*** MODIFY INPUT (CHANGE DIAMETERS TO RADII AND METERS *
C*** TO CENTIMETERS) *
C*** *
      DO 50 N22=1,3
      FANRAD(N22)=FANRAD(N22)*100./2.
50  CONTINUE
      DO 60 N23=1,6
      B(N23)=B(N23)*100./2.
60  CONTINUE
      N6=1
      N7=4
C*****
C*** OPTIMIZATION ROUTINE (TRY EACH FAN COMBINATION) *
C*** *
      DO 10 N1=1,3
      DO 20 N2=N6,N7
      DO 30 N3=1,6
      DO 40 N4=1,2
C*****
      WTDA=0.0
      WTDB=0.0
      WTDD=0.0
      M=1591.5494*SPACE(N4)
      IF(B(N3).LT.231.0.OR.B(N3).GT.650.0)THEN
      WRITE(2,200)
200  FORMAT(1X,'FAN SPACING MUST BE GREATER THAN
      #4.62 M',/, 'AND LESS THAN 13 M')
      GO TO 888
      ENDIF
C*****
C*** PREDICT THE DAILY WEIGHT GAIN WHEN NO AIR CIRCULATOR *
C*** IS USED (ZERO AIR FLOW) *
C*** *
      WGUES0=A1*4.0*B(N3)**2/(M*2.0*3.1416)

```

```

C*****
C*** PREDICT THE DAILY WEIGHT GAIN DUE TO THE ALTERNATIVE *
C*** AIR CIRCULATOR *
C*** *
      WGUSS=(A1+Y1*SQRT(UGUSS)-C1*UGUSS)*4.0*B(N3)**2/(M*2.0*3.1416)
C*****
C*** NODE=1 : NECKS DOWN *
C*** NODE=2 : NECKS UP *
C*****
C*** NECKS DOWN
C***
      IF(NODE.EQ.1)THEN
C*****
C*** PREDICT THE DAILY WEIGHT GAIN IN THE *
C*** POTENTIAL FLOW REGION (SECTION ONE) *
C*** *
C***          B IS CONSTANT *
C***          UC/UMAX IS EXPONENTIAL *
C*** *
      C5=3.629
      A5=0.543/FANRAD(N1)
      W=0.6138
      R1=0.0
      R2=2.174*FANRAD(N1)
      CALL FA(WTDA,R1,R2,W,C5,A5,N2)
      UAVEA=UAVE1(W,A5,C5,R2,N2)
C*****
C*** PREDICT THE DAILY WEIGHT GAIN IN THE *
C*** TRANSITION REGION (SECTION TWO) *
C*** *
C***          B IS CONSTANT *
C***          UC/UMAX IS LINEAR *
C*** *
      R1=R2
      R2=231.0
      S=1.0514
      T=-0.5940
      P=S/FANRAD(N1)
      CALL FB(WTDB,R1,R2,W,P,T,N2)
      UAVEB=UAVE2(P,T,R1,R2,W,N2)
C*****
      IF(B(N3).EQ.231.0)THEN
      GO TO 1
      ENDIF
C*****
C*** PREDICT THE DAILY WEIGHT GAIN IN THE *
C*** FULLY DEVELOPED FLOW REGION (SECTION *
C*** THREE) *
C*** *
C***          B IS LINEAR *
C***          UC/UMAX IS LINEAR *
C*** *
      H=0.1094
      I=12.16
      R1=231.0
      D=0.207819
      J=6.3225
      K=549.9371
      L=-9826.5106
      R2=B(N3)
      S=1.0514
      T=-0.5940
      P=S/FANRAD(N1)
      ELSE
C*****
C*** NECKS UP *
C*** *
C*****
C*** SECTION ONE: B IS CONSTANT *
C***          UC/UMAX IS EXPONENTIAL *
C*** *
      W=0.76335
      C5=4.606
      A5=0.483/FANRAD(N1)
      R1=0.0
      R2=2.174*FANRAD(N1)
      CALL FA(WTDA,R1,R2,W,C5,A5,N2)
      UAVEA=UAVE1(W,A5,C5,R2,N2)
C*****
C*** SECTION TWO: B IS CONSTANT *
C***          UC/UMAX IS LINEAR *
C*** *
      R1=R2
      R2=231.0
      S=1.02182

```

```

T=-0.24201
P=S/FANRAD(N1)
CALL FB(WTDB,R1,R2,W,P,T,N2)
UAVEB=UAVE2(P,T,R1,R2,W,N2)
C*****
IF(B(N3).EQ.231.0)THEN
GO TO 1
ENDIF
C*****
C*** SECTION THREE: B IS LINEAR *
C*** UC/UMAX IS LINEAR *
C*** *
H=0.185968
I=-7.5636
D=0.252024
J=12.06670
K=398.2836
L=-9700.050
R1=231.0
R2=B(N3)
S=1.02182
T=-0.24201
P=S/FANRAD(N1)
C*****
ENDIF
C*****
C*** CALCULATE THE WEIGHT GAIN IN SECTION *
C*** THREE,THE FOUR CORNERS AND THE SPARE *
C*** AREA. ALSO, CALCULATE THE AVERAGE *
C*** VELOCITY IN SECTION THREE. *
C*** *
CALL SIMP(WTDD,CORNER,UAVED,R1,R2,H,I,T,P,D,J,K,L,N2)
CORNER=CORNER*4.0
SPARE=SP(D,J,K,L,H,I,P,T,R2,N2)
C*****
C*** SUM THE WEIGHT GAINS AND AVERAGE THE AVERAGE *
C*** VELOCITIES *
C *
1 CONTINUE
WTD=WTDA+WTDB+WTDD+CORNER+SPARE
UAVE=(UAVEA+UAVEB+UAVED)/3.0
C*****
C*** CALCULATE THE REQUIRED NUMBER OF CEILING FANS *
C*** *
FAREA=4.0*B(N3)**2/10000.
FNUM=AREA/FAREA
FNUM1=FNUM
FNUM=AINT(FNUM)
C*****
C*** CALCULATE THE FLOOR AREA NOT ACCOUNTED FOR BY THE *
C*** FANS *
C*** *
FFRAC=FNUM1-FNUM
EXTRA=FAREA*FFRAC
C*****
C*** CALCULATE THE INITIAL INVESTMENT OF THE CEILING FANS *
C*** AND THE ALTERNATIVE AIR CIRCULATOR. ALSO, CALCULATE *
C*** THE DIFFERENCE IN THE INITIAL INVESTMENTS. *
C*** *
INVEST=FCOST(N1)*FNUM
TCBLOW=BCOST*BNUM
BDIFF=INVEST-TCBLOW
C*****
C*** CALCULATE THE SALVAGE VALUE OF THE CEILING FANS. *
C*** ALSO, CALCULATE THE DIFFERENCE IN THE SALVAGE *
C*** VALUES OF THE CEILING FANS AND AIR CIRCULATORS *
C*** *
SALV=SALVAG(N1)*FNUM
SAL=SALV-BSAL*BNUM
IF(SAL.LE.0.0)SAL=0.0
C*****
C*** CALCULATE THE KILOWATT HOURS REQUIRED BY THE CEILING *
C*** FANS AND THE ALTERNATIVE AIR CIRCULATORS. ALSO, *
C*** CALCULATE THE DIFFERENCE IN THE KILOWATT HOURS *
C*** REQUIRED BY THE TWO TYPES OF FANS. *
C*** *
TOTKWH=FNUM*WATTS(N2)/1000.*DAYS*24.0
ECOST=TOTKWH*ELECOS
BELEC=BNUM*BWATTS/1000.*DAYS*24.0
BPOW=BELEC*ELECOS
DELEC=ECOST-BPOW

```

```

C*****
C*** COMPARE THE MONETARY VALUE OF THE WEIGHT GAINS *
C*** 1) CEILING FANS COMPARED TO ALTERNATIVE FANS *
C***
      GAIN01=(MTD-WGUESS)*FNUM*BVAL*DAYS
      GAIN1=GAIN01-DELEC
      GAIN11=FPY*GAIN1
C*** *
C*** 2) CEILING FANS COMPARED TO NO FANS *
C*** *
      GAIN02=(MTD-WGUESO)*FNUM*BVAL*DAYS
      GAIN2=GAIN02-ECOST
      GAIN22=FPY*GAIN2
C*****
C*** CALCULATE THE BREAK-EVEN PERIODS *
C*** 1) CEILING FANS COMPARED TO ALTERNATIVE FANS *
C***
      IF(BDIFF.LE.0.0) THEN
      BEPC=0.0
      IF(GAIN11.LE.0.0)BEP=99.
      ELSE
      CALL ECON(BEPC,BDIFF,INT,SAL,GAIN11)
      ENDIF
C*** *
C*** 2) CEILING FANS COMPARED TO NO FANS *
C*** *
      CALL ECON(BEP,INVEST,INT,SALV,GAIN22)
C*****
C*** PREDICT THE MINIMUM BREAK-EVEN PERIOD AND THE *
C*** MAXIMUM 10 YEAR BENEFIT FOR THE COMPARISON OF *
C*** CEILING FANS VERSUS ALTERNATIVE AIR CIRCULATORS *
C*** *
C*** 1) INITIAL INVESTMENT FOR CEILING FANS IS *
C*** LESS THAN THE INITIAL INVESTMENT OF THE *
C*** ALTERNATIVE AIR CIRCULATORS *
C*** *
      IF(BEPC.EQ.0.0)THEN
      BEN=DURA*GAIN11+ABS(BDIFF)
      IF(BEN.GT.BENMAX)THEN
      BENMAX=BEN
      P1=-BDIFF
      P2=GAIN11
      P3=UAVE
      P4=UC(N2)
      P5=SPACE(N4)
      P6=B(N3)*2.0/100.
      P7=FANRAD(N1)*2.0/100.
      P8=GAIN01*FPY
      P9=-DELEC*FPY
      P10=FNUM
      P11=EXTRA
      NEY1=1
      ENDIF
      ELSE
C*** *
C*** 2) INITIAL INVESTMENT OF THE CEILING FANS IS *
C*** GREATER THAN THE INITIAL INVESTMENT OF THE *
C*** ALTERNATIVE AIR CIRCULATORS *
C*** *
      IF(BEPC.LT.BMIN)THEN
      BMIN=BEPC
      Q1=BDIFF
      Q2=GAIN11
      Q3=UAVE
      Q4=UC(N2)
      Q5=SPACE(N4)
      Q6=B(N3)*2.0/100.
      Q7=FANRAD(N1)*2.0/100.
      Q8=GAIN01*FPY
      Q9=-DELEC*FPY
      Q10=FNUM
      Q11=EXTRA
      NEY2=1
      ENDIF
      ENDIF
C*****
C*** PREDICT THE CEILING FAN PARAMETERS FOR THE OPTIMUM *
C*** BENEFIT (MINIMUM BREAK-EVEN PERIOD AND MAXIMUM TEN *
C*** YEAR BENEFIT) *
C*** *

```

```

IF(BEP.LT.B8MIN)THEN
B8MIN=BEP
V1=INVEST
V2=GAIN22
V3=UAVE
V4=UC(N2)
V5=SPACE(N4)
V6=B(N3)*2.0/100.
V7=FANRAD(N1)*2.0/100.
V8=GAINO2*FPY
V9=ECOST*FPY
V10=FNUM
V11=EXTRA
NEY3=1
ENDIF
C*****
C*** THESE STATEMENTS PRINT OUT ALL THE POSSIBLE *
C*** COMBINATIONS OF FAN CHARACTERISTICS *
C*** *
FAKE1=B(N3)*2.0/100.
FAKE2=FANRAD(N1)*2.0/100.
FAKE3=GAINO2*FPY
FAKE4=ECOST*FPY
WRITE(3,291)BEP,INVEST,GAIN22,UAVE,UC(N2),SPACE(N4)
*,FAKE1,FAKE2,FAKE3,FAKE4,FNUM,EXTRA
291 FORMAT(1X,F5.1,1X,F8.0,1X,F8.0,1X,F6.3,1X,F6.3,1X,F6.3
*,/,1X,F6.2,1X,F6.3,1X,F8.0,1X,F6.0,1X,F6.0,1X,F8.2,/)
C*****
C*** THESE STATEMENTS ARE A PART OF THE OPTIMIZATION *
C*** ROUTINE *
C*** *
40 CONTINUE
30 CONTINUE
20 CONTINUE
IF(N1.EQ.1)THEN
N6=5
N7=8
ELSE
N6=9
N7=12
ENDIF
10 CONTINUE
C*****
C*** PRINT THE RESULTS OF THE CEILING FAN COMPARISON *
C*** WITH THE ALTERNATIVE AIR CIRCULATOR *
C*** *
WRITE(2,299)
299 FORMAT(1X,'CEILING FANS COMPARED TO ALTERNATIVE AIR CIRCULATORS',/)
IF(NEY1.EQ.1)THEN
WRITE(2,300)FPY,BENMAX,P1,P2,P3,P8,P9,P11
300 FORMAT(1X,'IMMEDIATE BENEFIT',/
*,1X,'BREAK-EVEN PERIOD IS ZERO !',/
*,1X,'*** ',F3.0,' FLOCKS OF HEAT STRESSED BROILERS***',/
*,1X,'BENEFIT AFTER TEN YEARS = $ ',F8.0,/
*,1X,'PURCHASE OF CEILING FANS IS CHEAPER BY $ ',F8.0,/
*,1X,'YEARLY BENEFIT (NOT INCLUDING PURCHASE SAVINGS) = $ ',F8.0,/
*,1X,'AVERAGE VELOCITY IMPINGING BROILERS = ',F6.3,' M/S',/
*,1X,'YEARLY VALUE OF ADDITION WEIGHT GAIN = $ ',F8.0,/
*,1X,'YEARLY MONETARY SAVING FOR ELECTRICITY = $ ',F6.0,/
*,1X,'YOU CANNOT BUY A FRACTION OF A CEILING FAN THEREFORE '
*,F8.2,/, ' SQ M OF FLOOR AREA HAS NOT BEEN ACCOUNTED FOR.',////)
ENDIF
IF(NEY1.EQ.1) GO TO 777
IF(NEY2.EQ.1)THEN
WRITE(2,301)FPY,BMIN,Q1,Q2,Q3,Q8,Q9,Q11
301 FORMAT(1X,'*** ',F3.0,' FLOCKS OF HEAT STRESSED BROILERS***',/
*,1X,'BREAK-EVEN PERIOD = ',F5.1,' YEARS',/
*,1X,'PURCHASE OF CEILING FANS IS $ ',F8.0,' MORE',/
*,1X,'YEARLY BENEFIT = $ ',F8.0,/
*,1X,'AVERAGE VELOCITY IMPINGING BROILERS = ',F6.3,' M/S',/
*,1X,'YEARLY VALUE OF ADDITION WEIGHT GAIN = $ ',F8.0,/
*,1X,'YEARLY MONETARY SAVING FOR ELECTRICITY = $ ',F6.0,/
*,1X,'YOU CANNOT BUY A FRACTION OF A CEILING FAN THEREFORE '
*,F8.2,/, ' SQ M OF FLOOR AREA HAS NOT BEEN ACCOUNTED FOR.')
ENDIF
777 CONTINUE
IF(NEY1.NE.1.AND.NEY2.NE.1)THEN
WRITE(2,295)
295 FORMAT(1X,'BREAK-EVEN PERIOD DOES NOT EXIST')

```

```

      ENDIF
      WRITE(2,302)
302 FORMAT(1X,'*****')
      $,////)
C
C
C*****
C*** PRINT THE OPTIMUM SOLUTION *
C*** CEILING FANS VERSUS NO AIR CIRCULATORS *
C*** *
      IF(NEY3.EQ.1)THEN
        WRITE(2,303)FPY,BBMIN,V1,V2,V3,V4,V5,V6,V7,V8,V9,V10,V11
303 FORMAT(1X,'*** ',F3.0,' FLOCKS OF HEAT STRESSED BROILERS***',/
      $,1X,'BREAK-EVEN PERIOD = ',F5.1,' YEARS',/
      $,1X,'PURCHASE OF CEILING FANS IS $ ',F8.0,/
      $,1X,'YEARLY BENEFIT = $ ',F8.0,/
      $,1X,'AVERAGE VELOCITY IMPINGING BROILERS = ',F6.3,' M/S',/
      $,1X,'CHARACTERISTIC VELOCITY = ',F6.3,' M/S',/
      $,1X,'BROILER SPACING = ',F6.3,' SQ M /BROILER',/
      $,1X,'FAN SPACING = ',F6.2,' M',/
      $,1X,'FAN DIAMETER = ',F6.3,' M',/
      $,1X,'YEARLY VALUE OF ADDITION WEIGHT GAIN = $ ',F8.0,/
      $,1X,'YEARLY COST OF ELECTRICITY = $ ',F6.0,/
      $,1X,'NUMBER OF CEILING FANS NEEDED = ',F6.0,/
      $,1X,'YOU CANNOT BUY A FRACTION OF A CEILING FAN THEREFORE '
      $,F8.2,/, ' SQ M OF FLOOR AREA HAS NOT BEEN ACCOUNTED FOR.')
      ELSE
        WRITE(2,294)
294 FORMAT(1X,'BREAK-EVEN PERIOD DOES NOT EXIST')
      ENDIF
      WRITE(2,292)
292 FORMAT(1X,'*****')
888 CONTINUE
      STOP
      END
C
C
C
C*****
C*** INTEGRATE OVER SECTION ONE *
C*** *
      SUBROUTINE FA(WTDA,R1,R2,W,C5,A5,N2)
      IMPLICIT REAL *4(A-M,O-Z)
      COMMON A1,Y1,C1,M,UC(12)
C*****
C*****
C NUMERICAL INTEGRATION BY SIMPSON'S RULE *
C*****
C*****
C
C
C*****
C*** SET UP INTEGRATION PARAMETERS *
C*****
      A=R1
      B=R2
      N=10
      FN=FLOAT(N)
      HH=(B-A)/FN
      TMOH=HH+HH
C*****
C*** SET UP SUMMING VARIABLES *
C*****
      SUM4=0.0
      SUM2=0.0
C*****
C*** GIVE X ITS STARTING VALUE FOR LOOP *
C*****
      X=A+HH
C*****
C*** INITIALIZE LOOP COUNTER *
C*****
      NN=1
C*****
C*** THE SUMMING LOOP *
C*****
16 SUM4=SUM4+FAA(X,W,C5,A5,N2)
      SUM2=SUM2+FAA(X+HH,W,C5,A5,N2)
      IF(NN.GE.N-3) GO TO 36
      NN=NN+2
      X=X+TMOH
      GO TO 16

```

```

C*****
C*** MULTIPLY INTEGRAND BY CONSTANTS *
C*****
36 CONTINUE
  MTDA=1.0/M*HH/3.0*(4.0*SUM4+2.0*SUM2+FAA(A,M,C5,A5,N2)
  *+4.0*FAA(B-HH,M,C5,A5,N2))+FAA(B,M,C5,A5,N2))
  RETURN
  END
C
C
C
C
C*****
C*** INTEGRAND FOR WEIGHT GAIN IN SECTION ONE *
C*** *
  REAL FUNCTION FAA(R,M,C5,A5,N2)
  IMPLICIT REAL *4(A-M,O-Z)
  COMMON A1,Y1,C1,M,UC(12)
  ABC=UC(N2)*M*EXP(A5*R)/C5
  FAA=(A1+Y1*SQRT(ABC)-C1*ABC)*R
  RETURN
  END
C
C
C
C
C*****
C*** AVERAGE VELOCITY IN SECTION ONE *
C*** *
  REAL FUNCTION UAVE1(M,A5,C5,R2,N2)
  IMPLICIT REAL *4(A-M,O-Z)
  COMMON A1,Y1,C1,M,UC(12)
  UAVE1=UC(N2)*M/(A5*R2*C5)*(EXP(A5*R2)-1.0)
  RETURN
  END
C
C
C
C
C*****
C*** INTEGRAND FOR WEIGHT GAIN IN SECTION TWO *
C*** *
  REAL FUNCTION FBB(R,M,P,T,N2)
  IMPLICIT REAL *4(A-M,O-Z)
  COMMON A1,Y1,C1,M,UC(12)
  Z1=UC(N2)*M/(P*R+T)
  FBB=R*(A1+Y1*SQRT(Z1)-C1*Z1)
  RETURN
  END
C
C
C
C*****
C*** INTEGRATE OVER SECTION TWO *
C*** *
  SUBROUTINE FB(MTDB,R1,R2,M,P,T,N2)
  IMPLICIT REAL *4(A-M,O-Z)
  COMMON A1,Y1,C1,M,UC(12)
C*****
C NUMERICAL INTEGRATION BY SIMPSON'S RULE *
C*****
C
C*****
C*** SET UP INTEGRATION PARAMETERS *
C*****
  A=R1
  B=R2
  N=10
  FN=FLOAT(N)
  HH=(B-A)/FN
  TMOH=HH+HH

```

```

C*****
C*** SET UP SUMMING VARIABLES *
C*****
      SUM4=0.0
      SUM2=0.0
C*****
C*** GIVE X ITS STARTING VALUE FOR LOOP *
C*****
      X=A+HH
C*****
C*** INITIALIZE LOOP COUNTER *
C*****
      NN=1
C*****
C*** THE SUMMING LOOP *
C*****
      15 SUM4=SUM4+FBB(X,M,P,T,N2)
          SUM2=SUM2+FBB(X+HH,M,P,T,N2)
          IF(NN.GE.N-3) GO TO 35
          NN=NN+2
          X=X+TWOH
          GO TO 15
C*****
C*** MULTIPLY INTEGRAND BY CONSTANTS *
C*****
      35 CONTINUE
          HTDB=1.0/M*HH/3.0*(4.0*SUM4+2.0*SUM2+FBB(A,M,P,T,N2)
          *+4.0*FBB(B-HH,M,P,T,N2)+FBB(B,M,P,T,N2))
          RETURN
      END
C
C
C
C*****
C*** AVERAGE VELOCITY IN SECTION TWO *
C*** *
      REAL FUNCTION UAVE2(P,T,R1,R2,M,N2)
      IMPLICIT REAL *(A-M,O-Z)
      COMMON A1,Y1,C1,M,UC(12)
      UAVE2=UC(N2)*M/((R2-R1)*P)*(ALOG(T+P*R2)-ALOG(T+P*R1))
      RETURN
      END
C
C
C
C*****
C*** INTEGRAND FOR THE WEIGHT GAIN IN SECTION THREE *
C*** *
      REAL FUNCTION F(X,H,I,P,K,L,T,D,J,N2)
      IMPLICIT REAL *(A-M,O-Z)
      COMMON A1,Y1,C1,M,UC(12)
      AAA=(D+J/X+K/X**2+L/X**3)/(P/H*(X-I)+T)
      F=(X-I)*(A1+Y1*SQRT(UC(N2))*AAA)
      * -C1*UC(N2)*AAA
      RETURN
      END
C
C
C
C*****
C*** INTEGRAND FOR THE WEIGHT GAIN IN THE CORNER *
C*** *
      REAL FUNCTION G(R,H,I,P,K,L,T,D,J,R2,N2)
      IMPLICIT REAL *(A-M,O-Z)
      COMMON A1,Y1,C1,M,UC(12)
      X=H*R+I
      AAA=(D+J/X+K/X**2+L/X**3)/(P*R+T)
      G=(A1+Y1*SQRT(UC(N2))*SQRT(AAA)-C1*UC(N2))*AAA)
      *(1.4142*R2-R)
      RETURN
      END
C
C
C

```



```

C*****
C*** INTEGRAND FOR THE VELOCITY IN SECTION THREE *
C*** *
REAL FUNCTION U(X,H,I,T,D,J,K,L,P)
IMPLICIT REAL *(A-M,O-Z)
AAA=D+J/X+K/X**2+L/X**3
BBB=(X-I)/H
U=1.0/(P*BBB+T)*AAA
RETURN
END

C
C
C
C*****
C*** INTEGRATE OVER SECTION THREE *
C*** *
SUBROUTINE SIMP(WTDD,CORNER,UAVED,R1,R2,H,I,T,P,D,J,K,L,N2)
IMPLICIT REAL *(A-M,O-Z)
COMMON A1,Y1,C1,M,UC(12)
C*****
C*****
C NUMERICAL INTEGRATION BY SIMPSON'S RULE *
C*****
C*****
C
C
C*****
C*** SET UP INTEGRATION PARAMETERS *
C*****
A=H*R1+I
B=H*R2+I
N=10
FN=FLOAT(N)
HH=(B-A)/FN
TWOH=HH+HH
C*****
C*** SET UP SUMMING VARIABLES *
C*****
SUM4=0.0
SUM2=0.0
C*****
C*** GIVE X ITS STARTING VALUE FOR LOOP *
C*****
X=A+HH
C*****
C*** INITIALIZE LOOP COUNTER *
C*****
NN=1
C*****
C*** THE SUMMING LOOP *
C*****
12 SUM4=SUM4+F(X,H,I,P,K,L,T,D,J,N2)
SUM2=SUM2+F(X+HH,H,I,P,K,L,T,D,J,N2)
IF(NN.GE.N-3) GO TO 32
NN=NN+2
X=X+TWOH
GO TO 12
C*****
C*** MULTIPLY INTEGRAND BY CONSTANTS *
C*****
32 CONTINUE
WTDD=1.0/(M*H**2)*HH/3.0*(4.0*SUM4+2.0*SUM2+F(A,H,I,P,K,L,T,D,J,
N2)+4.0*(B-HH,H,I,P,K,L,T,D,J,N2)+F(B,H,I,P,K,L,T,D,J,N2))

C
C
C
C*****
C*** INTEGRATE OVER THE CORNER *
C*** *
C*****
C*****
C NUMERICAL INTEGRATION BY SIMPSON'S RULE *
C*****
C*****
C
C
C*****
C*** SET UP INTEGRATION PARAMETERS *
C*****

```

```

A=R2
B=R2*1.4142
N=10
FN=FLOAT(N)
HH=(B-A)/FN
TWOH=HH+HH
C*****
C*** SET UP SUMMING VARIABLES *
C*****
SUM4=0.0
SUM2=0.0
C*****
C*** GIVE X ITS STARTING VALUE FOR LOOP *
C*****
X=A+HH
C*****
C*** INITIALIZE LOOP COUNTER *
C*****
NN=1
C*****
C*** THE SUMMING LOOP *
C*****
13 SUM4=SUM4+G(X,H,I,P,K,L,T,D,J,R2,N2)
SUM2=SUM2+G(X+HH,H,I,P,K,L,T,D,J,R2,N2)
IF(NN.GE.N-3) GO TO 33
NN=NN+2
X=X+TWOH
GO TO 13
C*****
C*** MULTIPLY INTEGRAND BY CONSTANTS *
C*****
33 CONTINUE
CORNER=2.0/(M*2.0*3.1416)*HH/3.0*(4.0*SUM4+2.0*SUM2
+G(A,H,I,P,K,L,T,D,J,R2,N2)
+4.0*G(B-HH,H,I,P,K,L,T,D,J,R2,N2)+G(B,H,I,P,K,L,T,D,J,R2,N2))
C
C
C
C*****
C*** INTEGRATE THE VELOCITY OVER SECTION THREE *
C*** *
C*****
C NUMERICAL INTEGRATION BY SIMPSON'S RULE *
C*****
C
C
C
C*****
C*** SET UP INTEGRATION PARAMETERS *
C*****
A=H*R1+I
B=H*R2+I
N=10
FN=FLOAT(N)
HH=(B-A)/FN
TWOH=HH+HH
C*****
C*** SET UP SUMMING VARIABLES *
C*****
SUM4=0.0
SUM2=0.0
C*****
C*** GIVE X ITS STARTING VALUE FOR LOOP *
C*****
X=A+HH
C*****
C*** INITIALIZE LOOP COUNTER *
C*****
NN=1
C*****
C*** THE SUMMING LOOP *
C*****
14 SUM4=SUM4+U(X,H,I,T,D,J,K,L,P)
SUM2=SUM2+U(X+HH,H,I,T,D,J,K,L,P)
IF(NN.GE.N-3) GO TO 34
NN=NN+2
X=X+TWOH
GO TO 14

```

```

C*****
C*** MULTIPLY INTEGRAND BY CONSTANTS *
C*****
34 CONTINUE
UAVED=UC(N2)/(H*(R2-R1))*HH/3.0*(4.0*SUM4+2.0*SUM2+
*U(A,H,I,T,D,J,K,L,P)
*4.0*U(B-H,H,I,T,D,J,K,L,P)+U(B,H,I,T,D,J,K,L,P))
RETURN
END

C
C
C
C
C*****
C*** PREDICT THE DAILY WEIGHT GAIN IN THE SPARE AREA NOT *
C*** INCLUDED IN THE CIRCLE AND CORNERS THAT FORM THE *
C*** IMAGINARY SQUARE VENTILATED BY A FAN *
C*** *
REAL FUNCTION SP(D,J,K,L,H,I,P,T,R2,N2)
IMPLICIT REAL *4(A-M,O-Z)
COMMON A1,Y1,C1,M,UC(12)
CC=H*R2+I
UAVEE=UC(N2)/(P*R2+T)*(D+J/CC+K/CC**2+L/CC**3)
SP=(A1+Y1*SQRT(UAVEE)-C1*UAVEE)*0.1721*R2**2/(M*2.0*3.1416)
RETURN
END

C
C
C
C
C*****
C*** PREDICT THE BREAK-EVEN PERIOD *
C*** *
SUBROUTINE ECON(BEP,P,I,S,A)
IMPLICIT REAL *4(A-M,O-Z)
ATEST=(I*S-A)/(I*P-A)
IF(A.LE.0.0.OR.ATEST.LT.1.0)THEN
BEP=99.
ELSE
BEP=ALOG((I*S-A)/(I*P-A))/ALOG(1.0+I)
ENDIF
RETURN
END

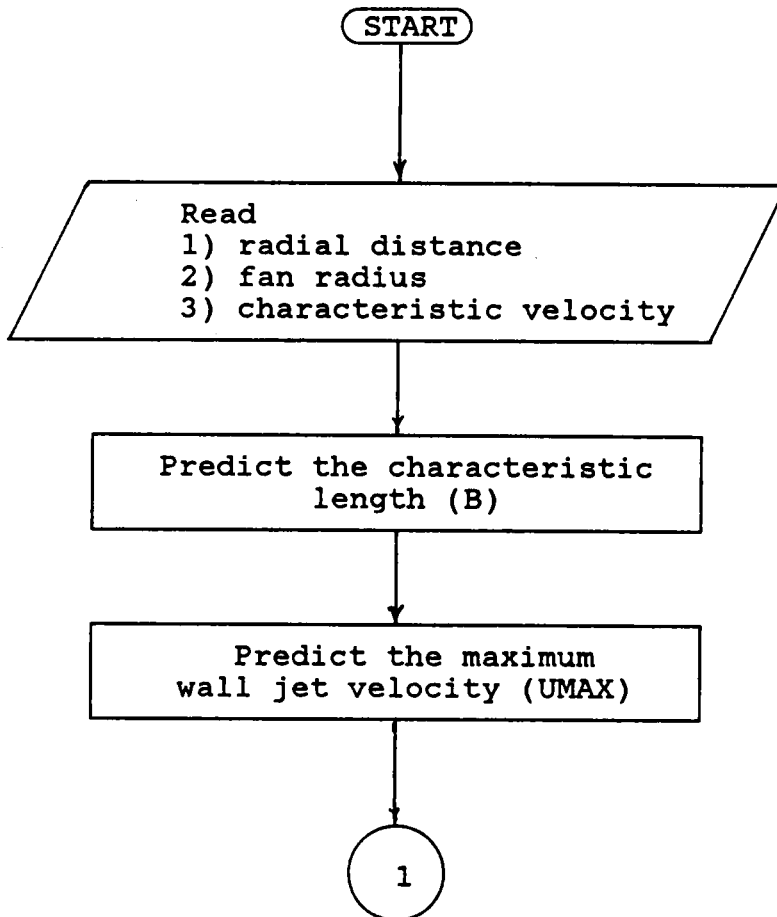
```

## APPENDIX B

### WINTER ROUTINE: USER MANUAL

Two calculator routines were developed to predict the velocity of the wall jet one centimeter above the litter. The routine entitled NECKDN was developed for the case of broilers with necks down. Likewise, the routine entitled NECKUP was developed for the case of broilers with necks up. The routines were coded in Reverse Polish Notation for use with the HP-41C series of calculators.

NECKDN and NECKUP prompt the user for (1) the radial distance corresponding to the desired velocity one centimeter above the litter, (2) the fan radius and (3) the characteristic velocity of the fan at a given speed. Input units are displayed during prompting. The coding for NECKDN and NECKUP are in TABLES 8 and 9 respectively.



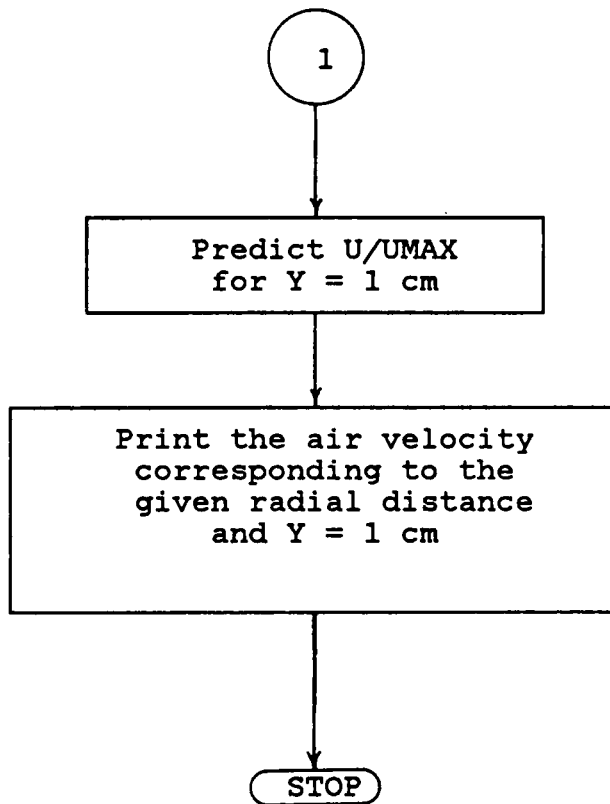


FIGURE 60. FLOWCHART FOR WINTER ROUTINES  
NECKDN AND NECKUP.

Table 8. Coding for NECKDN for  
the HP-41C Series of Calculators

01 LBL "NECKDN"	28 Y X
02 "RADIUS CM"	29 -28.188614
03 PROMPT	30 *
04 STO 01	31 STO 06
05 "FANRAD CM"	32 RCL 04
06 PROMPT	33 1/X
07 STO 02	34 X 2
08 "UC M/S"	35 13.016155
09 PROMPT	36 *
10 STO 03	37 ST+ 06
11 RCL 01	38 RCL 04
12 .1094	39 1/X
13 *	40 1.099557
14 12.16	41 *
15 +	42 .207819
16 STO 04	43 +
17 RCL 01	44 RCL 06
18 RCL 02	45 +
19 /	46 RCL 05
20 1.0514	47 1/X
21 *	48 *
22 .5940	49 RCL 03
23 -	50 *
24 STO 05	51 "M/S ="
25 RCL 04	52 ARCL X
26 1/X	53 AVIEW
27 3	54 END

Table 9. Coding for NECKUP for  
the HP-41C Series of Calculators

01 LBL "NECKUP"	28 Y X
02 "RADIUS CM"	29 -1.8649
03 PROMPT	30 *
04 STO 01	31 STO 06
05 "FANRAD CM"	32 RCL 06
06 PROMPT	33 1/X
07 STO 02	34 X 2
08 "UC M/S"	35 -0.95922
09 PROMPT	36 *
10 STO 03	37 ST+ 06
11 RCL 01	38 RCL 04
12 .185968	39 1/X
13 *	40 2.22311
14 7.5636	41 *
15 -	42 0.354282
16 STO 04	43 +
17 RCL 01	44 RCL 06
18 RCL 02	45 +
19 /	46 RCL 05
20 1.02181	47 1/X
21 *	48 *
22 .24201	49 RCL 03
23 -	50 *
24 STO 05	51 "M/S ="
25 RCL 04	52 ARCL X
26 1/X	53 AVIEW
27 3	54 END



## APPENDIX C

### UNCERTAINTY ANALYSIS

The uncertainty of the multiple sample experimental data, commonly called the standard deviation of the mean, was calculated by

$$\sigma_m = \sigma/\sqrt{n} \quad (28)$$

where

$\sigma$  = standard deviation

$n$  = number of measurements

(Holman, 1978).

Upper and lower bounds of the uncertainty were calculated because the uncertainty of the independent variables vary with the magnitude of the dependent variables.

The estimated uncertainty of  $r$  ranged between  $\pm 0.2$  and  $0.5$  cm or  $\pm 2$  to  $0.1\%$ , respectively. The uncertainty of  $R$  was  $\pm 0.2$  cm or  $\pm 0.25\%$ . Therefore, the uncertainties of  $r$  and  $R$  were negligible. The lower and upper bounds of the multiple sample uncertainties were 1)  $\pm 0.67$  to  $1.32$  cm for  $B$ , 2)  $\pm 0.013$  to  $0.039$  m/s for  $U_{MAX}$ , 3)  $\pm 0.003$  to  $0.006$  for  $Y/B$  and 4)  $\pm 0.004$  to  $0.025$  for  $U/U_{MAX}$ .

Upper and lower bounds of the uncertainty of the wall jet predictions were calculated by the Kline and McClintock uncertainty method for single samples (Holman, 1978). Uncertainty of the dependent variables were calculated using the estimated uncertainties of the independent variables. The uncertainty intervals were calculated by

$$Z_{\text{FUNC}} = \pm \left[ \left( \frac{\partial \text{FUNC}}{\partial x_1} Z_{x_1} \right)^2 + \left( \frac{\partial \text{FUNC}}{\partial x_2} Z_{x_2} \right)^2 + \dots + \left( \frac{\partial \text{FUNC}}{\partial x_n} Z_{x_n} \right)^2 \right]^{\frac{1}{2}} \quad (29)$$

where FUNC is a function of  $x_1, x_2 \dots x_n$ .

The uncertainties of the prediction of Y/B were  $\pm 0.00038$  and  $0.0019$ .

The uncertainties of the prediction of U/UMAX were  $\pm 0.0047$  and  $0.018$ .

The overall lower and upper bounds were the sum of the multiple sample uncertainties and the prediction uncertainties and are expressed as

$$(\text{OVERALL BOUND})_{\text{LOWER}} = (Z_{\text{FUNC}})_{\text{LOWER}} + (\sigma_m)_{\text{LOWER}} \quad (30)$$

and

$$(\text{OVERALL BOUND})_{\text{UPPER}} = (Z_{\text{FUNC}})_{\text{UPPER}} + (\sigma_m)_{\text{UPPER}} \quad (31)$$

The overall bounds for Y/B were  $\pm 0.003$  and  $0.008$ . The overall bounds for U/UMAX were  $\pm 0.009$  and  $0.043$ .

Overall lower and upper bounds for Y/B and U/UMAX were used to calculate the uncertainty bounds for velocity. Lower and upper bounds of velocity predictions were  $\pm 0.017$  and  $0.072$  m/s. Bounds of weight gain predictions were  $\pm 0.002$  and  $0.003$  N/(broiler.day). Weight gain multiple sample uncertainties were  $\pm 0.064$  and  $0.093$  N/(broiler.day). The overall weight gain uncertainties were the sum of the multiple sample uncertainties and prediction uncertainties. Lower and upper bounds of the overall weight gain uncertainties were  $\pm 0.070$  and  $0.096$  N/(broiler.day)

Weight gain multiple sample uncertainties resulting from the data reported by Drury (1966) were much larger than the weight gain prediction uncertainties. Hence, the overall weight gain uncertainties were relatively large. Mean weight gains were used to calculate equation 24 (Drury, 1966). Therefore, the summer routine predictions are based on the mean values of broiler weight gain.

**The vita has been removed from  
the scanned document**